ON THE CELLULAR STRESS RESPONSE

TO

STAPHYLOCOCCUS AUREUS ALPHA - TOXIN

D i s s e r t a t i o n
zur Erlangung des Grades
"Doktor der Naturwissenschaften"

am Fachbereich Biologie
der Johannes Gutenberg-Universität
in Mainz

Gunnaporn Veerachato
geb. in Bangkok, Thailand

Mainz, 2006

Dekan: .....

1. Berichterstatter:.....

2. Berichterstatter:.....

Tag der mündlichen Prüfung:.....

ON THE CELLULAR STRESS RESPONSE

TO

STAPHYLOCOCCUS AUREUS ALPHA - TOXIN

A Thesis

Submitted to the Faculty of Graduate Studies and Research

In Fulfillment of the Requirements

For the Degree of Doctor of Natural Sciences (Dr. rer. nat.)

In the Department of Biology

Johannes Gutenberg-University of Mainz

Mainz

By

Gunnaporn Veerachato

Winter, 2006

ABSTRACT

Staphylococcus aureus α-hemolysin was the first bacterial toxin recognized to form pores in the plasma membrane of eukaryotic cells. It is secreted as a water-soluble monomer that upon contact with target membranes forms an amphiphatic heptameric beta-barrel which perforates the bilayer. As a consequence, red cells undergo colloidosmotic lyses, while some nucleated cells may succumb to necrosis or programmed cell death. However, most cells are capable of repairing a limited number of membrane lesions, and then respond with productive transcriptional activation of NF-kB. In the present study, by using microarray and semiquantitative reverse transcriptase polymerase chain reaction (RT-PCR), data from a previously performed serial analysis of gene expression (SAGE) were extended and verified, revealing that immediate early genes (IEGs) such as *c-fos, c-jun* and *egr-1* are strongly induced at 2-8 h after transient toxin treatment. Activating protein 1 (AP-1: c-Fos, c-Jun) binding activity was increased accordingly. As IEGs are activated by growth factors, these findings led to the discovery that α-toxin promotes cell cycle progression of perforated cells in an EGFR-dependent fashion.

Although the amount of *c-fos* mRNA rose rapidly after toxin treatment, c-Fos protein expression was observed only after a lag of about 3 h. Since translation consumes much ATP, which transiently drops after transient membrane perforation, the suspicion arised that membrane-perforation caused global, but temporary downregulation of translation. In fact, eIF2α became heavily phosphorylated minutes after cells had been confronted with the toxin, resulting in shutdown of protein synthesis before cellular ATP levels reached the nadir. GCN2 emerged as a candidate eIF2α kinase, since its expression rapidly increased in toxin-treated cells. Two hours after toxin treatment, *GADD34* transcripts, encoding a protein that targets the catalytic subunit of protein phosphatase 1 (PP1) to the endoplasmic reticulum, were overexpressed. This was followed by dephosphorylation of eIF2α and resumption of protein synthesis. Addition of tautomycetin, a specific inhibitor of PP1, led to marked hyperphosphorylation of eIF2α and significantly reduced the drop of ATP-levels in toxin-treated cells. A novel link between two major stress-induced signalling pathways emerged when it was found that both translational arrest and restart were under the control of stress-activated protein kinase (SAPK) p38. The data provide an explanation for the indispensible role of p38 for defence against the archetypal threat of membrane perforation by agents that produce small transmembrane-pores.

ACKNOWLEDGEMENT

I would like to express my gratitude to all those who gave me the possibility to complete this thesis. Most of all I would like to thank my research advisors, Profs. Sucharit Bhakdi and Jürgen Markl for giving me the great opportunity in my life to do my Ph.D in Germany and I would like to thank Prof. Bhakdi for the financial support.

I sincerely thank my group leader Dr. Matthias Husmann for not only professionalism in working but also and most importantly a kind person. His trust and scientific excitement inspired me in the most important moments of making right decisions. His valuable comments and recommendations eliminated many ambiguous points from the manuscript. I am really glad to work with him and learn to be professional from him.

I am deeply indebted to Dr. Prapat Suriyaphol whose help, stimulating suggestions and patient encouragement enabled me to pass the difficult times and complete this work. Prapat, your labourious job is done. I am very grateful and would like you to be proud of me.

My best regards I want to give to Drs. Roman Kurek, Steffen Schmidt, Prof. Thomas Hankeln, and Ms. Sasithorn Chotewutmontri for professional advice in microarray. I would like to pay tribute to Dr. Shan-Rui Han who taught me how to deal with RNA. My special thanks to Claudia Neukirch, who did the [^{35}S] Met labeling and Wiesia Bobkiewicz for toxin preparation.

I would like to thank Drs. Katrin Dersch and Ulrike Haugwitz, my tutors while I was learning German at the Volkshochschule. Jetzt kann ich Deutsch sprechen (wenn auch nur ein bisschen) und in Deutschland zurechtkommen!

There are those whose spiritual support is even more important. Especially, I would like to give my special thanks to my parents Wg.Cdr. Rangsarit and Assoc.Prof. Gaysorn Veerachato together with my Thai and German friends who brighten up my days in Germany: Duangporn, Somruedee, Thipphaya, Ongkarn, Bhuwadol, Conny, Fatima, Sabine, Silvia, and Ricarda.

TABLE OF CONTENTS

LIST OF ABBREVIATIONS

β-PFT	β-pore-forming toxin
6PGDH	6-phosphogluconate dehydrogenase
Å	armstrong
aa-dUTP	5-(3-aminoallyl(-2'-deoxyuridine 5'-triphosphate))
AC	adenylate cyclase
AP-1	activating protein 1
ASK	apoptosis signal regulating kinase
ATF	activating transcription factor
ATM	ataxia telangiectasia mutated
ATP	adenosine 5'-triphosphate
ATR	ataxia telangiectasia and Rad3-related protein
Bcl-2	B-cell CLL/lymphoma
beta-ME	beta-mercaptoethanol
BiP	78 kDa glucose-regulated protein precursor
blvrb	biliverdin reductase B (flavin reductase (NADPH))
bona fide	genuinely or sincerely
bp	basepair(s)
BSA	bovine serum albumin
C. elegans	*Caenorhabditis elegans*
C/EBP	CCAAT/enhancer-binding protein
ca.	*circa* (approximately)
c-fos	FBJ murine osteosarcoma viral oncogene homolog
CHOP	C/EBP-homologous protein
c-jun	jun oncogene
COX	cyclooxygenase
CP	crossing point
CSR	cellular stress response
dATP	2'-deoxyadenosine 5'-triphosphate
dCTP	2'-deoxycytidine 5'-triphosphate
dGTP	2'-deoxyguanosine 5'-triphosphate
DKFZ	deutsches Krebsforchungsinstitut
DMSO	dimethyl sulfoxide
DNA	deoxyribonucleic acid
dNTP	deoxynucleoside triphosphate
dTTP	2'-deoxythymidine 5'-triphosphate
e.g.	*exempli gratia* (for example)
EDTA	ethylenediaminetetraacetic acid
EGFR	epidermal growth factor receptor
egr-1	early growth response factor 1
eIF2α	eukaryotic initiation factor 2, alpha subunit
EIF2AK	eukaryotic initiation factor 2, alpha subunit kinase
ELISA	enzyme-linked immunosorbent assay
ER	endoplasmic reticulum
ErbB	epidermal growth factor receptor (avian erythroblastic leukemia viral (v-erb-b) oncogene homolog)
ERK	extracellular signal-regulated kinase

ERK	extracellular signal-related kinases
FBS	foetal bovine serum
fwd	forward
G3PDH	glyceraldehyde 3-phosphate dehydrogenase
GADD	growth arrest and DNA-damage-inducible
GATA1	GATA binding protein 1/globin transcription factor1
GCN	general control non-derepressible-2
GM-CSF	granulocyte/macrophage colony-stimulating factor
GPCRs	G-protein-coupled receptors
GTP	guanosine-5'-triphosphate
h	hour(s)
HB-EGF	heparin-binding EGF-like growth factor
HER	human epidermal growth factor receptor
Herp	homocysteine-responsive endoplasmic reticulum-resident ubiquitin-like
Hmox-1	heme oxygenase-1
HPRT1	hypoxanthine phosphoribosyltransferase 1
HRI/	heme-regulated inhibitor
HRP	horseradish peroxidase
HSP	heat shock protein
IDH	NAD-isocitrate dehydrogenase
IEGs	immediate early genes
IgG	immunoglobulin G
IL	interleukin
iNOS	inducible nitric oxide synthase
ISR	integrated stress response
JNK	c-Jun N-terminal kinase
kDa	kilodalton(s)
LPS	lipopolyssaccharide
m	mutant α-toxin with arginine for histidine at residue 35
mA	milliampere(s)
MafA	v-maf musculoaponeurotic fibrosarcoma oncogene homolog A (avian)
MAPK	mitogen-activated protein kinase
MAPKAPK	MAPK-activated protein kinase
MAPKK/MKK	MAPK kinase
MAPKKK	MAPKK kinase
MEF	myocyte-enhancer factor
MEK	MAPK/ERK kinase
MEKK	MEK kinase
Met-tRNAi	initiating methionyl-tRNA
min	minute(s)
M-MLV	Moloney Murine Leukemia Virus
MMP	matrix metalloprotease
MNC	peripheral blood mononuclear cells
MNK	MAPK interaction protein kinase
MRSA	methicillin-resistant *S. aureus*
MSK	mitogen- and stress-activated kinase
NAD	nicotinamide adenine dinucleotide

NADPH	nicotinamide adenine dinucleotide phosphate hydrogen
NF-κB	nuclear Factor kappa B
NLK	nemo-like kinase
Nurr77	an orphan nuclear receptor
O.D	optical density
ORP150	150 kDa oxygen-regulated protein
p38α/β/γ/δ	p38 proteins α/β/γ/δ
PBS	phosphate buffered saline
p-c-Jun	phosphorylated c-Jun
PCR	polymerase chain reaction
p-eIF2α	phosphorylated eIF2α
PEK	pancreatic eIF2α kinase
PERK	PKR-like ER kinase
PFT	pore-forming toxin
PKC	protein kinase C
PKR	double-stranded RNA-dependent protein kinase
PLC-γ	phospholipase C-γ
PMA	phorbol myristate acetate
PP	protein phosphatase
PP1c	catalytic subunit of PP1
p-PERK	phosphorylated PERK
ppp1r15a	protein phosphatase 1, regulatory (inhibitor) subunit 15A
PRAK	p38-regulated/activated kinase
rev	reverse
RIPA buffer	radio-immunopreicipitation assay bufer
RNA	ribonucleic acid
ROS	reactive oxygen species
rps3a	ribosomal protein S3A
rRNA	ribosomal RNA
RT-PCR	reverse transcriptase polymerase chain reaction
RTK	receptor tyrosine kinase
s	second(s)
S. aureus	*Staphylococcus aureus*
SAGE	serial analysis of gene expression
SAPK	stress-activated protein kinase
SDS	sodium dodecyl sulfate
SDS-PAGE	sodium dodecyl sulfate polyacrylamide gel electrophoresis
SLO	streptolysin O
SRE	serum responsive elements
ssat	spermidine/spermine N(1)-acetyltransferase
TAK	TGF beta activated kinase
TAO	thyroid-associated ophthalmopathy
TAPI	tumor necrosis factor-α protease inhibitor
TC	tautomycetin
TCF	ternary complex factors
temp	temperature
TGF	transforming growth factor
TIGR	Institute for Genomic Research
TMPS	triple membrane-passing signal

TNF-α	tumor necrosis factor alpha
TPA	12-O-tetradecanoylphorbol-13-acetate
TRE	TPA responsive elements
TSS	toxic shock syndrome
UPL No.	Universal Probe Library number(s)
UPR	unfolded protein response
UV	ultraviolet
V. cholerae	*Vibrio cholerae*
v/v	volume per volume
VCAM	vascular cell adhesion molecule
VCC	*Vibrio cholerae* cytolysin
via	by way of
vs.	*versus* (against)
w	wild-type α-toxin
w/v	weight per volume

1. INTRODUCTION

1.1 *Staphylococcus aureus*

S. aureus is a Gram positive spherical bacterium which on microscopic examination appears in pairs, short chains, or bunched, grape-like clusters. It is frequently found in humans on external sites, such as the nostrils (1, 2) or the skin (3) and also transiently in the oropharynx (4) and faeces (5). Therefore, colonization of *S. aureus* does not cause disease. However, once the bacterium penetrates into tissues, it can cause more frequent and varied diseases than most other pathogens, ranging from minor skin infections and abscesses, to life-threatening diseases such as pneumonia, meningitis, endocarditis, toxic shock syndrome (TSS), and septicemia. Over the last decade, methicillin-resistant *S. aureus* (MRSA) strains have emerged as serious pathogens in the hospital and community settings (6), as well as initial cases of *S. aureus* with intermediate or, more recently, high-level resistance to vancomycin (7), makes MRSA infection more difficult to manage and costly to treat.

One reason that contributes to the pathogenesis of the bacteria is the multifaceted arsenal of toxins that can be elaborated by the microorganism, including agents that disrupt the integrity of target cell membranes, superantigens, and a multitude of hydrolytic enzymes. These virulence factors have the capacity to cripple host defence and elicit a broad range of pathologic effects in target cells.

1.2 Staphylococcal α-hemolysin

Staphylococcal α-hemolysin is water soluble, 33 kDa single-chain polypeptide of 293 amino acid residues, with no cysteine (8). It is the archetypal member of β-pore-forming toxins (β-PFTs),

which insert into the membrane to form a β-barrel (9-11). α-Toxin monomer, upon binding to a target cell, oligomerizes cooperatively and inserts into lipid bilayers to form cylindrical heptameric pores (12). It has been demonstrated that pores formed at <10 μg/ml toxin doses in keratinocytes and lymphocytes are very small (<12 – 15 Å effective diameter) (13, 14). Thus, they are freely permissive only to monovalent ions whereas small molecules such as propidium iodide are restricted. Most recently, it has been shown that the membrane-perforating β-barrel motif of α-toxin is highly conserved in evolution, and serves as the attack element of cytolysins from Gram-positive (*S. aureus*) and Gram-negative bacteria (*Vibrio cholerae*) (15, 16).

The biological relevance of α-toxin as a virulence factor has been demonstrated in several studies. It is a major determinant of bacterial pathogenicity (10) since mutant strains lacking α-toxin have dramatically reduced ability to kill mice (17). The attack of α-toxin on endothelial cells and thrombocytes together with the secondary reactions lead to pulmonary edema supporting the view that lethal action is probably due to effects on cells maintaining homeostasis (10). The toxin was found to trigger DNA-degradation in human T-lymphocytes in a manner resembling endonuclease activation during programmed cell death (14). It is also capable to induce apoptosis in Jurkat T cells, peripheral blood mononuclear cells (MNC) (18), and in endothelial cells (19). In addition, *S. aureus* α-toxin induced a molecular chaperone heat shock protein 70 (HSP 70), a member of a minimal stress proteome involving in the cellular stress response (CSR) in order to promote leakage of calcein from liposomes (20).

1.3 The cellular stress response

The CSR is a defence reaction of cells to environmental changes. It is triggered primarily by macromolecular damage or oxidative burst. The functions of CSR are to assess and counteract stress-induced damage, temporarily increase tolerance of such damage, and/or remove terminally damaged cells by programme cell death (apoptosis). Sensors of membrane, protein, and DNA damage as well as redox sensors, molecular chaperones, and energy metabolism sensors are important for CSR signalling networks. The CSR is a characteristic of all cells. More than 300 proteins involved in key aspects of the CSR are conserved in all organisms (21) but only 44 proteins have known functions and are regarded as "the minimal stress proteome". This consists of a spectrum of sensors as shown in Table 1. In cells exposed to ionizing radiation or highly reactive chemicals, oxidative burst occurred and a large amount of reactive oxygen species (ROS) was produced (22), which represents a critical second messenger for CSR signalling network (23). The capacity of the CSR depends on the proteome expressed in a cell at a particular time and is therefore species- and cell type-dependent. The key regulators of the CSR in eukaryotes include MAPKs (mitogen-activated protein kinases) (24) together with 14-3-3 (25), Bcl-2 (B-cell CLL/lymphoma) (26), ATM (ataxia telangiectasia mutated) and ATR (ataxia telangiectasia and Rad3-related protein) kinases (27), and insulin receptor-like kinases (28). MAPKs and the transcription factor AP-1 can also be activated by products of membrane lipid peroxidation, which is a common form of damage in response to stress, possibly via generation of H_2O_2 as a signalling intermediate (29, 30).

Table 1. Minimal stress proteome in the cellular stress response and their key responses (31).

Types of sensors	Proteins	Key functions
lipid membrane damage sensors	long-chain fatty acid ABC transporter multifunctional beta oxidation protein long-chain fatty acid CoA ligase	changing membrane lipid composition membrane lipid peroxidation triggers oxidative burst and produces H_2O_2.
DNA damage sensors	MutS/MSH MutL/MLH RecA/RadA/Rad51 TopI/III, Mre11/Rad32 Rad50 MutT/MTH	recognition of DNA damage *e.g.* DNA single strand breaks
protein damage sensors	FtsH Lon serine protease protease II/prolyl endopetidase aromatic amino acid amino-transferase aminobutyrate aminotrans-ferase	unfolded protein response (UPR), protein degradation
molecular chaperones	DnaK/HSP70 DnaJ/HSP40 GrpE HSP60 (heat shock protein60) petidyl-prolyl isomerise (cyclophilin)	recognition of unfolded proteins
energy metabolism sensors	citrate synthase Ca^{2+}/Mg^{2+}-transporting ATPase ribosomal RNA methyl-transferase enolase phosphoglucomutase	control of glycolysis, pentose phosphate pathway, and the Krebs cycle
redox sensors and redox regulation	*e.g.* aldehyde reductase glutathione reductase thioredoxin, peroxiredoxin superoxide dismutase quinone oxidoreductase MsrA G3PDH (glyceraldehyde 3-phosphate dehydrogenase) 6PGDH (6-phosphogluconate dehydrogenase)	*e.g.* free radical scavenging system, production of a cofactor of antioxidant NADPH, conversion of superoxide radicals to H_2O_2 and H_2O, respectively

1.3.1 Mammalian mitogen-activated protein kinase (MAPK) signalling cascades

MAPKs are a family of serine/threonine protein kinases that mediate fundamental biological processes and cellular responses to external stress signals (32). MAPK activity is regulated through three-tiered cascades composed of MAPKs, MAPK kinases (MAP2Ks/MKKs/MEKs), and MAP2K or MEK kinases (MAP3Ks/MEKKs) (33). Several MAPK activate specific effector kinases (MAPKAPKs: MAPK-activated protein kinases) are inactivated by MAPK phosphatases (34).

Mammals express at least six distinctly regulated groups of MAPKs (35), including i.) ERK-1/2 (extracellular signal-related kinases-1/2) (36, 37), ii.) JNK1/2/3 (Jun amino-terminal kinases 1/2/3), iii.) p38α/β/γ/δ, ERK6, and MXI, iv.) ERK5, v.) NLK (nemo-like kinase), and vi.) ERK3α/β (37). These MAPKs are activated by specific MAP2Ks: MKK1/2 for ERK1/2 (38), MKK3/4/6 for the p38s and, possibly, MKK6 for NLK (39, 40), MKK4/7 (JNKK1/2) for the JNKs (39, 41), MKK5 for ERK5 (42, 43), and ERK3 kinase for the ERK3s (44).

Each MAP2K can be activated by more than one MAP3K, increasing the complexity and diversity of MAPK signalling. Each individual MAPK cascade shares a number of upsteam and downstream kinases and transcription factors that interact and integrate these different pathways (45). In addition, each MAPK member has feedback loops that not only affect their own activation but also regulate the activation of other MAPK family members (46) (Fig. 1).

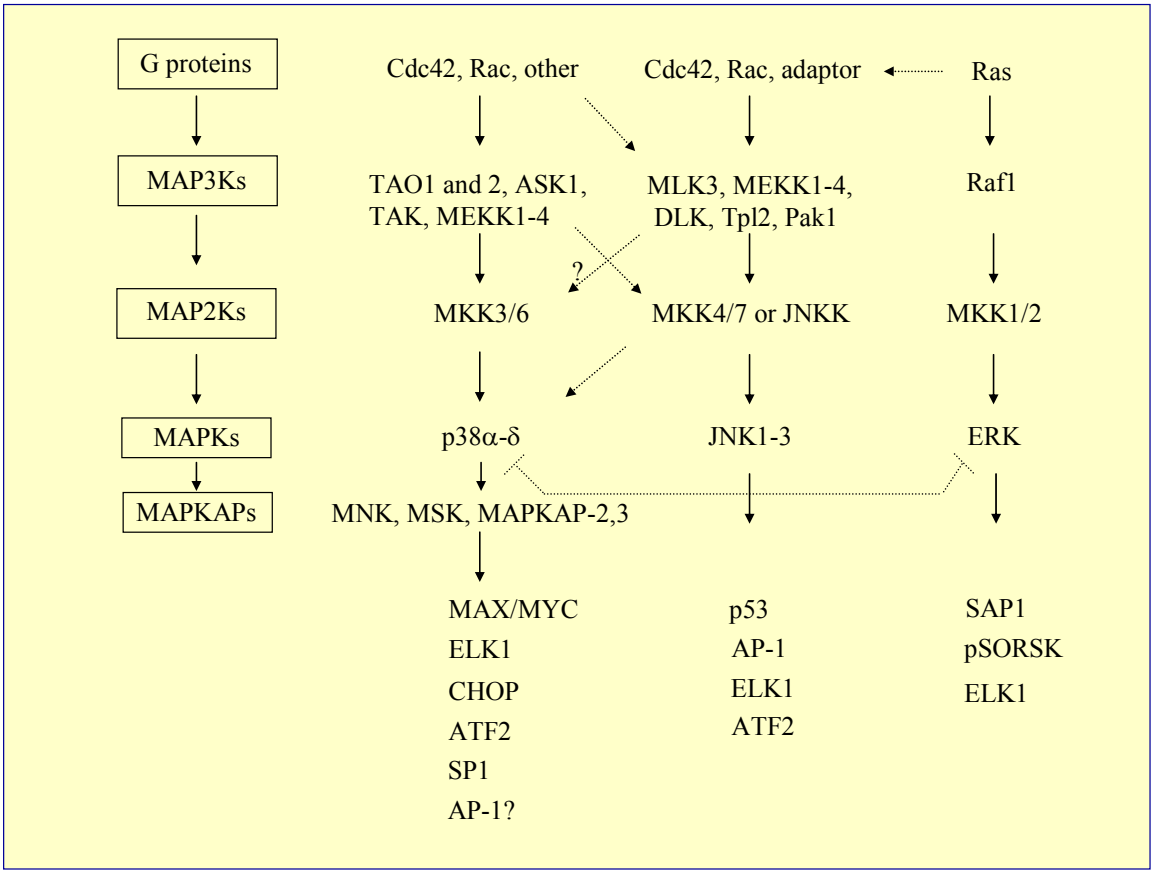

Fig. 1. The complex and interactive mitogen-activated protein kinase (MAPK) pathway. This figure demonstrates the activation pathway and the redundancy involved in transcription factor activation among the various MAPK members. Growth factors and other stimuli activate small G proteins that, in turn, activate a cascade of kinases. Phosphorylated MAPKs are transported into the nucleus and activate transcription factors like SAP1, AP-1. Modified from references (35, 45, 47).

Among all MAPKs, the p38 MAPK signalling pathway appears to play important roles in response of epithelial cells to subcytolytic concentrations of bacterial pore-forming toxins, including *Streptococcus pneumoniae* pneumolysin, *S. aureus* alpha-hemolysin, *Streptococcus pyogenes* streptolysin O (SLO), and *Bacillus anthracis* anthrolysin O (48). Neurotoxicity of *S. pneumoniae* pneumolysin, a major pneumococcal virulence factor, depends on p38 since SB203580, a potent and selective inhibitor of p38 MAPK, rescued human neuronal cells from

pneumolysin-induced death (49). p38 has been demonstrated to enhance the production of tumor necrosis factor alpha (TNF-α) in SLO treated mast cells (50). SLO has also been reported to activate p38 via apoptosis signal regulating kinase 1 (ASK1) and ROS (51). However, p38 MAPK was inhibited in anthrolysin O-attacked macrophages (52).

Response of p38 MAPK to stress

Four members of the p38 MAPK family have been cloned and characterized: p38α (53-55), p38β (p38-2) (56, 57), p38γ (ERK6 or SAPK3) (58), and p38δ (SAPK4) (59, 60). The p38 is in a subgroup of stress-activated protein kinases (SAPKs) within the MAPKs superfamily (35). It is therefore activated by cellular stresses like exposure to heat shock, protein synthesis inhibitors such as anisomycin, free radicals, ionizing radiation, and UV light (61, 62).

Mammalian p38 activation has also been observed in inflammatory responses, as in lipopolyssaccharide (LPS)-treated macrophages (53) or phorbol myristate acetate (PMA)-treated human neutrophils (63, 64). The activation of p38 pathway plays an essential role in: i. production of proinflammatory cytokines such as IL-1β (interleukin 1 beta), TNF-α (tumor necrosis factor alpha), and IL-6 (65); ii. induction of COX-2 (cyclooxygenase-2) (66), which controls connective tissue remodelling; iii. expression of iNOS (inducible nitric oxide synthase) (67, 68); iv. induction of VCAM-1 (vascular cell adhesion molecule-1) (69). The p38 pathway also plays a role in the proliferation and differentiation of cells of the immune system *via* induction of GM-CSF (granulocyte/macrophage colony-stimulating factor), CSF (colony-stimulating factor), and CD40 (70, 71). Several transcription factors have been shown to be activated by p38α such as ATF2 (activating transcription factor 2) (72, 73), ATF3 (74), TGFβ (75), GATA1 (GATA binding protein 1/globin transcription factor1), (76), MafA (v-maf musculoaponeurotic fibrosarcoma

oncogene homolog A (avian)) (77), MEF2 (myocyte-enhancer factor 2) (78) as well as C/EBP(CCAAT/enhancer-binding protein).

Several protein substrates of p38α were identified such as MAPKAPK2 or M2, M3 (or 3pk), MNK1 (MAP kinase interaction protein kinase), PRAK (p38-regulated/activated kinase) which is a stress-activated protein kinase, and MSK (mitogen- and stress-activated kinase) which is a protein that is activated by both stress and mitogens (79). Recently, p38 MAP kinase has been demonstrated to mediate transactivation of EGFR by hyperosmolar concentrations of sorbitol (80) and stress-induced internalization of EGFR (81).

1.3.2 Epidermal growth factor receptor (EGFR) signalling pathway

The EGFR is a member of a receptor tyrosine kinase (RTK) family which are a subgroup of transmembrane proteins with an intrinsic tyrosine kinase activity that determines various cellular functions as growth, differentiation, cell mobility or survival (82). The RTKs consist of four members: EGFR/ErbB1, HER2/ErbB2 (human epidermal growth factor receptor 2), HER3/ErbB3 and HER4/ErbB4 (83). The induction of EGFR can be processed in three ways. First and most commonly, direct stimulation of the EGFR occurs through binding of a ligand to the extracellular receptor domain. EGFR ligands such as EGF, TGFα or HB-EGF (heparin-binding EGF-like growth factor) are synthesized as transmembrane precursors and are proteolytically cleaved by metalloproteases to yield the mature growth factors, which subsequently activate receptors on the same or on adjacent cells (84). Ligand binding induces the formation of homo- or heterodimers which subsequently trigger the autophosphorylation of cytoplasmic tyrosine residues (85-87). These phosphorylated amino acids represent docking sites for a variety of signal transducers with enzymatic activity, such as PLC-γ (phospholipase C-γ), and adapter proteins, such as Shc, Grb2,

Nck, and Dok-R, which couple receptor activation to downstream pathways, calcium metabolism, and protein kinase C (PKC) signalling, transcription and phospholipid turnover (88). Concomitantly, these ligand-EGFR complexes cluster into clathrin coated pits, internalize into early endosomes, and eventually traffic to lysosomes for degradation (89, 90). However, growing evidence has shown that internalized EGF-EGFR complex may maintain its ability to generate cell signaling from endosomes, which can elicit cell survival through generation of antiapoptotic signals and promote cell proliferation (91, 92).

Second, EGFR family can be transactivated by G-protein-coupled receptors (GPCRs) in a ligand-independent pathway. The EGFR and HER2 are critical pathway elements in the signalling from GPCRs, cytokine receptors, membrane-depolarizing or stress-inducing agents, RTKs and integrins to a variety of cellular responses such as MAPK activation, gene transcription and proliferation (88, 93).

Third and recently, the triple membrane-passing signal (TMPS) mechanism of EGFR transactivation has been described with the critical involvement of the EGFR ligand binding domain for EGFR transactivation, as well as the possibility of intercellular transactivation between cocultured cells in a cell-density dependent manner. In the TMPS of the EGFR transactivation, GPCR-induced metalloprotease-mediated proteolytic cleavage of EGF-like growth factor precursors that leads to transactivation of the EGFR. This mechanistic signaling model for ligand-dependent interreceptor communication involves three transmembrane passages and couples GPCR activation to the Ras-MAPK pathway (88). Apart from GPCRs, p38 has also been shown to act upstream of EGFR in sorbitol treated HaCat cells and in stress-stimulated Vero cells (94). In human carcinoma cells, p38 activated the TMPS mechanism of EGFR transactivation, mediated by metalloproteases ADAM9, -10, and -17 (95) (Fig. 2).

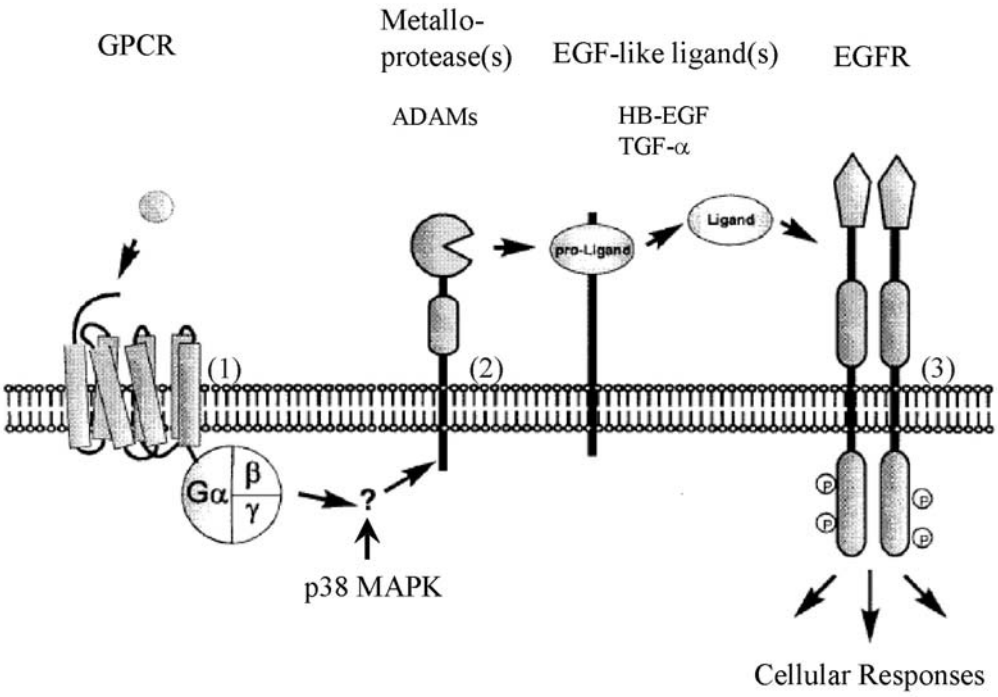

Fig. 2. Triple membrane-passing signal (TMPS) mechanism of EGFR transactivation. GPCR and p38 stimulation (1) lead to metalloprotease-dependent processing of EGF-like ligands (2), which in turn activate the EGFR and downstream signalling cascades (3). The TMPS transactivation involves as key elements pro-HB-EGF, an EGF-like growth factor precursor, and a metalloprotease activity. Modified from references (96).

EGFR transactivation could also be induced by TPA induction of shedding of certain EGFR ligands. This transactivation of the EGFR by TPA was related to the PKC/MAP kinases/AP-1 pathway, leading to TPA-induced tumor promotion (97).

Activating protein 1 (AP-1)

AP-1 is a protein complex composed of three Jun (c-Jun, Jun B, and Jun D) (98-102) and four Fos proteins (c-Fos, Fos B, Fra-1, and Fra-2) (103-107). It plays a key role in normal and abnormal epithelial cell growth and differentiation (108). Homodimerization of Jun proteins or heterodimerization between proteins of the two subfamilies results in AP-1 complexes which interact with a DNA-binding site known as TRE (TPA responsive elements; TPA: 12-O-

tetradecanoylphorbol-13-acetate) (109, 110) that resides within the promoter regions of genes it regulates, including cell cycle-related and AP-1 genes themselves (111, 112). EGFR tyrosine kinase inhibitor could inhibit induction of c-Fos by α-toxin in HaCat cells to promote cell survival (113). The other pathway that also leads to cell survival is the integrated stress response (ISR) (129, 130).

1.4 The integrated stress response

The ISR is the gene expression pathway that modulates protein biosynthesis by integrating various types of unrelated stress signals, which activate specific stress kinases, mediate the phosphorylation of eukaryotic initiation factor 2 at an alpha subunit (p-eIF2α), and thus attenuate translation. At the same time, the ISR also mobilizes stress-induced gene expression involved in cell growth and differentiation (114). It is the pro-survival gene expression program (115) since numerous genes in the ISR such as *GADD34* and *CHOP* promote cell survival and stress resistance (116-118). The ISR is conserved from yeast to mammals. Defects in the ISR are associated with the development of several important disease, including diabetes, Alzheimer disease, and viral infection (119-121).

Although phosphorylation of eIF2α causes overall attenuation of translation, a subset of specific mRNAs is preferentially translated in those conditions. They include transcription factors such as ATF4, which activate genes required for adaptation and survival during stress *e.g.* *Ppp1r15a* (GADD34), *Ddit3* (CHOP), *Herpud1* (Herp), *Hspa5* (BiP), and *Hmox-1* (heme oxygenase-1) (116, 122-125). GADD34 binds to proliferating cell nuclear antigen (PCNA), which is an essential protein for eukaryotic chromosomal DNA replication and repair (126) and is an

accessory protein of DNA polymerase δ (127), allowing essential protein synthesis and preventing programmed cell death (128).

ISR constitutes one arm of a larger coordinated program called the unfolded protein response (UPR) of ER stress (129). During hypoxia, several UPR proteins including BiP (immunoglobulin heavy chain binding protein), stress-inducible nuclear protein CHOP/GADD153, and ORP150 (150 kDa oxygen-regulated protein) are upregulated together with the expression of ATF4. ISR is an important mediator of hypoxia tolerance and tumor growth and this pathway is an attractive target for antitumor therapy. Inactivation of ISR could compromise cell survival and significantly impair tumor growth (130). Phosphorylated eIF2α plays a major role in ISR by attenuating mRNA translation whereas dephosphorylated form is important to initiate translation.

1.4.1 Role of eIF2α in initiation of translation

An early event in the initiation pathway is the association of eIF2 with the Met-tRNAi and GTP (131). This ternary complex can bind to the 40S ribosomal subunit carrying eIF3 complex to produce the 43S preinitiation complex (132, 133). mRNA binding to this complex involves the participation of the trimeric eIF4F complex, comprising the cap-binding protein eIF4E, the scaffold protein eIF4G, and the RNA helicase eIF4A, together with the helicase-stimulatory factor eIF4B (134). Joining of the 60S subunit and hydrolysis of the GTP, catalyzed by eIF5, leads to the formation of the 80S initiation complex which can commence protein synthesis. The GDP formed as a result of GTP hydrolysis remains associated with the eIF2 and is later exchanged for another molecule of GTP by eIF2B (135) (Fig. 3).

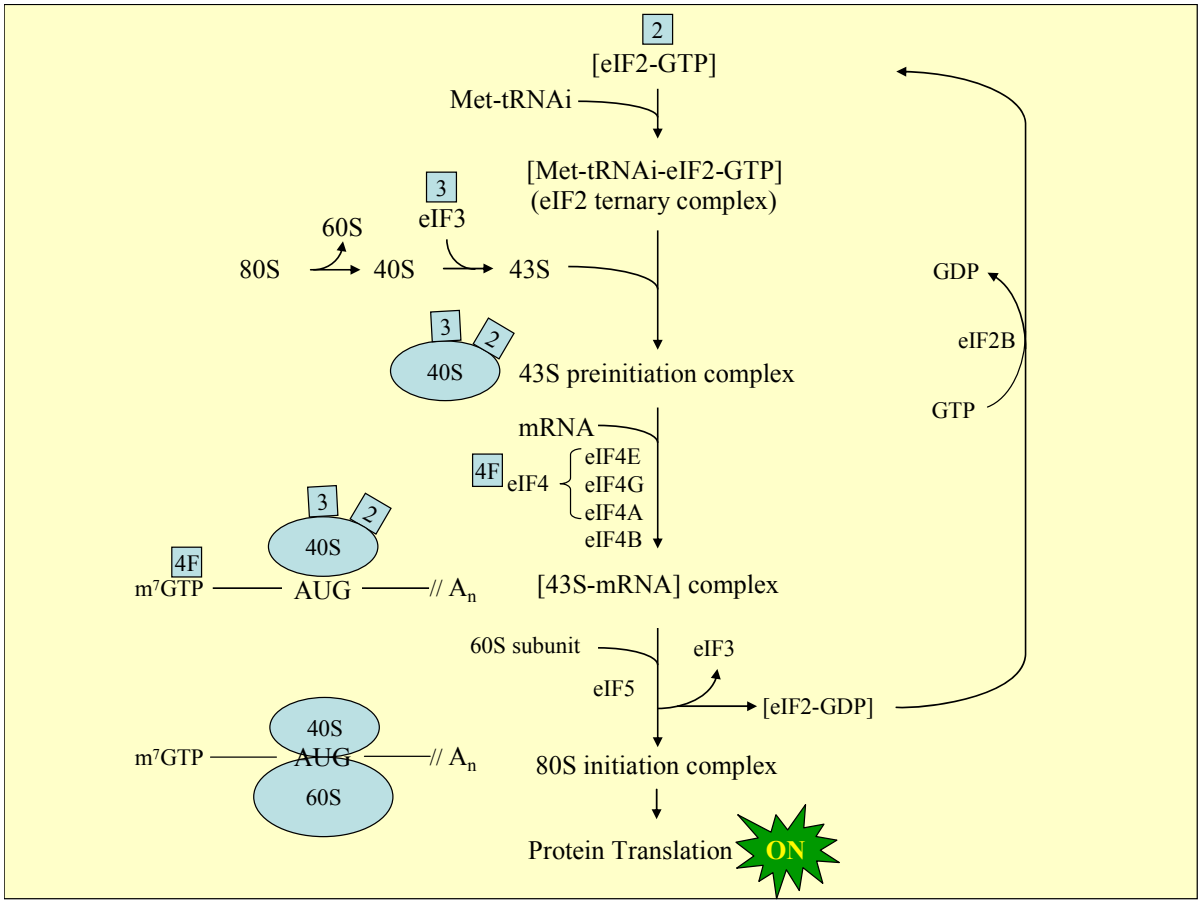

Fig. 3. Initiation of protein translation. Modified from 'Summary of the Initiation of Protein Synthesis' of reference (136).

1.4.2 Phosphorylated eIF2α signaling pathway

Eukaryotic cells recognize and process diverse stress signals that elicit cellular damage or alternatively induce apoptosis. An important contributor to stress adaptation is a family of protein kinases that phosphorylate eIF2α. Four different eIF2 kinases have been identified in mammals, and each contains unique regulatory regions that recognize a different set of stress conditions (137). The eIF2 kinase GCN2/EIF2AK4 (general control non-derepressible-2 or eIF2α kinase 4) is induced during amino acid deprivation (138, 139), UV irradiation and proteasome inhibition (137).

GCN2 is a kinase conserved from yeast to mammals (140). It is activated by uncharged tRNA (141), and couples amino acid availability to translation rates. It is a molecular sensor in $CD8^+$ T cells (142). Additional mammalian eIF2 kinases include i.) PEK/PERK/EIF2AK3 (pancreatic eIF2α kinase or PKR-like ER kinase or eIF2α kinase 3), which is activated in response to misfolded or unfolded proteins in the endoplasmic reticulum or ER stress (143), ii.) PKR (double-stranded RNA-dependent protein kinase) which participates in an anti-viral defence mechanism that is mediated by interferon (144), and iii.) HRI/EIF2AK1 (heme-regulated inhibitor) which balances heme availability with globin synthesis (114) and is activated by heme deprivation, oxidative stress, and heat stress in erythroid tissues (145) (Fig. 4).

Phosphorylated eIF2α has GTPase activity. That modification alters the capacity of eIF2α to be recharged by the nucleotide–exchange factor eIF2B by stabilizing the eIF2-GDP-eIF2B complex, inhibiting the turnover of eIF2B and impeding recycling of eIF2 to its active GTP-bound form. The reduction of eIF2-GTP reduces global translation, allowing cells to conserve resources and to initiate a reconfiguration of gene expression to effectively manage stress conditions (137).

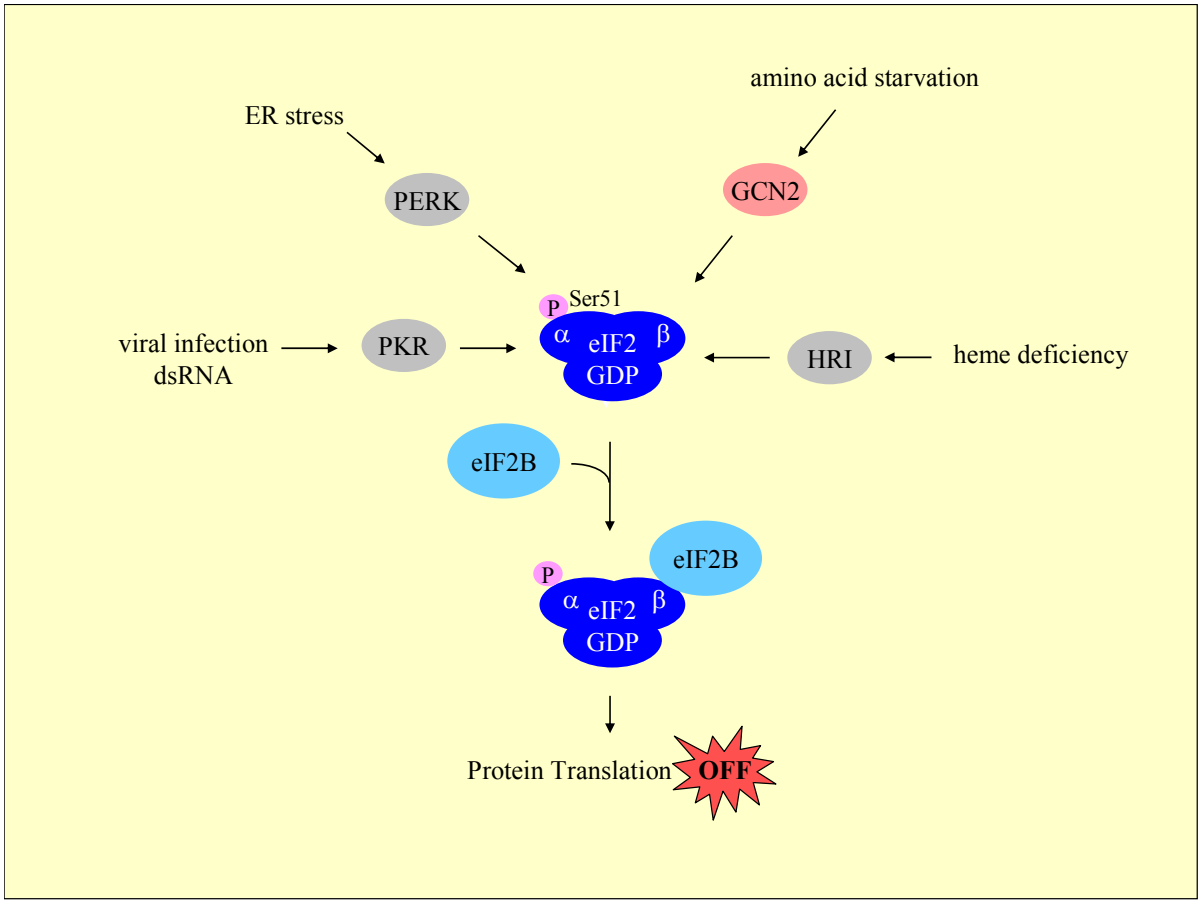

Fig. 4. Phosphorylated eIF2α signaling pathway. Modified from eIF2alpha signaling pathway: Cell Signaling Technology, Inc.

2. AIM OF THE PRESENT STUDY

Based on previous studies of the group, it was known that keratinocyte HaCat cells can survive an attack by α-toxin and mount a transcriptional response. However, few regulated transcripts had been characterized so far, and therefore the first goal of the present study was to identify a larger number of transcripts that are expressed at different levels in perforated *vs.* normal cells. It was anticipated that the studies on transcriptional changes followed by translational modulations would generate clues on the cellular reactions needed to cope with toxin-attack. They led to identification of a pathway that may be of relevance for cellular survival and discovered a novel, dual role of p38 MAPK in the control of protein synthesis in these cells.

3. MATERIALS AND METHODS

3.1 Cell culture and reagents

3.1.1 Cell culture and reagents

The keratinocyte cell line HaCat is derived from non-virally transformed human keratinocytes that have retained the capacity to differentiate (146); it was kindly provided by Dr. N. Fusenig [Deutsches Krebsforchungsinstitut (DKFZ), Heidelberg, Germany]. Cells were cultured in D-MEM:F-12 (1:1) plus GlutaMAX I (Gibco/Invitrogen) supplemented with 10% foetal bovine serum (FBS) (Gibco/Invitrogen) and 100 units/mL penicillin, and 100 µg/mL streptomycin (Gibco/Invitrogen). If not otherwise stated, cells were detached by trypsinization, counted and seeded in tissue culture plates (Nunc) of various formats, 24 h prior to application of the various treatment protocols, so that at the time of treatment the cell density had reached *ca.* 80%.

3.1.2 α-Toxin and antibodies

α-Toxin and α-toxin H35R mutant, a single amino acid exchange mutant that binds to cells without forming pores, were prepared and the hemolytic activity was measured as described previously (147).

Rabbit polyclonal antibodies against GCN2 (Cat. No. 3302) and phosphorylated eIF2α (p-eIF2α) at serine 51 (Cat. No.9721S) were purchased from Cell Signaling Technology. Rabbit polyclonal antibodies against eIF2α (Cat. No.sc-11386), PERK (Cat. No.sc-13073), and phosphorylated PERK (p-PERK) at threonine 981 (Cat. No.sc-32577-R) were from Santa Cruz

Biotechnology. Horseradish peroxidase (HRP)-conjugated anti-rabbit IgG (Cat. No.7074) was from Cell Signaling Technology.

3.1.3 Enzymes and markers

Recombinant DNaseI (RNase-free) (Cat. No.2235), SuperTaq (Cat. No. 2052), and M-MLV Reverse Transcriptase (Cat. No. 2044) were purchased from Ambion.

SuperSriptII Reverse Transcriptase (Cat. No. 18064-022) and Magic Mark XP Western Standard (220, 120, 100, 80, 60, 50, 40, 30, 20 kDa; Cat. No. LC5602) were from Invitrogen. One hundred basepair DNA ladder (100, 200, 300, 400, 500/517, 600, 700, 800, 900, 1000, 1200, 1517 bp; Cat. No. N3231L) was from New England Biolabs.

3.1.4 Chemicals

Microarray hybridization solution (salted based) (Cat. No. 1180-200000) was from MWG Biotech. SB203580 in solution (Cat. No.559398) and taotomycetin (Cat. No.580550) were purchased from Calbiochem/Merck KGaA. RNaseOUT recombinant ribonuclease inhibitor (Cat. No.10777-019) was from Invitrogen. Random decamers (Cat. No.5722G) were from Ambion. Cy3-ester (Cat. No. PA23001), Cy5-ester (Cat. No. PA25001), $pd(T)_{12\text{-}18}$ (Cat. No. 27-7858-01), Redivue L-[^{35}S] methionine (Cat.No.AG1094) were from Amersham Biosciences. aa-dUTP: 5-(3-aminoallyl(-2'-deoxyuridine 5'-triphosphate)) (Cat. No. A0410) was from Sigma-Aldrich.

3.2 Kits

PanHuman Starter Array (Cat. No. 2170-000000) was purchased from MWG Biotech. Human MMP-9 Primer Set (Cat. No. SP-10518) was from Maxim Biotech. Human MMP-9

Quantikine ELISA Kit (Cat. No. DMP900) was from R&D Systems. TransAM™ AP-1 Family Kit (Cat. No. 44296) and a Nuclear Extract Kit (Cat .No. 40010) were from Active Motif Europe. RNeasy Mini Kit (Cat. No. 74104), RNeasy Midi Kit (Cat. No.75144), RNase-Free DNase set (Cat. No.79254), QIAshredder Kit (Cat. No.79654), and QIAquick PCR Purification Kit (Cat. No.28104) were from Qiagen.

Human c-fos Relative RT-PCR Kit (Cat. No.5303), DNA-*free* Kit (Cat. No.1906), and QuantumRNA Classic 18S Internal Standard (Cat. No.1716) were from Ambion. One hundred mM dNTP set (Cat. No.27-2035-01) was from Amersham Biosciences.

Light Cycler TaqMan Master Kit (Cat. No. 0453 528 6001), Human Universal Probe Library Set (Cat. No. 0468 363 3001), ATP Bioluminescence Assay CLS II Kit (Cat. No. 1 699 695), and BM Chemiluminescence Blotting Substrate (POD) (Cat. No. 11 500 708 011) were from Roche.

Manufacturers:

Ambion (Europe), Cambridgeshire, UK
Amersham Biosciences/GE Healthcare Europe, Munich
Cell Signaling Technology, Frankfurt am Main
Invitrogen, Karlsruhe
Maxim Biotech/Biozol Diagnostica Vertrieb, Eching
Merck KGaA, Darmstadt
MWG Biotech, Ebersberg
New England Biolabs, Frankfurt am Main
Nunc, Wiesbaden
Qiagen, Hilden
R&D Systems, Wiesbaden-Nordenstadt
Roche, Mannheim
Santa Cruz Biotech, Heidelberg
Sigma-Aldrich Chemie, Munich

3.3 Primers

3.3.1 PCR primers

PCR primers were ordered from MWG Biotech. Sequences of PCR primers, length of PCR products, optimal annealing temperatures, and PCR cycles in RT-PCR study are shown in Table 2.

Table 2. Sequences of PCR primers, lengths of PCR products (amplicons), optimal annealing temperatures, and PCR cycles in RT-PCR study

Genes	Primers	Amplicons (bp)	Annealing temp (^{o}C)	Cycles
blvrb	fwd : aat gac ctc agt ccc acg ac rev : cgg atg tgg tca tca gtc ac	167	50	25
c-fos	fwd : atc gca gac cag agc cct ca rev : ggg atc ttg cag gca ggt cgg t	360	64	23
c-jun	fwd : ccc caa gat cct gaa aca ga rev : ccg ttg ctg gac tgg att at	168	55	25
egr-1	fwd : tcc ccg gtt gct acc tct ta rev : cct ggg aga aaa ggt tgc tg	285	55	25
ppp1r15a (GADD34)	fwd : gag gag gct gaa gac agt gg rev : aat tga ctt ccc tgc cct ct	161	50	25
mmp9	fwd : gaa gat gct gct gtt cag cg rev : act tgg tcc acc tgg ttc aa	216	68	30
Nurr77	fwd : cac cca ctt ctc cac acc tt rev : act tgg cgt ttt tct gca ct	201	55	28
rps3a	fwd : ccg gaa gaa gat gat gga aa rev : caa act tgg gct tct tca gc	179	55	25
ssat	fwd : ccg tgg att ggc aag tta tt rev : tcc aac cct ctt cac tgg ac	217	55	25

Note: fwd, rev, bp, temp represent forward primer(s), reverse primer(s), basepair(s), and temperature(s), respectively.

3.3.2 Real-time PCR primers

Real-time PCR primers were ordered from MWG Biotech. Sequences of primers, Universal Probe Library numbers, and length of PCR products in real-time PCR study are shown in Table 3.

Table 3. Sequences of PCR primers, Universal Probe Library numbers (UPL No.), and length of PCR products in real-time RT-PCR study

Genes	Primers	UPL No.	Amplicons (bp)
HPRT1	fwd : tga cct tga ttt att ttg cat acc rev : cga gca aga cgt tca gtc ct	73	102
GADD34	fwd : gct tct ggc aga ccg aac rev : gta gcc tga tgg ggt gct t	28	99

3.4 ATP- measurements

HaCat cells were seeded at a density of 3 x 10^4 per well into 96-well tissue culture plates. Cells were loaded with 500 ng/ml α-toxin at 4°C for 40 min and subsequently cultured at 37°C. In the tautomycetin (TC)-treated condition, cells were pretreated with 5 μM TC at 37°C for 1 h prior to toxin treatment, and TC was presented throughout the experiment. Cellular ATP (% of untreated controls) was determined at 0, 1, 2, 6, 24 h after 40 min-toxin treatment with the ATP Bioluminescence Assay Kit CLS II (Roche), using a Lumat 9705 instrument (Berthold Technologies, Bad Wildbad).

3.5 Microarray

3.5.1 Array design.

The PanHuman Starter Array consists of an array of oligonucleotide probes covering 161 human genes, 32 replicas, and 7 arabidopsis controls; each oligo is spotted as duplicate. For a complete list of genes present in this array, see http://ecom2.mwgdna.com/download/arrays/starter_arrays/gene_id/html/gene_id_starterkit_human.html.

3.5.2 RNA isolation

HaCat cells were seeded at a density of 5 x 10^6 per flask into T75 flasks. Toxin treatment was performed 2 d later. Cells were treated with 0.2 µg/ml wild-type or H35R mutant α-toxin at 37°C. After 2 h, medium was changed. Cells were trypsinized at 2, 8, and 24 h after the beginning of toxin treatment. Total RNA was isolated using the RNeasy Midi Kit as recommended by the supplier. The remaining of genomic DNA was eliminated by RNase-Free DNase I treatment during the isolation as described by the manufacturer.

3.5.3 Aminoallyl labelling

First-Strand cDNA was synthesized according to the protocol from the Institute for Genomic Research (TIGR) with some modifications. Twenty µg of total RNA was combined with 2 µg $pd(T)_{12-18}$. The mixture was heated to 70°C for 10 min and quick-chilled on ice. Reverse transcription was performed at 42°C for 3 h after the addition of 10 mM DTT, 0.5 mM each dATP, dCTP, dGTP, 0.3 mM dTTP, 0.2 mM aa-dUTP, 40 U RNaseOUT recombinant ribonuclease inhibitor, and 200 U Superscript™ II. After that RNA was hydrolyzed with 200 mM NaOH and 100 mM EDTA at 65°C for 15 min prior to the addition of HCl to neutralize pH. The experiment was performed in quadruplicate. Unincorporated aa-dUTP and free amines were removed by QIAquick PCR Purification Kit as recommended by the supplier except the phosphate wash buffer (5 mM KPO_4, pH 8.0 in 80% EtOH) and phosphate elution buffer (4 mM KPO_4) were substituted for the Qiagen supplied buffers because the Qiagen buffers contain free amines which compete with the Cy dye coupling reaction. The aminoallyl-labeled cDNA (aa-cDNA) was dried and resuspended in 4.5 µl of freshly prepared 0.1 M Na_2CO_3, pH 9.0. The following steps were performed in the dark in order to prevent photobleaching of the Cy dyes. Each aa-cDNA from

wild-type or H35R mutant α-toxin treatment was coupled to 4.5 µl NHS ester Cy3 or Cy5 dye in DMSO at room temperature for 1 h. Any uncoupled Cy dye was quenched with 2.5 M hydroxylamine for 15 min. The uncoupled dye was then removed, using Qiagen QIAquick PCR Purification Kit as described by the manufacturer except 5x reaction volume of Buffer PB was used in the first step and dH_2O was used to elute sample instead of Buffer EB.

The labelling reaction was analysed at an optical density (O.D) at 260 nm for cDNA and either 550 nm for Cy3 or 650 nm for Cy5, as appropriate. The total picomoles of cDNA synthesized were calculated using the following formula:

$$\text{pmol nucleotides} = \frac{O.D_{260} \times \text{volume (µl)} \times 37\ \text{ng/µl} \times 1000\ \text{pg/ng}}{324.5\ \text{pg/mol}}$$

Note: One OD_{260} unit of single-stranded DNA = 37 µg/ml

Average molar mass of dNTP = 324.5

The total picomoles of dye incorporation (Cy3 and Cy5 accordingly) was calculated using:

$$\text{pmol Cy3} = \frac{O.D_{550} \times \text{volume (µl)}}{0.15}$$

$$\text{pmol Cy5} = \frac{O.D_{650} \times \text{volume (µl)}}{0.25}$$

$$\text{nucleotides/dye ratio} = \frac{\text{pmol cDNA}}{\text{pmol Cy dye}}$$

Note: Extinction coefficient of Cy3 = 150,000 $M^{-1}cm^{-1}$ at 550 nm

Extinction coefficient of Cy5 = 250,000 $M^{-1}cm^{-1}$ at 650 nm

Samples with the dye incorporation of more than 200 pmol and a ratio of less than 50 nucleotides/dye molecules, which is optimal for hybridizations, were considered for the next steps of experiments. Subsequently, the two differentially labelled probes (Cy3 *vs.* Cy5), which would be hybridized to the same microarray slide, were combined and completely dried in a speed vac.

3.5.4 cDNA array hybridization

PanHuman Starter Array was hybridized to aminoallyl-labeled cDNA probes. The hybridizations were performed according to the manufacturer's instructions. The probes were incubated with 120 µl hybridization solution (salted based) at 95^{o}C for 3 min. The spots on array were located by Microarray Gene Frames (MWG Biotech). The probe mixture was added to the array slide in a hybridization chamber (MWG Biotech) within the Microarray Gene Frame and a coverslip was laid over the array. The chamber was covered with aluminium foil and incubated in a water bath at 42^{o}C for 24 h. To wash an array slide, it was plunged 4-5 times in 37^{o}C prewarmed low (2x SSC and 0.1% SDS: sodium dodecyl sulfate), medium (1x SSC), and high (0.5x SSC) stringency wash buffers, respectively. The slide was briefly centrifuged. Microarray images were visualized by using an Affymetrix 428 Array Scanner (MWG Biotech). The resulting fluorescence was measured after excitation at two different wavelengths: 532 nm (green laser) and 635 nm (red laser).

3.5.5 Microarray data analysis

The array images were overlaid and quantified by using the ImaGene software version 5.5 (Biodiscovery, El Segundo, CA, USA). For these analyses, local background for each spot was corrected, and signals lower than 50 were flagged and eliminated.

After red and green foreground (R*f* and G*f*, respectively) and background intensities (R*b* and G*b*, respectively) for each spot were obtained, they were analyzed by R Software version 2.2.1 of the R Foundation for Statistical Computing (Vienna, Austria) to select differentially expressed genes. The background-corrected intensities are G and R where usually G = G*f* – G*b* and R = R*f* – R*b*. The log-differential expression ratio is M = $\log_2$ G/R for each spot. The log-intensity of the

spot is A = ½ $\log_2$ RG, a measure of the overall brightness of the spot. (The letter M is a mnemonic for *minus* as M = log G – log R while A is a mnemonic for *add* as A = (log R + log G)/2). Base-2 logarithms were used for M and A calculation so that M refers to units of 2-fold change of expression and A is in units of 2-fold increase in brightness. On this scale, M = 0 repersents equal expression, M = 1 represents a 2-fold change between the RNA samples, M = 2 represents a 4-fold change, and so on. Any negative values of R and G were excluded from any analysis on the logarithmic scale (148).

MA plots (149) was used to show the intensity-dependant ratio of raw microarray data. The plots differ in the axes used. The MA plot uses M as the y-axis and A as the x-axis. The M-A data was normalized by the global lowess method, which is a nonlinear regression of M against the average A. The method is based on overlaping windows that slide from the beginning to the end of intensity range across the data. In these windows, It computes local linear regressions that are joined together to form a smooth lowess regression curve. This normalization takes into account intensity artefacts. The lowess normalization procedure subtracts a lowess regression curve from the data to linearize it. The curve itself is calculated by a regression process, which essentially calculates the dependence of the ratio on the intensity and puts it in a mathematical (as supposed to a graphical plot) context.

Fold differences >1.6 were considered. Genes demonstrating variable pattern in three independent experiments and genes that showed weak intensity were excluded from the analyses.

3.6 RT-PCR

Except total RNA that was also used in microarray experiment, RNA was extracted from HaCat cells, seeded at a density of 7 x 10^5 per well into 6-well plates. Cells were loaded with 100

ng/ml wild-type or H35R mutant α-toxin at 37°C and were collected at indicated time points with the change of medium after 2 h. Cells were trypsinized or lyzed *in situ* and total RNA was isolated using the RNeasy Mini Kit as recommended by the supplier. Genomic DNA was eliminated by DNA-*free* Kit treatment after the isolation as described by the manufacturer.

First-Strand cDNA was synthesized according to the protocol from Ambion. Two µg of total RNA was combined with 5 µM random decamers and 0.5 mM of each dATP, dCTP, dGTP, dTTP (dNTPs). The mixture was heated to 85°C for 3 min and quick-chilled on ice. Reverse transcription was performed at 42°C for 1 h after the addition of 10 U RNaseOUT recombinant ribonuclease inhibitor, and 100 U M-MLV reverse transcriptase.

For the design of the primers, gene sequences were searched in the NCBI Entrez search system. Primer sequences were designed using Primer3 Program (http://frodo.wi.mit.edu/cgi-bin/primer3/primer3_www.cgi). The sequences of the primers are shown in Table 2. The primers of *c-fos* and *mmp-9* genes were from Human *c-fos* Relative RT-PCR Kit and Human MMP-9 Primer Set, respectively. If not indicated otherwise, each PCR was performed in a 50-µl reaction mixture containing 100 ng cDNA, 0.2 mM of each dNTPs, 0.2 µM forward and reverse primers, and 1.25 U SuperTaq DNA polymerase (Ambion). The final concentration of Mg^{2++} was 1.5 mM. To obtain meaningful results, all PCR products were determined for a linear range of cycles, which is a period of the PCR in which the amplification efficiency is at its maximum and remains constant over a number of cycles. The PCR would remain in the linear range for only a limited number of cycles. In order to obtain the linear range, the PCR mixture was split into 4-5 aliquots and was subjected to PCR. Aliquots were then removed every 3-5 cycles, starting with cycle 20, ending with cycle 30-35 and the cycle number in the middle of the linear range was selected for further experiments.

The hot start PCR reaction was run in a 94^{o}C preheat thermal cycler (Master Cycler, Eppendorf, Hamburg, Germany) for 20-35 cycles of 45 s denaturation at 95^{o}C, 45 s annealing at the optimal annealing temperature (Table 2.), and 45 s extension at 72^{o}C, and then cooling at 4^{o}C. Amplification without template was performed as a negative PCR control. Amplified DNA was run on a 1% agarose gel (Carl Roth, Karlsruhe, Germany) and visualized with ethidium bromide for size verification.

3.6.1 Duplex Relative RT-PCR Analysis

Genes of interest were coamplified with ribosomal 18S RNA (amplicon 489 bp) for selected cycles, under conditions described above. The optimal ratio of 18S primers:competimers for each RT-PCR primer pair was determined. The ratio in which the level of 18S product was most similar in either wild-type or H35R mutant α-toxin-treated samples was selected. For most of the genes, duplex PCR was proceeded at ratio between 1:9 to 4:6 of 18S primers:competimers, as proposed by the manufacturer. Since the amount of 18S rRNA is abundant in cells, the 18S RNA competimers were used to reduce 18S RNA amplification signal and modulate the amplification efficiency of a PCR template without affecting the performance of other targets in a duplex PCR. The competimers are identical to 18S RNA primers, but are modified at their 3' end to block extension of DNA polymerase. Mixing 18S RNA primers with increasing amounts of 18S RNA competimers allowed a decrease of amplification efficiency of 18S RNA template without loss of relative quantitation.

3.7 Western blots

Subconfluent cell monolayers grown in 6-well plates were washed once in PBS (0.8% (w/v) NaCl, 0.02% (w/v) KCl, 0.144% (w/v) $Na_2HPO_4.7H_2O$ and 0.024% (w/v) KH_2PO_4, pH 7.4) and solubilized *in situ* by the addition of 80 µl of 2x SDS-loading buffer (10%(v/v) glycerin, 5%(v/v) 2-ME, 2%(w/v) SDS, and bromophenol blue); lysates were transferred to Eppendorf tubes and incubated at 95°C for 5 min and were separated by 7.5% SDS-PAGE at 20 mA per gel until the dye front was closed to the bottom. Separated proteins were transferred to nitrocellulose membranes (Schleicher & Schuell, Dassel, Germany) by semi-dry blotting, using Trans-Blot SD Transfer Cell (Bio-Rad Laboratories, Munich, Germany) at 100 mA in transfer buffer (48 mM Tris, 39 mM Glycine, 0.0375% (w/v) SDS, and 20% methanol) for 1 h. The membranes were stained with Ponceau S (0.5% (w/v) Ponceau S in 1% acetic acid). Non-specific binding sites were blocked by 5% (w/v) dry milk powder in TBST (50 mM Tris, 150 mM NaCl and 0.1% (v/v) Tween-20, pH 7.5). After 1 h, the blots were incubated with primary antibody (diluted 1:1000 to 1:5000 in 5% BSA in TBST) with shaking for 4 h at room temperature or at 4°C overnight. Unbound reagents were removed and background was reduced by three washing steps of 10 min each in TBST with shaking. Subsequently, anti-rabbit IgG-horseradish peroxidase (HRP) conjugate (Cell Signaling Technology) (diluted 1:2,000 - 1:10,000 in blocking buffer) was added to detect bound proteins of interest. After 1 h of incubation at room temperature, the membranes were repeatedly washed three times and the bound HRP conjugates were developed by a BM Chemiluminescence Blotting Substrate Kit and exposed to X-ray film for 1 to 30 min.

Bound antibodies were stripped off membranes after the first round of detection by incubating membranes at 50°C for 30 min in 10 mM Tris-HCl, 100 mM NaCl, 2% (w/v) SDS,

5mM beta-ME, pH 7.4 on a shaker. Membranes were washed three times prior to being blocked again and processed for the second round of development.

All Western blot experiments were repeated at least once, and representative data are depicted.

3.8 Metabolic Labeling of Cells.

HaCat cells were seeded at a density of 3.5 x 10^5 cells per well into 6-well plates. Cells were treated with 100 ng/ml toxin in DMEM plus 10% FBS for 1 h and were starved in DMEM lacking methionine (Gibco Invitrogen, Cat. No. 31966-021) supplemented with 10% dialyzed FBS. After 15 min, cells were pulse-labeled with Redivue L-[^{35}S] methionine at a concentration of 10 μCi/well for 30 min., and washed twice with ice-cold PBS plus 1 mM EDTA. Cells were harvested or reincubated for 3 h in unlabelled medium. In order to collect cells, samples were scraped off and lysed in a radio-immunopreicipitation assay (RIPA) buffer (50 mM Tris-HCl, pH 8.0, 150 mM NaCl, 1.0% Igepal CA-630 (NP-40), 0.5% sodium deoxycholate, and 0.1% SDS). Radiolabeled proteins were separated by 12.5% SDS-PAGE at 150 mA for 1 h 10 min and visualized by autoradiography.

3.9 Real-time PCR

Gene quantification was performed with a Light Cycle 24 (Roche Applied Science, Mannheim, Germany). Primers were designed from GenBank sequences (http://www.ncbi.nlm.nih.gov/) with the aid of Universal Probe Library Assay Design Center (https://www.roche-applied-science.com/sis/rtpcr/upl/adc.jsp) of Roche Applied Science. The

sequences of the primers are shown in Table 3. Each PCR was performed in a 20-µl reaction mixture containing 0.1 µM Universal Probe Library probe, Ready-to-use hot start PCR reaction mix (reaction buffer, $MgCl_2$, and dNTP mix), and 1 U FastStart Taq DNA polymerase (LightCycler TaqMan Master Kit). The final concentrations of primers and Mg^{2++} were 0.2 µM and 3.5 mM, respectively. The thermal cycling conditions were as follows: pre-incubation for 10 min at 95°C, followed by 45 amplification cycles of 10 s denaturation at 95°C, 30 s annealing at 60°C, and 1 s extension at 72°C, and then cooling for 30 s at 40°C. Data collection was performed during each extension phase. A negative control (10 mM Tris-HCl, pH 8.5) was included in each run.

Relative quantification

The relative expression ratios were calculated by a mathematical model. The crossing point (CP) values used were provided from real-time PCR instrumentation. The fold change in expression of the *GADD34* gene in cells treated with wild-type α-toxin ± SB203580 was normalized to an endogenous reference gene *HPRT1* and relative to the untreated control at various time points. Real-time PCR was performed on the corresponding cDNA synthesized using a mathematical delta-delta method (150), where $\Delta\Delta CP = (CP_{GADD34} - CP_{HPRT1})_{treatment} - (CP_{GADD34} - CP_{HPRT1})_{control}$. The treatment group represented samples treated with wild-type α-toxin ± SB203580 and the control group represented the samples of untreated cells. Two independent experiments were performed. For the untreated control sample, ΔΔCP equals zero and 2^0 equals one, so that the fold change in gene expression relative to the untreated control equals one, by definition. For the treated samples, evaluation of $2^{-\Delta\Delta CP}$ indicates the fold change in gene expression relative to the untreated control.

Another mathematical model that was used to calculate the relative expression ratios was efficiency calibrated method, included an efficiency correction for real-time PCR efficiency of the individual transcripts (151), as follows:

$$\text{Ratio} = \frac{(E_{\text{target}})^{\Delta \text{CP } \textit{GADD34} \text{ (control – sample)}}}{(E_{\text{ref}})^{\Delta \text{CP } \textit{HPRT1} \text{ (control – sample)}}}$$

The relative expression ratio of a target gene was computed based on its real-time PCR efficiencies (E) and the crossing point difference (ΔCP) for a treated sample versus a control. Under the optimal and identical real-time amplification condition that $E_{\text{target}} = E_{\text{ref}} = 2$, the delta-delta mathematic method (ratio = $2^{-\Delta\Delta CP}$) would be applicable. However, since good E values could be varied from 1.85 – 2.05 (Dr.Dierk Evers, Roche Diagnostics - personal communication), E = 1.85 and 2.05 was used in the Equation above in order to find the range of possible ratio.

3.10 Nuclear extract

Nuclear protein extracts were obtained from HaCat treated with α-toxin and untreated cells by using the Nuclear Extract Kit according to the manufacturer's instruction. The entire procedure was performed at 4°C. Briefly, cells in 145-mm plates were washed with ice-cold PBS/phosphatase inhibitors, subsequently scraped, and centrifuged at 300 x g for 5 min. The pellet containing nuclei was resuspended in 1x hypotonic buffer. After 15 min incubation, the suspension was briefly vigorously vortexed and centrifuged at 14,000 x g for 30 s. The supernatant (cytoplasmic fraction) was kept at –70°C. The nuclear pellet was resuspended in 1x complete lysis buffer (Nuclear Extract Kit). The suspension was incubated for 30 min on a rocking platform, set at 150 rpm, and vortexed prior to centrifugation at 14,000 x g for 10 min. Finally, the supernatant, containing nuclear fraction, was collected, aliquoted, and stored at –70°C.

3.11 AP-1 binding assay

c-Fos and phosphorylated c-Jun (p-c-Jun) DNA-binding activites were measured using the TransAM™ AP-1 Family Kit according to the manufacturer's instruction. Briefly, twenty μg of nuclear protein samples were incubated for 1 h in a 96-well plate coated with an oligonucleotide that contains a TRE (5'-TGAGTCA-3'), to which c-Fos or p-c-Jun in nuclear extracts specifically binds. After washing, c-Fos (1:1000 dilution) or p-c-Jun antibodies (1:500 dilution) were added to the plates and were incubated for 1 h. Subsequently, a secondary HRP-conjugated antibody (1:1000 dilution) was added to detect bound proteins. Following 1 h incubation, specific binding was detected by colorimetric estimation at 450 nm with a reference wavelength of 655 nm.

3.12 MMP 9 ELISA

Aliquots of supernatants of cells treated with α-toxin and untreated cells were stored at -20°C. Pro and/or active MMP-9 were measured using the Human MMP-9 Quantikine ELISA Kit as described in the manufacturer's protocol. This assay employs the quantitative sandwich enzyme immunoassay technique. Briefly, supernatant samples were incubated for 2 h in a 96-well plate coated with a monoclonal antibody specific for MMP-9. After washing, a MMP-9 conjugated enzyme polyclonal antibody was added to these wells and incubated for 1 h. Specific binding was detected by colorimetric estimation at 450 nm with a reference wavelength of 540 nm.

4. RESULTS

4.1 Transient depletion of ATP levels in HaCat cells induced by low concentrations of α-toxin.

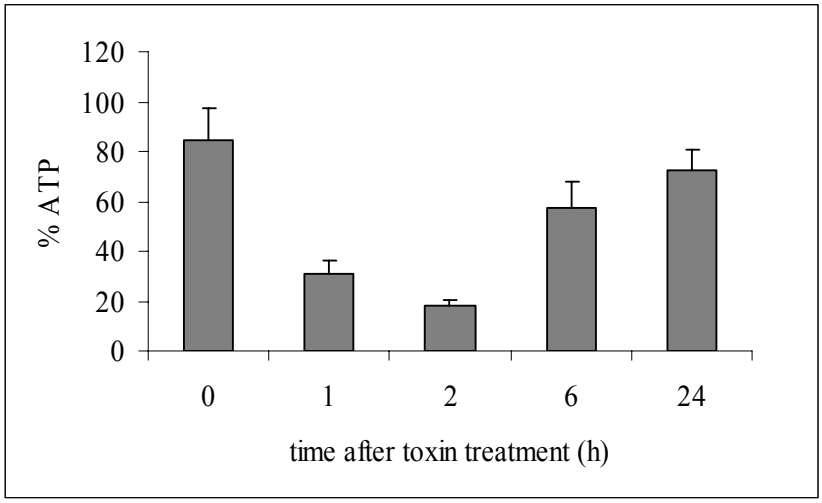

Fig. 5. Transient drop of cellular ATP levels after α-toxin treatment. Cellular ATP (% of untreated control) was determined at various time points after cells were treated with 500 ng/ml α-toxin at 4°C for 40 min and subsequently cultured at 37°C for 0, 1, 2, 6, and 24 h. The results of the indicated time points are from three independent experiments, each performed in quadruplicate; means ± SD are shown.

HaCat cells were treated with α-toxin, leading to the transient drop of ATP levels. The result showed recovery of cells from toxin treatment, which recapitulated the work of Husmann et al., 2006 (51). ATP levels were at 85(± 12)% at 0 h and dropped to 31(± 6)% and 18(± 2)% at 1 and 2 h, respectively. However, cells treated with α-toxin were able to replenish their ATP-stores to 57(± 11)% and 73(± 8)% at 6 and 24 h, respectively (Fig. 5).

4.2 Transcription profile screening by microarray

Previous work had shown that cell recovery was accompanied by the activation of NF-κB-dependent transcription of genes, which led to *de novo* synthesis of cytokines in the target cells (152). Subsequently, an unbiased screen of transcripts was performed using SAGE and the data indicated that α-toxin provoked a comprehensive change in the transcriptome of toxin-treated cells.

In the present work, a microarray was employed to i.) explore the cheaper approach to analyzing transcriptome changes, and ii.) establish this technique in the lab. MWG PanHuman Starter Array with 161 genes was chosen for a set of pilot experiments. Microarray analysis again demonstrated up- and downregulation of genes in cells temporarily treated with wild-type and H35R mutant α-toxin for 2 h and 24 h. MA-plots were used to display the intensity-dependent ratio of microarray data before and after normalization (Fig. 6). M as the y-axis represents differential expression ratio and A as the x-axis represents overall brightness of the spot.

As shown in Table 4, more than 30 genes were found differentially expressed with at least a 1.6 fold change in mRNA levels. Mean values of both up- and downregulated genes, which were shown at least in three independent experiments, were identified. Interestingly, contrary to *c-myc* gene, *mig* gene was shown to be upregulated at 2 h but downregulated at 24 h. The finding of differential gene expression of certain genes at different time points ensured the validity of array results.

However, due to the low depth of sampling, only a few genes on the PanHuman Starter Array slide overlapped with the previous SAGE data (*e.g. c-fos*). As a next step, genes were chosen from SAGE and array data for confirmation by RT-PCR.

Table 4. List of genes found to be differentially regulated in cells treated with wild-type relative to H35R mutant toxins in microarray analysis.

Gene names	Accession no.	Fold regulation
1. Genes that were upregulated at 2 h		
mig (monokine induced by gamma interferon)	NM_002416	2.66
csk (C-terminal src tyrosine kinase)	NM_004383	2.51
polB ((beta polymerase (DNA directed))	NM_002690	2.18
c-fos (v-fos fbj murine osteosarcoma viral oncogene homolog	NM_005252	2.15
dusp1 (dual specificity phosphatase 1)	NM_004417	2.00
h2afg (h2a histone family, member g)	NM_021065	1.68
smarca4 (swi/snf related, matrix associated, actin dependent regulator of chromatin, subfamily a, member 4)	NM_003072	1.68
2. Genes that were downregulated at 2h		
glrx (lutaredoxin (thioltransferase))	NM_002064	2.42
s100a8 (s100 calcium-binding protein a8)	NM_002964	2.41
msh6 (muts homolog 6 (*Escherichia coli*))	NM_000179	2.22
ceacam7 (carcinoembryonic antigen-related cell adhesion molecule 7)	NM_006890	2.04
c-myc (v-myc myelocytomatosis viral oncogene homolog (avian))	NM_002467	2.02
spp1 (secreted phosphoprotein 1 (osteopontin, bone sialoprotein i, early t-lymphocyte activation 1)	NM_000582	2.02
sep2 (septin 2)	NM_015129	1.83
cd14 (cd14 antigen precursor)	NM_000591	1.78
mpo (myeloperoxidase)	NM_000250	1.73
3. Genes that were upregulated at 24h		
ask (activator of s phase kinase)	NM_006716	1.90
c-myc (v-myc myelocytomatosis viral oncigene homolog (avian))	NM_002467	1.90
hsp70 (heat shock protein 70)	NM_002467	1.88
cdk4 (cyclin-dependent kinase 4, isoform 1)	NM_000075	1.77
top1 (topoisomerase (dna) I)	NM_003286	1.71
ccnh (cyclin h)	NM_001239	1.67
atf4 (activating transcription factor 4)	NM_001675	1.66
cdk7 (cyclin-dependent kinase 7)	NM_001799	1.66
4. Genes that were downregulated at 24h		
hspb1 (heat shock 27kd protein 1)	NM_001540	2.44
s100a8 (s100 calcium-binding protein a8)	NM_002964	2.35
dsg2 (desmoglein 2 preproprotein)	NM_001943	2.24
atp1b3 (atpase, na+/k+ transporting, beta 3 polypeptide)	NM_001679	1.98
mig (monokine induced by gamma interferon)	NM_002416	1.98
casp8 (caspase 8, isoform c)	NM_033356	1.76
polr2j (dna directed rna polymerase ii polypeptide j, isoform b)	NM_032959	1.76

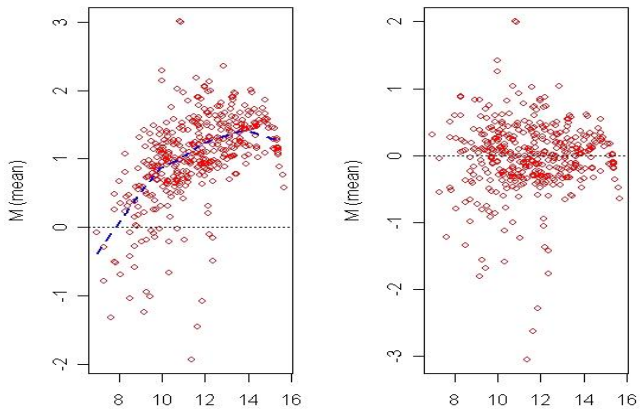

Fig. 6. Effect of normalization on microarray data. MA-plots of samples treated with wild type and H35R mutant toxins both before and after normalization are demonstrated.

4.3 Confirmation of selected mRNAs by RT-PCR

In order to ensure the validity of selected SAGE and array results, RT-PCR was performed. A duplex relative RT-PCR using ribosomal RNA (18S rRNA) as internal standard was carried out to evaluate mRNA levels semi-quantitatively. Ribosomal RNA expression has been reported to be more faithful compared to GADPH and β–actin (153, 154). Fig. 7, 8, 9, 10, 11, 12, 13, and 14 illustrate the expression levels of *blvrb*, *c-fos*, *c-jun*, *egr-1*, *GADD34*, *Nurr77*, *rps3a*, and *ssat*, respectively, in cells transiently treated with wild-type and H35R mutant toxins for 0 to 24 h, using a duplex relative RT-PCR assay. The data from these experiments are displayed as follows:

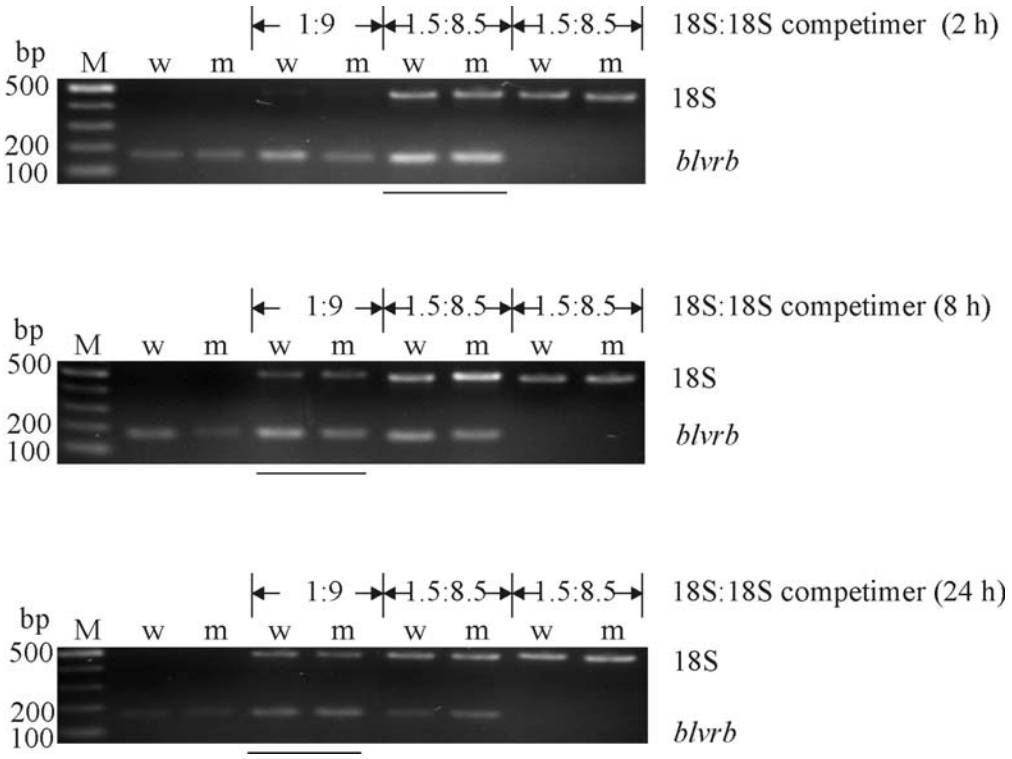

Fig. 7. Expression levels of *blvrb* (biliverdin reductase B (flavin reductase (NADPH)) in cells transiently treated with wild type (w) and H35R mutant toxins (m) for 2 h, 8 h, and 24 h, using a duplex relative RT-PCR assay. The RT-PCR was performed using i.) primers for *blvrb* alone, ii.) primers for *blvrb* and 18S rRNA at 1:9-1.5:8.5 different ratios of 18S rRNA primer:competimer, and iii.) primers of 18S rRNA at 1.5:8.5 ratio of 18S rRNA primer:competimer. An optimal 18S rRNA primer:competimer ratio for *blvrb* gene is underlined. M represents 0.5 μg of 100 bp DNA ladder marker. bp represents base pairs. The time points when cells are harvested are in brackets.

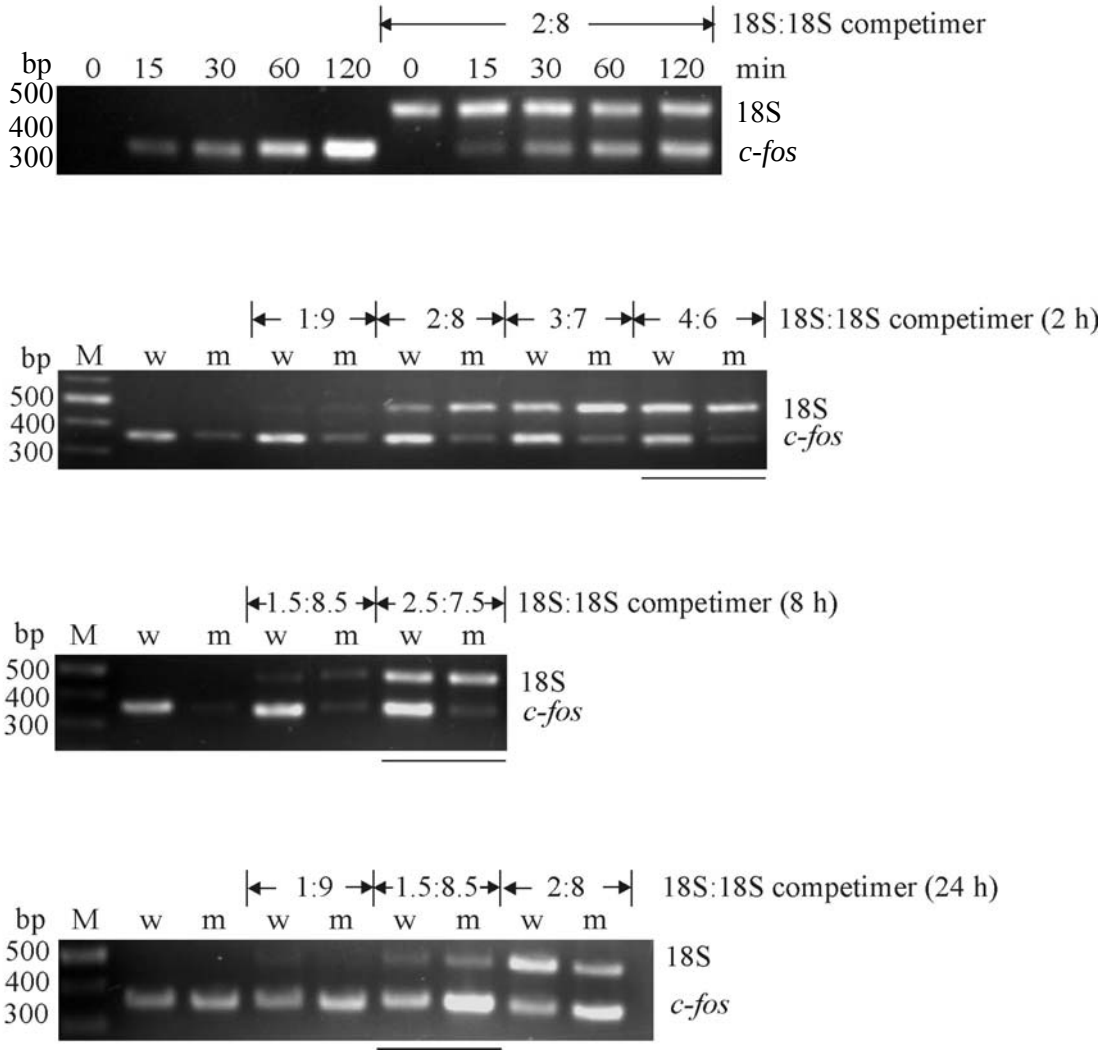

Fig. 8. Expression levels of *c-fos* (FBJ murine osteosarcoma viral oncogene homolog) in cells transiently treated with wild type (w) and H35R mutant toxins (m) for 0 to 24 h, using a duplex relative RT-PCR assay. An optimal 18S rRNA primer:competimer ratio for *c-fos* gene is underlined.

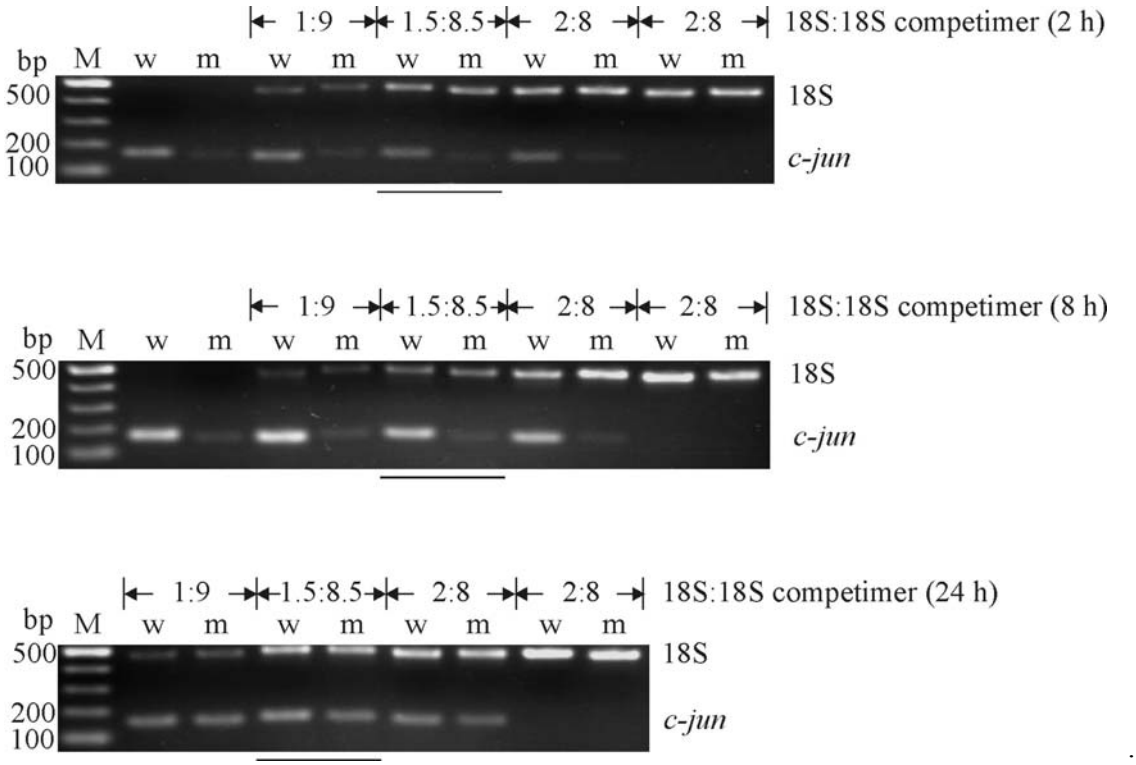

Fig. 9. Expression levels of *c-jun* (jun oncogene) in cells transiently treated with wild type (w) and H35R mutant toxins (m) for 2 h, 8 h, and 24 h, using a duplex relative RT-PCR assay. An optimal 18S rRNA primer:competimer ratio for *c-jun* gene is underlined.

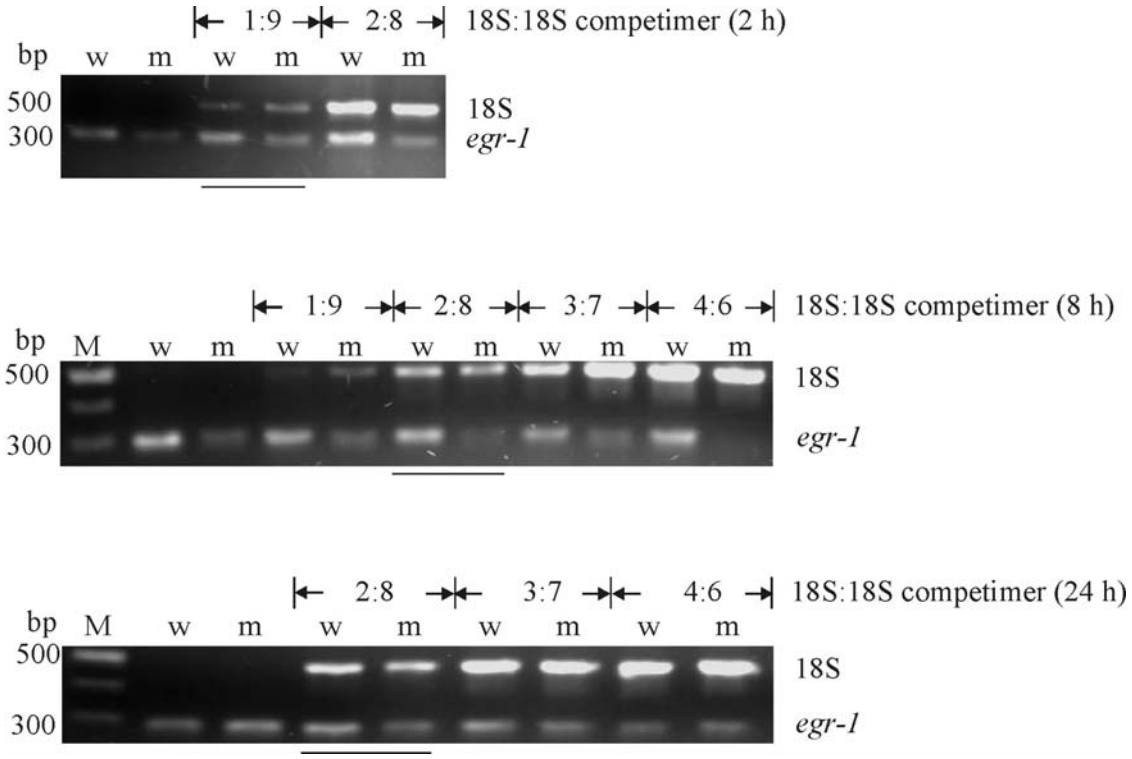

Fig. 10. Expression levels of *egr-1* (early growth response factor 1) in cells transiently treated with wild type (w) and H35R mutant toxins (m) for 2 h, 8 h, and 24 h, using a duplex relative RT-PCR assay. An optimal 18S rRNA primer:competimer ratio for *egr-1* gene is underlined.

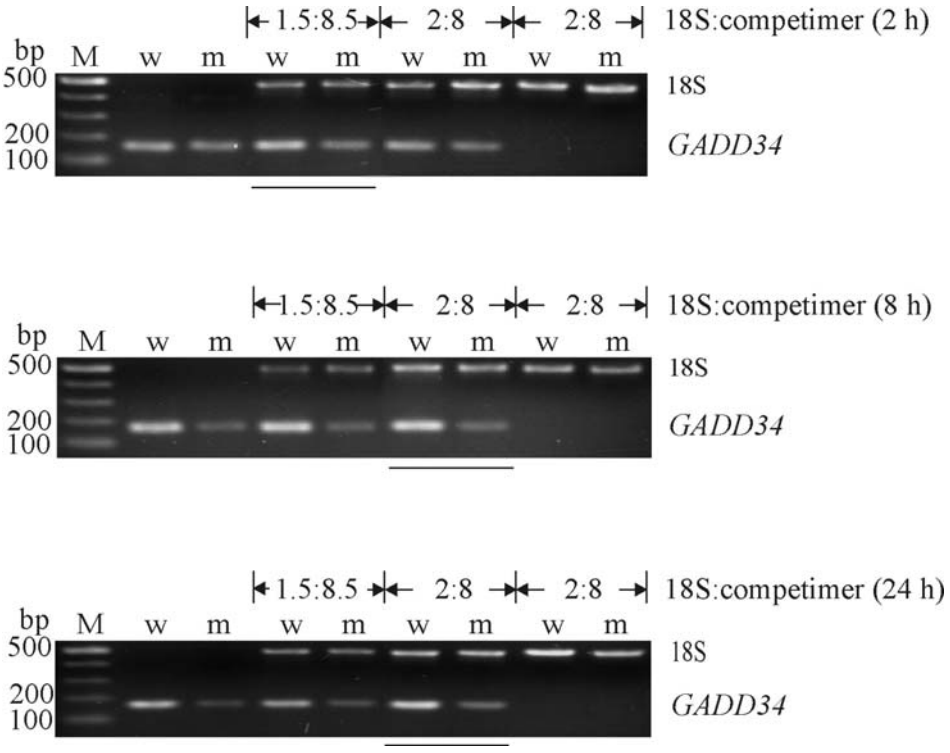

Fig. 11. Expression levels of *GADD34* (growth arrest and DNA-damage-inducible 34) in cells transiently treated with wild type (w) and H35R mutant toxins (m) for 2 h, 8 h, and 24 h, using a duplex relative RT-PCR assay. An optimal 18S rRNA primer:competimer ratio for *GADD34* gene is underlined.

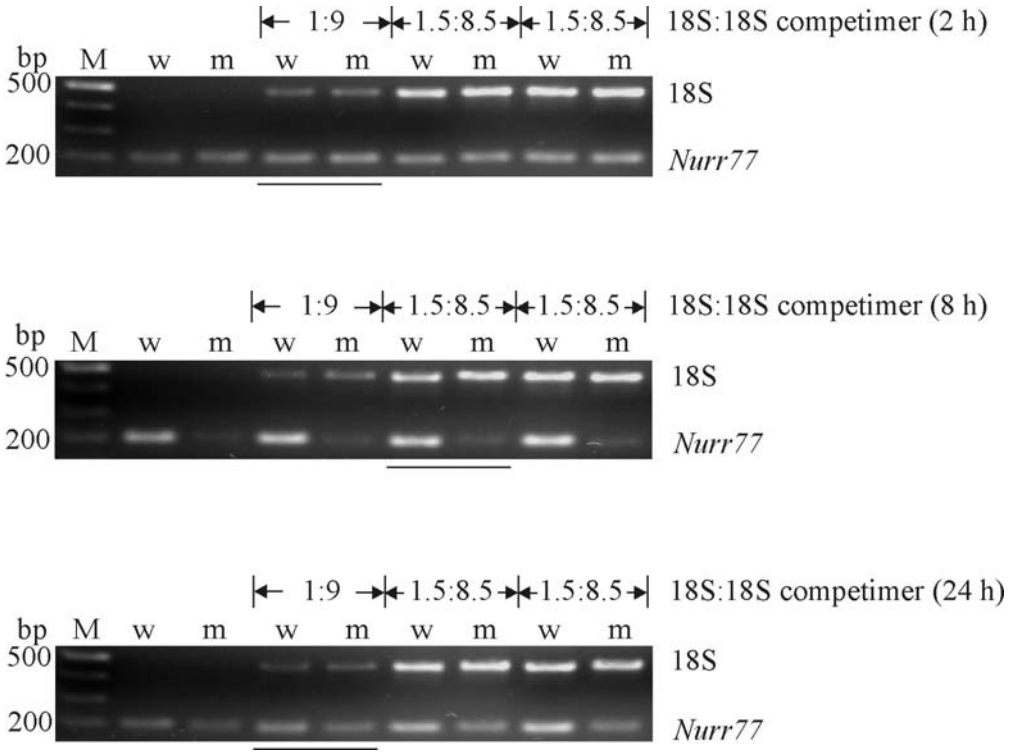

Fig. 12. Expression levels of *Nurr77* (an orphan nuclear receptor) in cells transiently treated with wild type (w) and H35R mutant toxins (m) for 2 h, 8 h, and 24 h, using a duplex relative RT-PCR assay. An optimal 18S rRNA primer:competimer ratio for *Nurr77* gene is underlined.

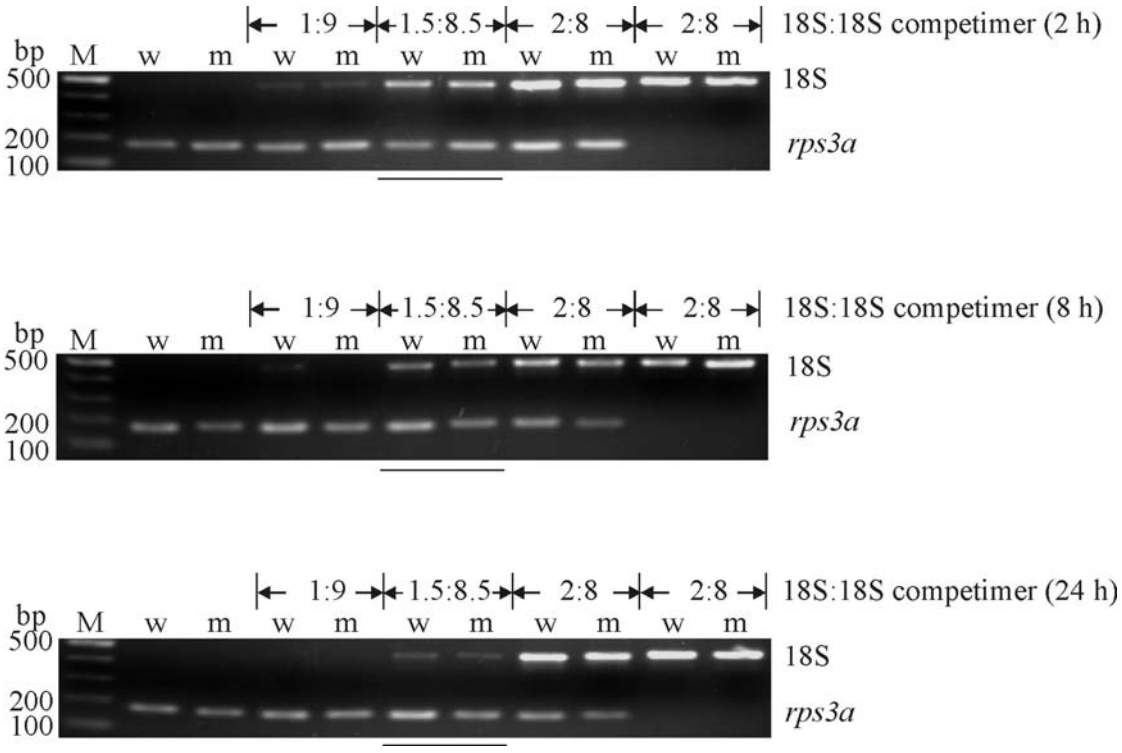

Fig. 13. Expression levels of *rps3a* (ribosomal protein S3A) in cells transiently treated with wild type (w) and H35R mutant toxins (m) for 2 h, 8 h, and 24 h, using a duplex relative RT-PCR assay. An optimal 18S rRNA primer:competimer ratio for *rps3a* gene is underlined.

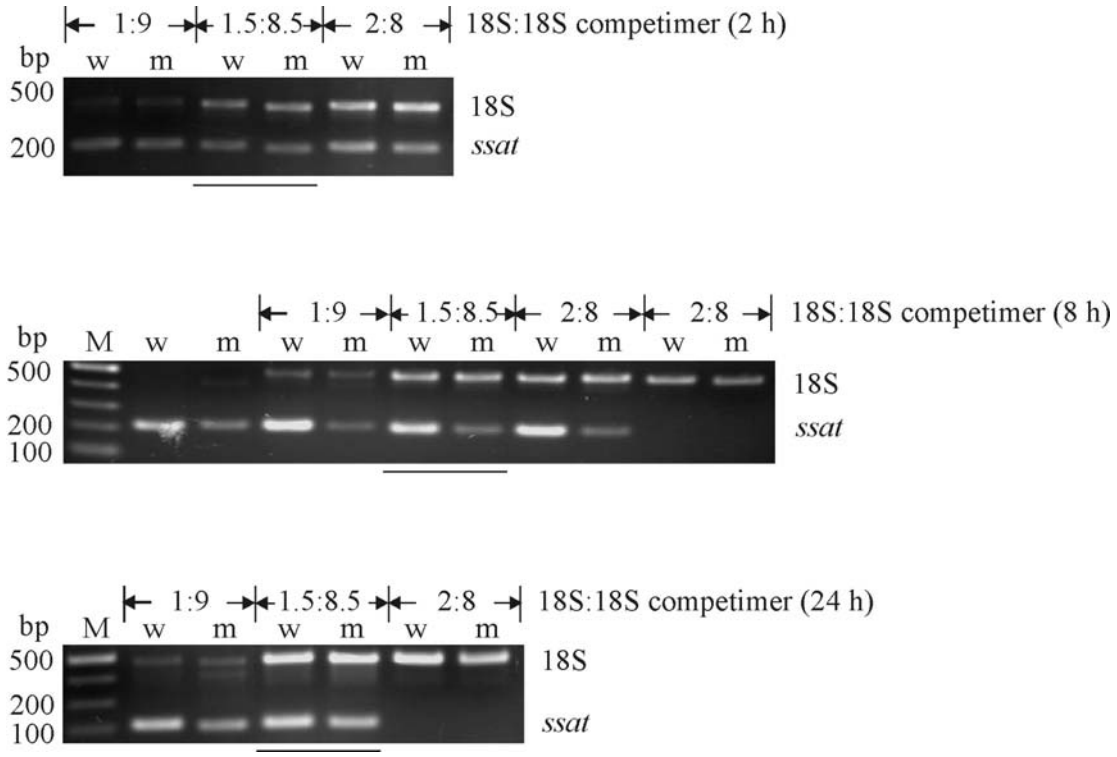

Fig. 14. Expression levels of *ssat* (spermidine/spermine N(1)-acetyltransferase) in cells transiently treated with wild type (w) and H35R mutant toxins (m) for 2 h, 8 h, and 24 h, using a duplex relative RT-PCR assay. An optimal 18S rRNA primer:competimer ratio for *ssat* gene is underlined.

4.4 Clustering of transcription profile

The results of differentially confined expressed genes are clustered according to their functions in Table 5. Immediate early genes (IEGs), encoding transcription factors such as c-Fos, c-Jun, and Egr-1, were found to be strongly induced at 2-8 h after toxin treatment. Other genes that were upregulated in RT-PCR at 8 h and confirmed SAGE data included one of the IEGs *Nurr77*, *blvrb*, *rps3a*, and *ssat*. *rps3a* Gene encodes a ribosomal protein: v-fos transformation effector protein, which is a component of the 40S subunit (155). *polB* and *GADD34* were also observed at 2 h after toxin treatment. Pol II, protein encoded by *polB*, is a repair polymerase. GADD34 plays a role in regulation of protein translation (156, 157).

The activation of c-Fos and c-Jun plays an important role in cell death and proliferation (158) and can be inducible by an epidermal growth factor (EGF) (159, 160). The finding that these IEGs are transcribed in perforated cells led to the discovery that α-toxin-treated cells proliferate in an EGFR fashion (113).

4.5 AP-1 activation is induced after 6 h of toxin treatment

Whereas RT-PCR demonstrated that immediate early mRNAs already accumulated at 15 min after toxin treatment, c-Fos protein was expressed with considerable delay at 3 h. AP-1 binding to a serum response element was also observed at 6 h, after cells recuperated from wild-type toxin treatment compared to the untreated cells and cells treated with H35R mutant toxin (Fig. 15 and 16). The AP-1 binding activities waned at 24 h.

Table 5. Clusters of up- and downregulated genes, analyzed by microarray and RT-PCR, at 2 h, 8 h, 24 h after transient toxin treatment according to data from GeneCards (http://www.genecards.org/index.shtml).

Molecular functions	2 h	8 h	24 h
Transcription factor & Transcription coactivator	upreg.: *egr1*, *c-jun*, *smarca4*, *c-fos*	upreg.: *c-fos*, *c-jun*, *egr1*, *Nurr77*	upreg.: *atf4*, *c-myc*, *Nurr77*, *cdk7*, *egr1*
	downreg.: *c-myc*		
Protein kinase	upreg.: *csk* (Ser/Thr kinase)		upreg.: *cdk4*, *cdk7*
Protein binding		upreg.: *rps3a*	upreg.: *ash*, *atf4*, *cdk4*, *rps3a*
	downreg.: *c-myc*, *spp1*		downreg.: *dsg2*, *hspb1*
Enzymes			
- Oxidoreductase	downreg.: *mpo*	upreg.: *blvrb*	
- Transferase	upreg.: *polB*	upreg.: *ssat*	upreg.: *cdk7*
			downreg.: *polr2j*
- Hydrolase	upreg.: *dusp*		
	downreg.: *asah*		
ATP binding	upreg.: *csk*		upreg.: *cdk7*
	downreg.: *msh6*		
Metal ion binding	upreg.: *egr1*	upreg.: *egr1*, *Nurr77*	upreg.: *egr1*, *Nurr77*
	downreg.: *cpa3*		
Ca^{2+} binding	downreg.: *s100a8*, *mpo*		downreg.: *dsg2*, *s100a8*
Translation control	upreg.: *GADD34*	upreg.: *GADD34*	upreg.: *GADD34*

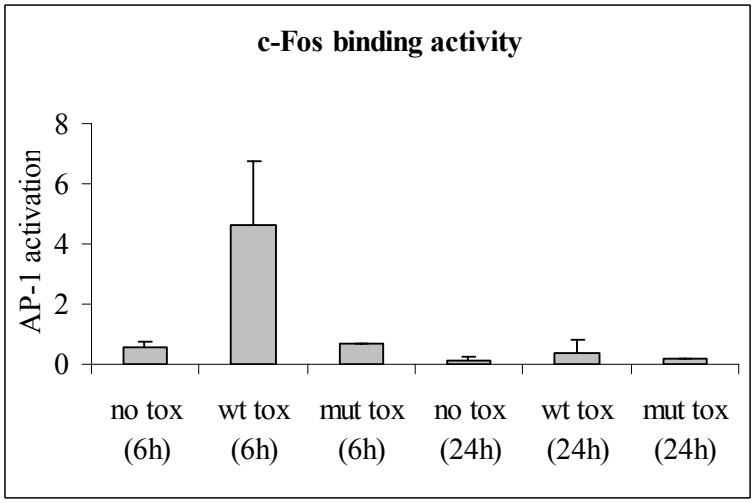

Fig. 15. c-Fos profiling for DNA binding activation upon toxin treatment. Nuclear extracts from HaCat cells (untreated or stimulated by wild-type and H35R mutant α-toxin) were assayed by ELISA at 20 μg/well for c-Fos activity. No tox, wt tox, and mut tox represent data from untreated cells, cells transiently treated with wild-type α-toxin, and cells treated with mutant α-toxin, respectively. The numbers in brackets represent cell-harvested time points.

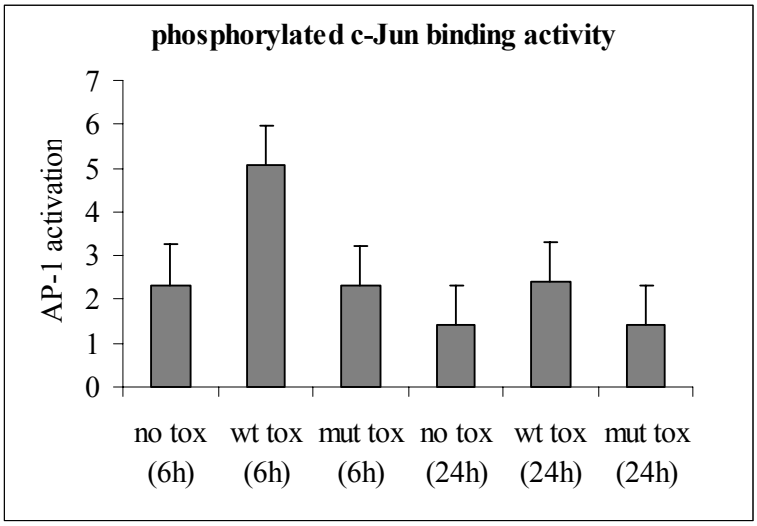

Fig. 16. Phosphorylated c-Jun (p-c-Jun) profiling for DNA binding activation upon toxin treatment. Nuclear extracts from HaCat cells (untreated or stimulated by wild type and H35R mutant α-toxin) were assayed by ELISA at 20 μg/well for p-c-Jun activity.

AP-1 activation values were calculated from ratio of sample O.D/positive control O.D. c-Fos AP-1 activation values of untreated cells, wild-type α-toxin-treated cells, and mutant α-toxin-treated cells at 6 h were 0.54 (±0.18), 4.62 (±2.16), and 0.67 (±0.02), respectively. c-Fos AP-1 activation values of untreated cells, wild-type α-toxin-treated cells, and mutant α-toxin-treated cells at 24 h were 0.12 (±0.10), 0.39 (±0.43), and 0.19 (±0.00), respectively. c-Jun AP-1 activation values of unperforated cells, wild-type α-toxin-perforated cells, and mutant α-toxin-perforated cells at 6 h were 2.33 (±1.06), 5.06 (±1.93), and 2.31 (±1.39), respectively. c-Jun AP-1 activation values of unperforated cells, wild-type α-toxin-perforated cells, and mutant α-toxin-perforated cells at 24 h were 1.41 (±0.05), 2.41 (±1.35), and 1.40 (±0.92), respectively.

The effect of toxin on AP-1 function was further examined by investigating one of the AP-1-regulated gene products, MMP-9 (metalloprotease-9) (161, 162).

4.6 MMP-9 is not induced by increased AP-1 activity

The promoter of MMP-9 possess three AP-1 enhancer element-binding sites. Accumulated data indicate that TNF-α may activate or induce MMP-9 expression through pathways leading to activation of NF-κB and AP-1 in several tumor lines (163, 164). However, MMP-9 induction by α-toxin was not observed at the transcription level (Fig. 17) or at the protein expression level (Fig. 18). In addition, TNF-α treatment failed to induce MMP-9 in cells that had previously been treated with α-toxin (Fig. 18).

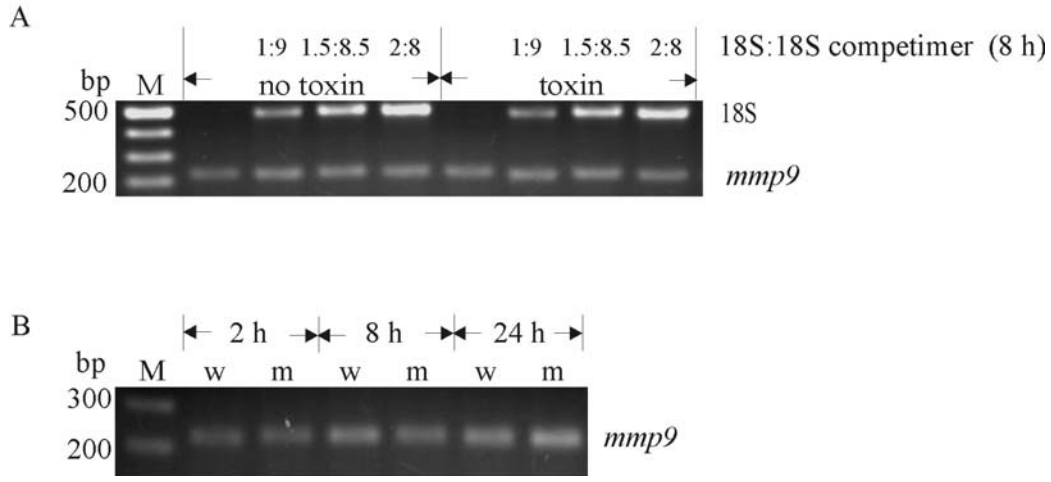

Fig. 17. A.) Expression levels of *mmp9* in cells transiently treated with toxin for 8 h compared to the untreated cells. The RT-PCR was performed using primers for *mmp9* and 18S rRNA at 1:9-2:8 different ratios of primer:competimer. Coamplification of *mmp9* with 18S RNA did not modify *mmp9* amplification signals. **B.)** Expression levels of *mmp9* in cells temporarily treated with wild type (w) and H35R mutant toxins (m) for 2 h, 8 h, and 24 h. M represents 0.5 μg of 100 bp DNA ladder marker. bp represents base pairs.

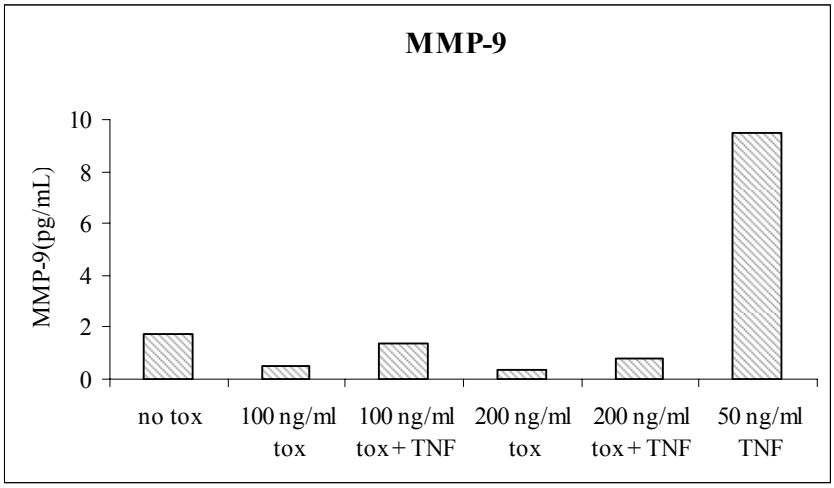

Fig. 18. α-Toxin does not induce MMP-9 protein expression. The MMP-9 protein levels, measured by ELISA, were markedly reduced at 24 h after transient treatment of HaCat cells with 100 or 200 ng/ml α-toxin. Toxin-dependent suppression of MMP-9 was also observed in cells that were stimulated by 50 ng/ml TNF-α.

Cells were transiently treated with 100 and 200 ng/ml α-toxin for 2 h. After change of medium, 50 ng/ml TNF-α was added for 22 h. The MMP-9 levels were measured in untreated cells, cells treated with 100 ng/ml toxin, 100 ng/ml toxin plus TNF-α, 200 ng/ml toxin, 200 ng/ml toxin plus TNF-α, and TNF-α alone were 1.73 (±0.11), 0.47 (±0.04), 1.36 (±0.01), 0.34 (±0.02), 0.82 (±0.01), 9.49 (±0.41) pg/ml, respectively.

The unexpected down regulation of MMP-9 levels was observed although MMP-9 is a *bona fide* AP-1-regulated gene product (165). These data suggest that AP-1-mediated gene regulation underlies additional restrictions in α-toxin-treated cells, and further studies need to be done to identify AP-1- regulated gene products in toxin-treated HaCat cells. One potentially important candidate is *c-jun*, which is in fact upregulated during α-toxin attack, and known both to be a target of AP-1 and to be required for cell cycle progression.

Conceivably, restricted gene expression is pivotal at times of ATP shortage. Control may occur at various levels. In contrast to MMP-9, which was inhibited of the RNA-level, *c-fos* mRNA was massively overexpressed at 30 min post-toxin treatment. However, translation of *c-fos* seemed to lag significantly behind. Translation is a highly energy consuming process, and at times of massive ATP-shortage as cells experience following perforation, it would appear meaningful for cells to restrict translation to a minimal set of proteins which are absolutely required to manage the crisis. Such a response has been described previously as the “integrated stress response”. The following sections will deal with this issue in the context of a perforated cell.

4.7 Alpha-toxin and protein translation

4.7.1 *S. aureus* α-toxin induces eIF2α phosphorylation

One critical step in translational control is the phosphorylation of eIF2α since it stops initiation of translation. Therefore analysis of the phosphorylation status of eIF2α was performed. Western blot experiments revealed that α-toxin at concentrations ≥100 ng/ml induced phosphorylation of eIF2α in HaCat cells. Activation commenced within 30 min after treatment and waned after 6 h (Fig. 19 -21). Far less p-eIF2α was observed when the non-lytic, bindable α-toxin mutant H35R was employed (Fig. 20). Levels of total eIF2α were similar in all lysate preparations.

To determine the effects of eIF2α phosphorylation after toxin treatment, [^{35}S]Met incorporation was measured following the exposure of HaCat cells to α-toxin. There was a significant reduction in protein synthesis in HaCat cells after 1 h of toxin treatment with recovery of protein synthesis following 4 h of the treatment. By comparison, protein synthesis levels of non-treated cells remained constant throughout the experiment (Fig. 22).

Since the phosphorylation of eIF2α appears to be critically dependent on a family of eIF2α kinases, it was of interest to further investigate which kinases possibly activated eIF2α following α-toxin treatment.

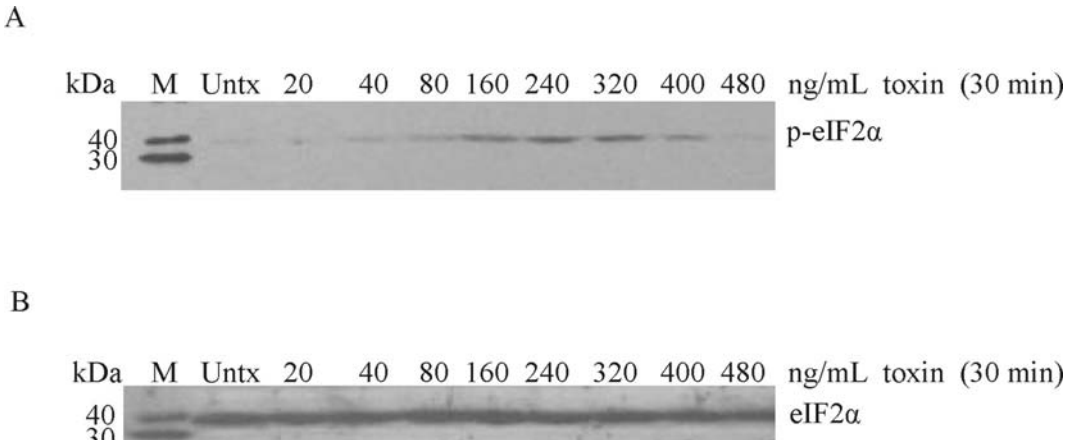

Fig. 19. Western blot of p-eIF2α (A) and total eIF2α (B) with lysates from HaCat cells transiently treated with α-toxin for 30 min for the indicated concentrations.

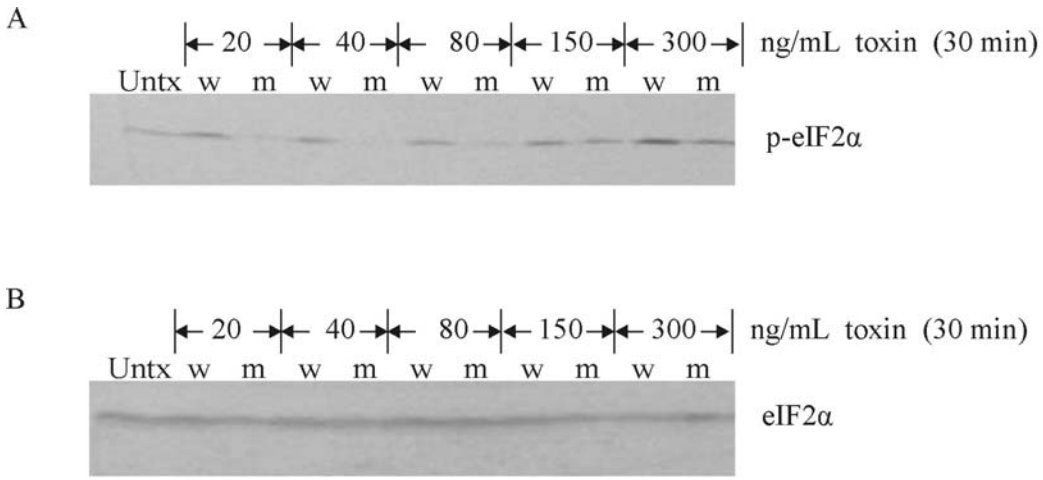

Fig. 20. Western blot of p-eIF2α (A) and total eIF2α (B) with lysates from HaCat cells transiently treated with wild type (w) and H35R mutant (m) α-toxin for 30 min for the indicated concentrations.

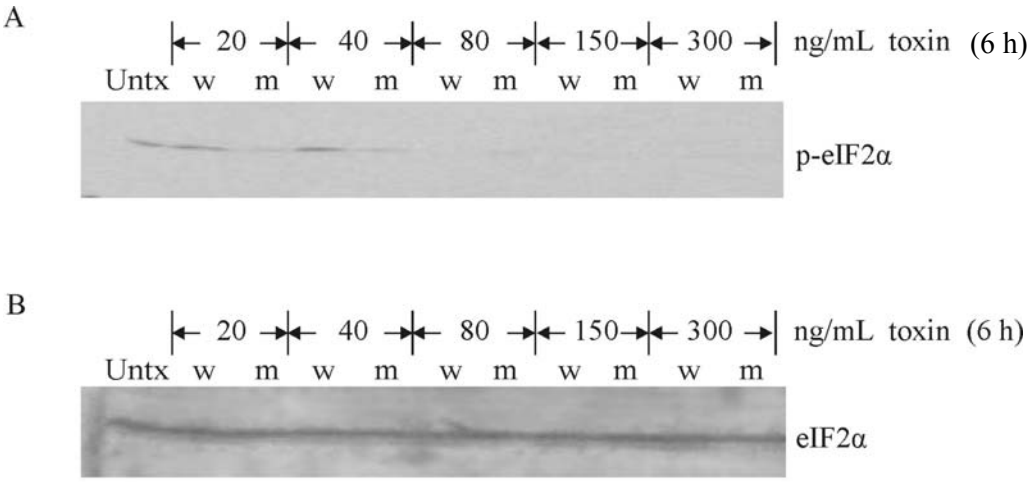

Fig. 21. Western blot of p-eIF2α (A) and total eIF2α (B) with lysates from HaCat cells transiently treated with wild-type (w) and H35R mutant (m) α-toxin for 6 h for the indicated concentrations.

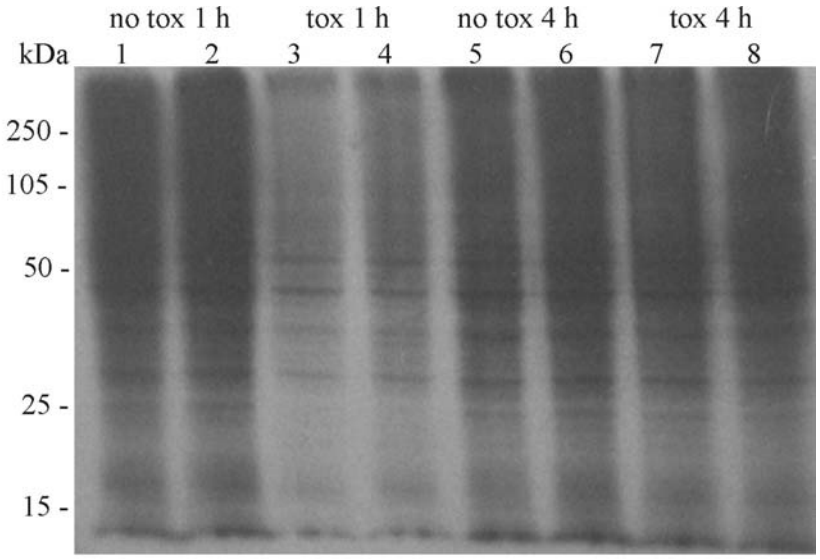

Fig. 22. Phosphorylation of eIF2α reduces translation in response to α-toxin treatment. HaCat cells were exposed to 100 ng/ml α-toxin or to medium for 1 h and were starved in medium lacking methionine. After 15 min, cells were radiolabeled with [^{35}S]Met for 30 min, washed, and harvested or reincubated for 3 h in unlabeled medium. Radiolabeled proteins were separated by SDS-PAGE, and visualized by autoradiography. A representative image from one of two independent experiments with the same result is shown.

4.7.2 GCN2 is induced prior to eIF2α phosphorylation in toxin-treated cells

As eIF2α kinases PERK and GCN2 can phosphorylate the alpha subunit of eIF2 (166, 167), tt was investigated whether these pathways would be involved in eIF2α activation by α-toxin. In the presence or absence of α-toxin p-PERK signal intensities appeared to be the same. Total PERK levels of all samples also remained constant throughout the experiment. PERK signals were not affected by pretreatment of cells with SB203580 (Fig. 23). In contrast, GCN2 was markedly induced after only 10 min of toxin treatment and then the signal waned (Fig. 24 lanes 1, 3, 5, 7, 9). Therefore, GCN2 emerged as a candidate protein that could phosphorylate eIF2α following α-toxin treatment.

Since p38 MAPK has been previously described to be activated and required for rescue of α-toxin-treated cells (51), a possible link between p38 MAPK and GCN2 was soughted.

4.7.3 p38 is involved in activation of GCN2 and p-eIF2α in toxin-treated cells

SB203580, a p38 α/β-specific inhibitor, was used in toxin treatment experiments. It was found that the p38 inhibitor blocked both GCN2 induction (Fig. 24) and eIF2α phosphorylation (Fig. 25). These results established a possible novel link between p38 MAPK and translational control via GCN2 and eIF2α.

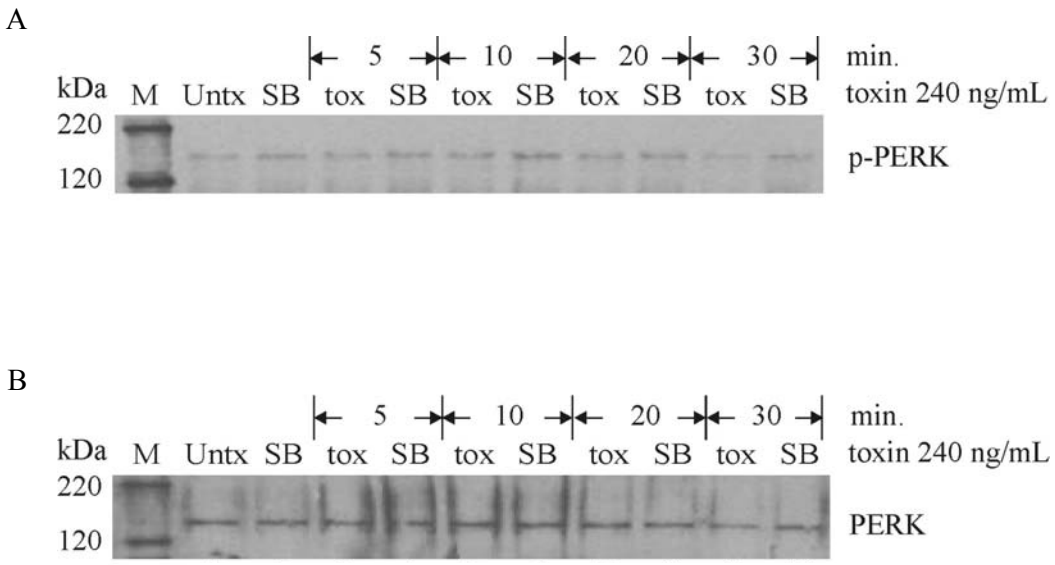

Fig. 23. Western blot of phosphorylated PERK (A) and total PERK (B) with lysates from HaCat cells transiently treated with 240 ng/ml α-toxin in the presence and absence of SB203580. Cells were pretreated with 10 μM SB203580 for 1 h prior to addition of 240 ng/ml α-toxin for the indicated times. Control cells were treated identically but received no toxin and/or SB203580. Representative images from one of two independent experiments with the same result are shown. M represents Magic Mark XP Western blot Standard with the protein sizes of 120 and 220 kDa. p-PERK signal intensities did not change upon the treatments with α-toxin and SB203580.

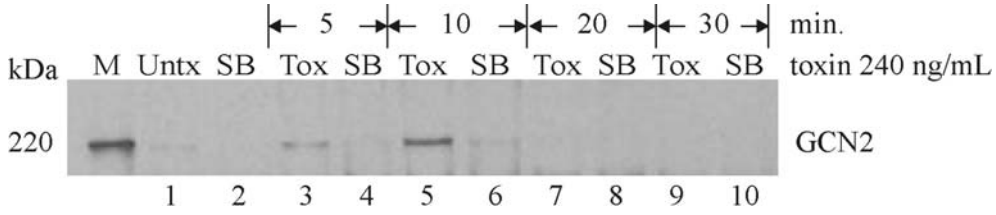

Fig. 24. Western blot of GCN2 with lysates from HaCat cells transiently treated with 240 ng/ml α-toxin in the presence and absence of SB203580. Cells were treated with the same conditions as Fig. 24. GCN2 signals markedly increased at 10 min after toxin treatment and could be inhibited by SB203580.

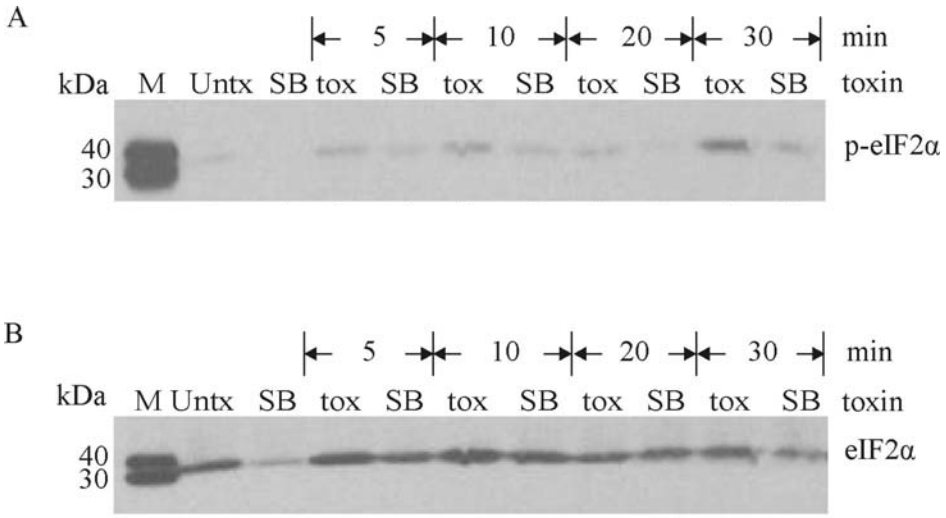

Fig. 25. Western blot of phosphorylated eIF2α (A) and total eIF2α (B) with lysates from HaCat cells transiently treated with 240 ng/ml α-toxin in the presence and absence of SB203580. Cells were pretreated with 10 μM SB203580 for 1 h prior to addition of 240 ng/ml α-toxin for the indicated times. M represents Magic Mark XP Western blot Standard with the protein sizes of 30 and 40 kDa.

4.8 α-Toxin induces expression of *GADD34*

GADD34 is capable to re-initiating protein synthesis by interacting with eIF2α (122, 168, 169). And since the synthesis of protein resumed at 4 h after toxin treatment (Fig. 22), it was of interest to study the effect of α-toxin on *GADD34* expression.

Real-time PCR revealed that α-toxin at the concentration of 100 ng/ml induced the expression of *GADD34* in HaCat cells (Fig. 26). *GADD34* expression levels was found to be induced by α-toxin at 2 h after toxin treatment. In the first experiment, the expression level of *GADD34* of cells treated with α-toxin for 15 min, 30 min, 1 h, and 2 h were 1.83 (1.70-1.87), 4.41 (3.97-4.41), 14.83 (11.80-15.14), and 25.81 (18.20-28.51), respectively. In the second experiment, the expression level of *GADD34* of cells treated with α-toxin for 15 min, 30 min, 1 h, 1.5 h, and 2 h were 0.69 (0.65-0.76), 1.78 (1.52-1.99), 1.71 (1.62-1.72), 2.35 (2.12-2.43), and 10.41 (8.84-10.24), respectively. The expression values were calculated under the optimal and identical real-time amplification condition that $E_{\text{target}} = E_{\text{ref}} = 2$ (*E* means the PCR efficiency). However, since the PCR efficiency could be varied, ranges of the possible expression values were shown in brackets. In both experiments, *GADD34* was upregulated within 2 h after toxin treatment.

Since it had been hypothesized that the mechanism activated eIF2α in response to α-toxin treatment, requiring p38 MAPK, further investigation whether p38 MAPK also played a role in *GADD34* expression was performed.

A

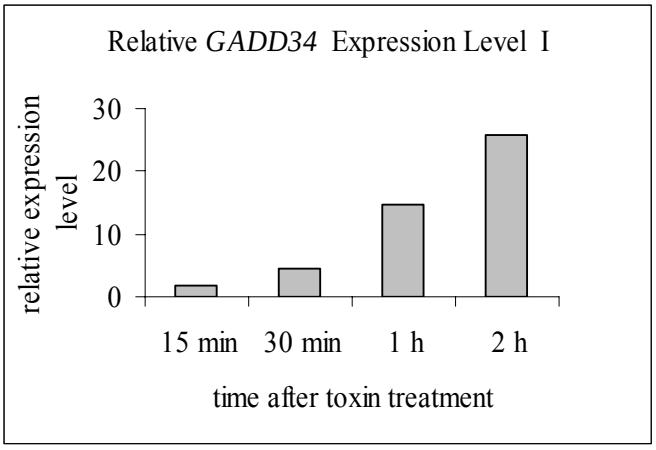

B

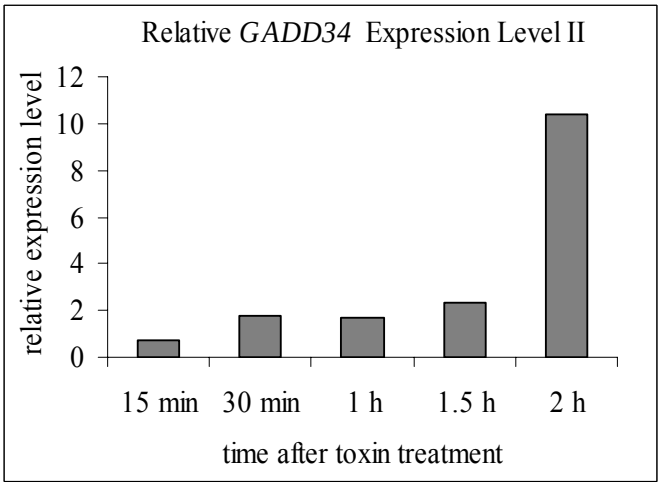

Fig. 26. Expression of *GADD34* mRNA in HaCat cells treated with α-toxin. Cells were treated with α-toxin for 15 min – 2 h. Untreated cells served as negative control. Total RNA was extracted and *GADD34* mRNA expression was detected by real-time PCR. *HPRT1* expression was used as an internal standard. Fig. A) and B) were from two independent experiments.

4.8.1 Inhibition of p38 blocks *GADD34* mRNA expression

The p38 MAPK-inhibitor SB203580 was applied to cells and the effect on the expression levels of *GADD34* after toxin treatment was assessed. As shown in Fig. 27, *GADD34* expression was found to be enhanced in cells treated with α-toxin but expression was reduced in the presence of SB203580 as compared to the samples treated with α-toxin alone. Actinomycin, which functions to inhibit RNA synthesis, served as a positive control.

In the first experiment, the expression level of *GADD34* of cells treated with actinomycin D, actinomycin D plus toxin, SB203580, SB203580 plus toxin, and α-toxin alone at 2 h were 0.38 (0.37-0.42), 1.06 (1.04-1.07), 1.01 (0.99-1.04), 4.59 (4.03-4.66), and 8.17 (6.62-8.57), respectively. In the second experiment, the expression levels of *GADD34* were 0.34 (0.34-0.38), 0.58 (0.58-0.60), 0.64 (0.63-0.67), 2.85 (2.50-2.99), and 4.44 (3.62-4.85), respectively. In both experiments, *GADD34* was downregulated in the presence of SB203580 compared to cells treated with toxin alone. GADD34 in concert with PP1 is capable of dephosphorylating eIF2α and restoring protein synthesis shutoff (122, 156).

A

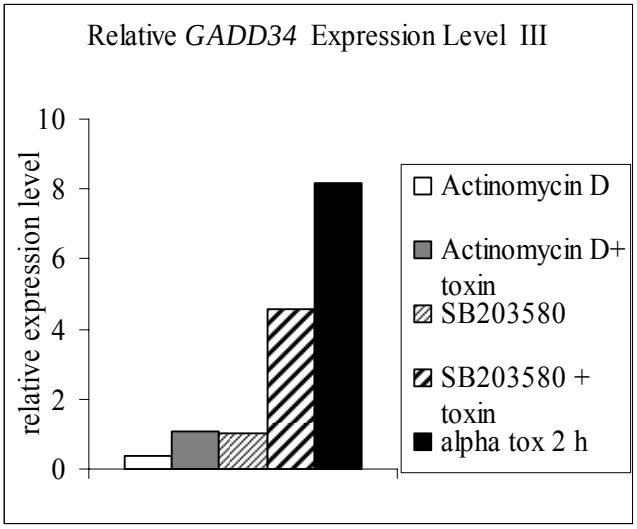

B

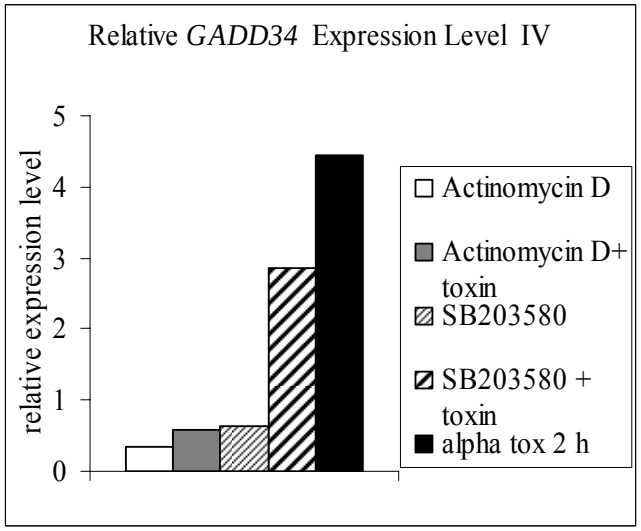

Fig. 27. Inhibition of p38 MAPK could reduce *GADD34* expression level. Cells were pretreated with 10 μM SB203580 for 1 h or with 1 μg/μl actinomycin D for 30 min prior to the addition of 100 ng/ml α-toxin for 2 h. Untreated cells served as negative control. Total RNA was extracted and *GADD34* mRNA expression was detected by real time PCR. *HPRT1* expression was used as an internal standard. Fig. 26 A) and B) were from two independent experiments.

4.8.2 Effect of PP1 on toxin-treated cells

The above results indicated that the cascade of eIF2α phosphorylation in HaCat cells treated with α-toxin possibly involved p38 MAPK and *GADD34*. To substantiate this contention, the effect of tautomycetin (TC), a specific inhibitor of PP1 (170, 171), on ATP levels after α-toxin treatment was assured.

As shown in Fig. 28, TC markedly blunted the fall of ATP-levels in toxin-treated cells (Fig. 28). Moreover, TC increased p-eIF2α levels either in untreated or toxin-treated cells. This effect was observed until 6 h after toxin treatment (Fig. 29). The results were in line with the hypothesis that protein synthesis consumes ATP. When translation is inhibited by p-eIF2α, ATP levels are consequently higher in the cells.

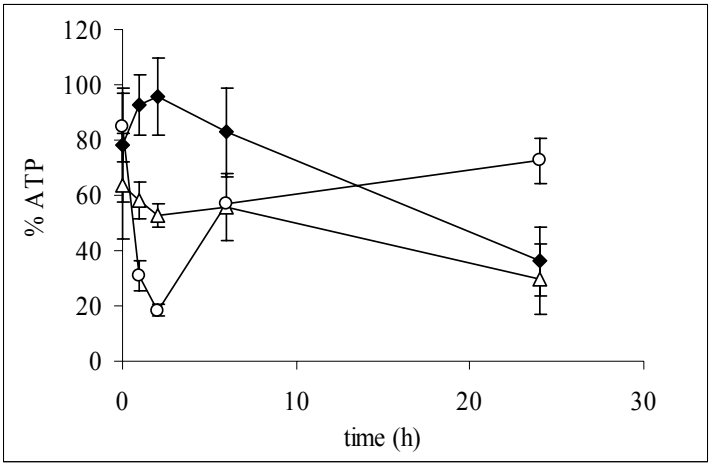

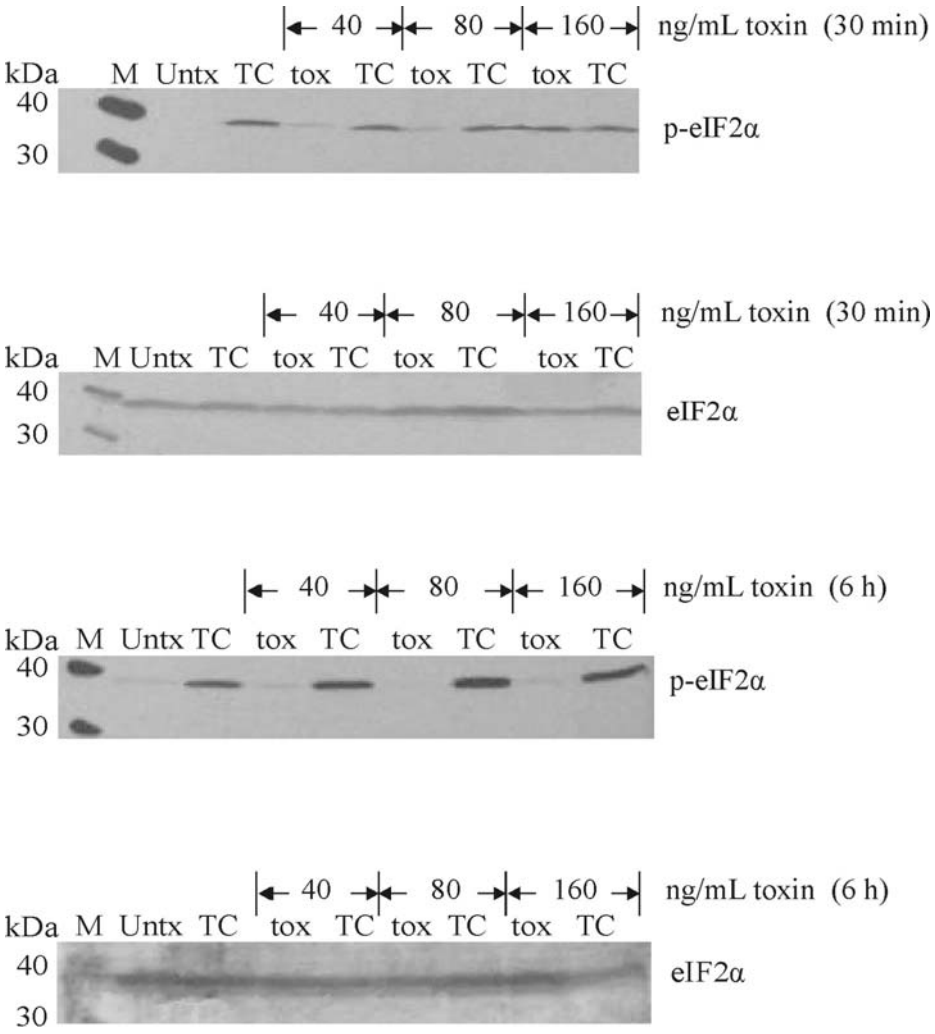

Fig. 29. Western blot of p-eIF2α and total eIF2α with lysates from HaCat cells transiently treated with wild type α-toxin for 30 min and 6 h in the presence and absence of tautomycetin (TC). Cells were pretreated with 50 μM TC for 1 h prior to addition of α-toxin for the indicated concentrations with the medium change at 2 h. Control cells were treated identically but received no toxin and/or TC.

5. DISCUSSION

In the present work molecular details of the stress response to transient perforation by *S. aureus* α-toxin, a prototypic membrane-pore-forming toxin were investigated in a human keratinocyte cell line.

Transcriptional changes in the wake of perforation

First it was shown that ATP levels dropped to *ca.* 20% at 2 h post-toxin treatment and then they were replenished to reach ≥75% at 24 h after treatment with 500 ng/ml α-toxin. Transient ATP depletion has been demonstrated in fibroblasts, bladder carcinoma and myelomonocytic leukemia cell lines treated with α-toxin (152). In fibroblasts, cellular recovery was reported to be consequence of closure of toxin channels (172, 173). Irreversible decrease of ATP levels has been seen in monocytes treated with *Bordetella pertussis* adenylate cyclase (AC) toxin (174, 175) and in intestine cells treated with *V. cholerae* cytolysin (VCC) where both toxins can form small pores in membranes and allow the efflux of potassium ions as *S. aureus* α-toxin (176-178). Hence, recovery of toxin-attacked cells depends on cell type, duration of treatment, and dose of toxin used. The reduction of ATP levels by α-toxin correlates with the impairment of mitochondrial function (13), and presumably the mechanism is the same as in VCC- treated intestine cells (177). In contrast, for *B. pertussis* AC toxin, an AC enzymatic activity possibly contributes to depletion of cellular ATP pool (174).

Additional insights into the consequences of transient membrane permeabilization by α-toxin were gained through transcript profiling using SAGE (113). In the present work, SAGE results were confirmed and extended by microarray and semiquantitative RT-PCR analysis. A massive over-expression of immediate early transcripts (*c-fos, c-jun, egr-1, Nurr77*) was observed within

2-8 h after toxin treatment. A nonlytic mutant toxin served as a negative control, thereby excluding a role of any potential contaminants in toxin preparations for effects observed with wild-type toxin. Moreover, negative results using this control support the view that effects obtained with wild-type toxin were due to transient membrane pore formation, rather than mere binding to target cells. Transient expression of *c-fos* has been documented in B lymphocytes within three hours after stimulation with *S. aureus* (179). *c-fos*, *c-jun*, and *egr-1* were also upregulated in the response of respiratory epithelium to the same period of infection by viable *S. aureus* (180). In accord with enhanced *c-fos* and *c-jun* mRNA levels, AP-1 was activated. In this context, it is of note that reduced AP-1 expression levels were found to be one indicator of successful therapy of *S. aureus* infections (181). Furthermore, it has been recently illustrated that infection of skin keratinocytes with the bacterium induces increased gene expression of *hBD-3*, an antimicrobial peptide, through AP-1 proteins (182).

The above data on IEG expression led to the unexpected finding that transient perforation by α-toxin activates the EGFR. EGFR activation is known to increase c-Fos protein and in fact AG1478, a specific inhibitor of the EGFR tyrosine kinase, inhibited c-Fos induction by α-toxin (113). Several publications from other groups have previously demonstrated induction of AP-1 (c-Fos and c-Jun) expression and cell proliferation *via* activation of the EGFR. For example in HaCat cells EGFR was tyrosine-phosphorylated within 15 min after UV B exposure and induced MAPKs and their effectors c-Fos and c-Jun within 50 min (183). In addition to c-Fos and c-Jun, another immediate early gene-encoded protein Egr-1, shown here to be overexpressed upon toxin treatment, also induces EGFR signalling cascades. The synthesis of Egr-1 in HaCat cells occurred 1 h after the stimulation by EGF and thrombin, suggesting that Egr-1 plays an integral part in EGF- and thrombin-induced proliferative signalling (184). Taken together, the analysis of

transcriptional changes in target cells led to the discovery of α-toxin effects that may be of relevance for regulation or disease. Analysis of the role of additional transcripts found in this work (see Table 5) is required and may yield more insights into the mechanisms involved in α-toxin-induced pathology.

In a related work in our lab, Western blots were performed to see whether c-Fos was also induced of the protein level. Confirmatory results were obtained, but conspicuously there was a marked delay between mRNA expression and protein expression of several hours, hinting at the possibility that translation was temporarily blocked.

Translational stop and go following toxin perforation

Recent work of others has shown that translational shutdown occurs in response to various types of stress, and therefore efforts were made to clarify whether this played a role in the present case. Downregulation of protein synthesis is mediated largely through phosphorylation of eIF2α at serine 51. eIF2α inhibits nucleotide exchange on the eIF2 complex, attenuating translation of most mRNAs and reducing protein synthesis (185, 186). In a series of Western blots eIF2α phosphorylation was demonstrated in HaCat cells shortly after attack by α-toxin (Fig. 19-21) This was followed by a massive reduction of protein synthesis at 1 h as measured by [^{35}S]Met incorporation (Fig. 22). Protein synthesis is a major ATP-consuming pathway (25-30%) in the hierarchy of ATP utilizing processes in mammals (187, 188). Thus, by immediately stopping translation of transcripts not absolutely required for short-term survival, cells will conserve ATP; this strategy would take effect more rapidly than eradication of undesired transcripts, as it would include the pool of transcripts already present at the time when stress ensues.

Although reduction of global translation allows cells to conserve resources and to initiate reconfiguration of gene expression to effectively manage stress conditions (137), profound and persistent translational repression might interfere with synthesis of new proteins that promote long-term resistance to the toxin. Therefore, translational suppression would need to be transient in order to save a beneficial effect. In fact, translational repression of HaCat cells in response to α-toxin treatment was released around 4 h post-toxin (Fig. 22).

The cellular mechanisms underlying translational recovery of α-toxin-treated HaCat cells were further investigated. *GADD34*, which is a stress-induced gene encoding a regulatory subunit of PP1 holoenzyme, was demonstrated to be upregulated in HaCat cells 2 h after α-toxin attack. GADD34 attenuates signalling in the integrated stress response (ISR) of eIF2α by recruiting the catalytic subunit of PP1 (PP1c) to the ER, leading to dephosphorylation of eIF2α (122, 168, 169). Inactivation of *GADD34* not only prevented eIF2α dephosphorylation but also inhibited recovery of protein synthesis in mouse embryonic fibroblasts treated with thapsigargin, an ER stress inducer, for 4-8 h (189). The prominent function of GADD34 as a mediator of translational recovery surfaces under the conditions of severe stress, with a requirement of high levels of protein synthesis such as in ischemic neurons in developing brain infarcts (190-192). Phosphorylation of eIF2α also occurs under physiological circumstances, such as in β cells of the endocrine pancreas during glycemic excursions (117, 193) and in the normal metabolism of the liver (194) and GADD34 activation may be an important modulator under these conditions. In cells treated with α-toxin and tautomycetin (TC), a specific inhibitor of PP1, depletion of ATP levels was blunted compared to cells treated with toxin alone (Fig. 28). In addition, massive phosphorylation of eIF2α was observed (Fig. 29). Taken together, these data support a role of PP1

in restarting protein synthesis. PP1 has been demonstrated to contribute to the cellular recovery from stress by acting as an eIF2α phosphatase (195, 196). The hyperphosphorylation of mammalian eIF2α during 4 h ischemic stress has shown to be related to a reduction of PP1-derived eIF2α phosphatase activity (197). A PP1 holoenzyme has been demonstrated to dephosphorylate Snf1, protein kinases that responsed to nutrient starvation and hypoxia in yeast (198, 199). When the nutrient supply rebounds, Snf1 is dephosphorylated by the associated PP1 complex, resulting reinitiation of anabolic pathways (200). PP1 thereby enables the cell to shift to its most energy-efficient and hence preferred fuels. Targeting of PP1 to eIF2α appears to be mediated by GADD34 (122, 168). Indeed, the GADD34/PP1 complex is an efficient eIF2α phosphatase *in vitro*. The complex is lost during hibernation of ground squirrels, and this correlates with a hyperphosphorylation of eIF2α and an inhibition of protein synthesis. Hence, the loss of GADD34-associated PP1 contributes to an eIF2α-mediated inhibition of translation during hibernation and on the contrary, dephosphorylation of eIF2α is involved in the recovery from hibernation (168, 201).

Phosphorylation of eIF2α is carried out by a family of protein kinases, including GCN2, PERK, HRI, and PKR. Since PKR induction is owing to the double-stranded RNA (dsRNA) or viral infection , PKR-dependent phosphorylation of eIF2α seems unlikely to occur in HaCat cells treated with α-toxin. Therefore eIF2α kinases PERK, HRI, and GCN2 are considered candidates in response to α-toxin treatment. Neither an increment of PERK phosphorylation nor an increase in PERK production was observed in toxin-treated cells (Fig. 23). In striking contrast, GCN2 was clearly overexpressed at 10 min after toxin exposure, prior to the induction of eIF2α (Fig. 24). This suggests that GCN2 is the relevant upstream kinase. However, phosphorylated GCN2 was

undetectable and the reason why GCN2 was expressed only at 10 min after toxin treatment was unclear.

Translational "stop and go" is due to a bimodal switch operated by p38

Membrane perforation by toxin leads to rapid activation of p38, which is absolutely required for survival in the case of α-toxin (51). Therefore, a potential link between the p38-pathway and translational downregulation was explored. Phosphorylation of both p38 MAPK and eIF2α have been documented in several conditions such as in mechanical forces of fibroblasts (202), in response of rat hepatocytes to ER stress inducer thapsigargin (203), in prostate cancer cells treated with the protease inhibitor β2-macroglobulin (204), and in myocardial ischemia and reperfusion (205), however, in the above publications the functional relationship has not been addressed. A role of p38 in an eIF2α phosphorylation cascade has been previously suggested, however, p38 has been placed downstream of PKR/eIF2α in that work (206-208). Upon osmotic shock in yeast cells, Hog1p (the only mammalian p38 homolog) activates GCN2p, which subsequently phosphorylates eIF2α in order to downregulate protein synthesis at the initiation level (209). However, a similar relationship between p38 MAPK and GCN2 eIF2α kinase in mammals has not been established so far. Strikingly, p38 inhibitor SB203580 blocked GCN2 expression and eIF2α phosphorylation (Fig. 24). As SB203580 also effectively inhibited α-toxin-mediated induction of the *GADD34* gene (Fig. 27), p38 turns out to be important for both translational shutoff and subsequent restart, by promoting sequential induction of GCN2, phosphorylation of eIF2α, and GADD34 expression. Thus, the present work provides the first link between the SAPK pathway mediated by p38 and the translational shutdown in mammals and hint at a novel bimodal repulatory switch triggered by p38. The findings also provide at least one potential explanation for the emerging role of the p38

pathway in innate defence against the archetypal threat of membrane perforation by small transmembrane-pores. Several publications have documented that p38 MAPK is a survival factor of cells treated with bacteria, including *S. aureus* and their toxins. Inhibition of p38 in α-toxin-treated cells led to disruption of the ATP level recovery and to cell death (51) and to the hypersensitivity of baby hamster kidney cells to PFT proaerolysin (210).

p38-the emerging master regulator of cell defence against PFT

The importance of the p38 pathway for defence against PFT may also be reflected by the fact that it is a target of another bacterial toxin, anthrax lethal factor (LF). MKK3 and MKK6, which act upstream of p38*hog*, are cleaved by LF, a component of lethal toxin (LT), thereby impairing their function (211). Inhibition of p38 MAPK by anthrax LF induces macrophage apoptosis (212). The p38 MAPK-signalling pathway is also important in defence toward bacterial infection and death in the nematode *Caenorhabditis elegans*, proposed to be a model host for several Gram-positive human bacterial pathogens, including *S. aureus* (213-215). *C. elegans* has three genes encoding p38 MAPKs: *pmk-1, -2,* and *-3* (216). p38 MAPK encoded by the *pmk-1* gene (PMK-1) can protect the worm from *Salmonella enterica* infection by a pro-apoptotic activity (217) whilst PMK-3 plays an anti-apoptotic role in the *C. elegans* hermaphrodite germ line (218). It has been demonstrated that *pmk-1* can also be transcriptionally upregulated by Cry5B, a member of the pore-forming Crystal toxin family, made by *Bacillus thuringiensis*. Animals lacking *pmk-1* are hypersensitive to Cry5B.

Phosphorylation of p38 MAPK appears to be a conserved response of epithelial cells to subcytolytic concentrations of bacterial PFTs, including *S. aureus* α-toxin and *S. pneumoniae* pneumolysin although both toxins are not structurally related. Thus, pore-formation, rather than

recognition of specific toxin motifs, seems to be an essential step in the p38 MAPK response to toxins. p38 Phosphorylation can be inhibited by high molecular weight osmolytes in human alveolar epithelial cells (48). p38 has been shown to act upstream of EGFR in sorbitol treated HaCat cells and in stress-stimulated Vero cells by control of shedding of pro-HB-EGF, which is a membrane-anchored form of heparin-binding EGF-like growth factor; one of the EGF ligand (94). In human carcinoma cells, p38 activated the TMPS mechanism of EGFR transactivation, mediated by metalloproteases ADAM9, -10, and -17 (also known as a tumor necrosis factor alpha-converting enzyme) (95). Since tumor necrosis factor-α protease inhibitor 2 (TAPI2), a specific inhibitor of the metalloproteases (219), could block α-toxin-mediated cell proliferation and phosphorylation of Shc (51): a crucial adaptor protein that mediates EGFR-dependent mitogenic signalling (219), TMPS seems to contribute to EGFR signalling in toxin-treated HaCat cells.

Taken together, the present work has identified novel facets of the cellular survival strategies after being attacked by α-toxin (Fig. 30). These mechanisms are likely to contribute to protect and regenerate epithelial barrier function after attack by pore-forming toxins. The work also raises new questions. The further analysis of such questions may lead to additional discoveries in the future and is hoped that these findings will eventually contribute to advances in diagnosis and therapy.

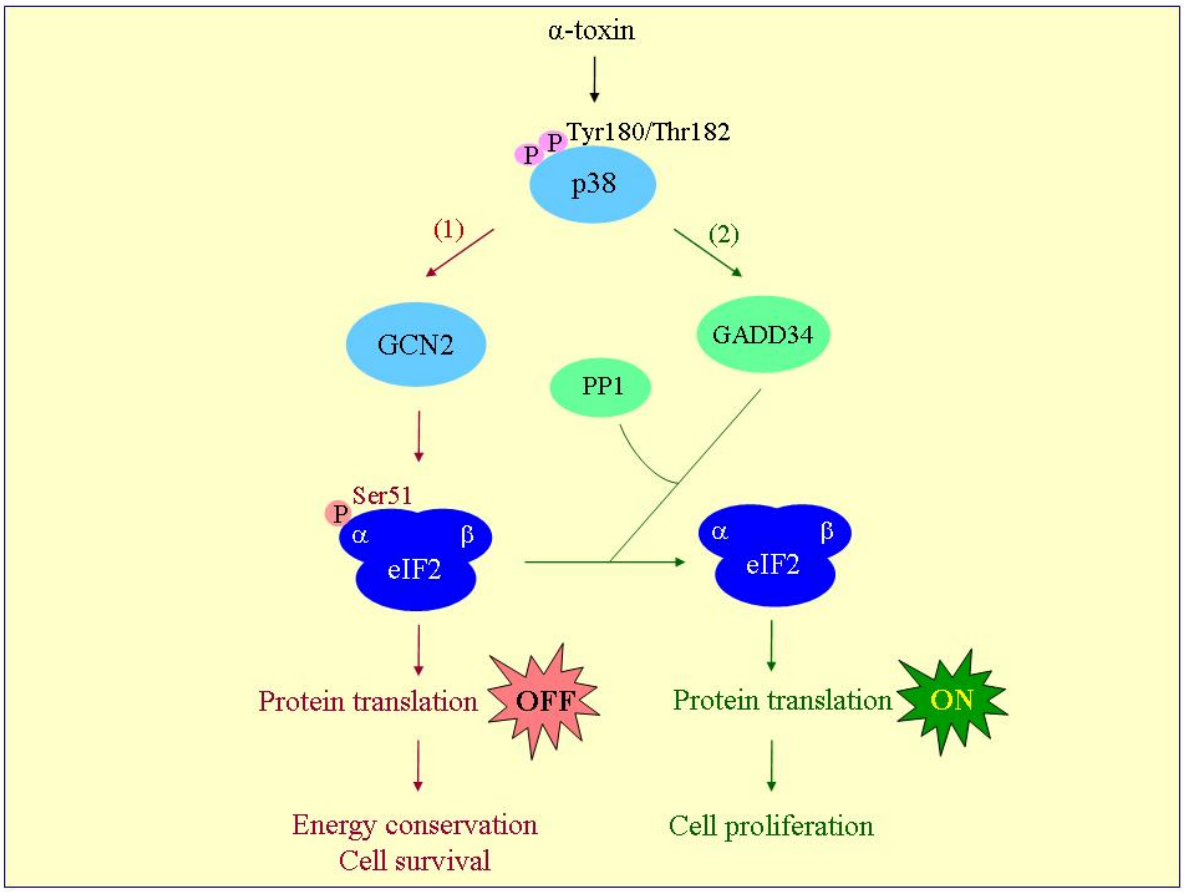

Fig. 30 Translational *stop and go* after membrane perforation by α-toxin. In the early phase after membrane perforation by α-toxin, translation is shut down (red lines, 1), thereby saving energy and increasing the chance of cellular survival. This response is triggered by p38 MAPK and mediated by GCN2, via phosphorylation of eIF2α, ultimately resulting in reduction of translation initiation. Once cells overcome the crisis, p38-induces GADD34, which targets PP1 to dephosphorylate eIF2α. Hence, translation resumes (green lines, 2).

6. PUBLICATIONS

1. Husmann M, Dersch K, Bobkiewicz W, Beckmann E, Veerachato G, Bhakdi S. Differential role of p38 mitogen activated protein kinase for cellular recovery from attack by pore-forming *S. aureus* alpha-toxin or streptolysin O. Biochem Biophys Res Commun. 2006 Jun 16;344(4):1128-34. Epub 2006 Apr 21. PMID: 16643845.

Following the observation that cells are able to recover from membrane lesions incurred by *Staphylococcus aureus* alpha-toxin and streptolysin O (SLO), we investigated the role of p38 in this process. p38 phosphorylation occurred in response to attack by both toxins, commencing within minutes after toxin treatment and waning after several hours. While SLO reportedly activates p38 via ASK1 and ROS, we show that this pathway does not play a major role for p38 induction in alpha-toxin-treated cells. Strikingly divergent effects of p38 blockade were noted depending on the toxin employed. In the case of alpha-toxin, inhibition of p38 within the time frame of its activation led to disruption of the recovery process and to cell death. In contrast, blockade of p38 in SLO permeabilized cells did not affect the capacity of the cells to replenish their ATP stores.

2. Haugwitz U, Bobkiewicz W, Han SR, Beckmann E, Veerachato G, Shaid S, Biehl S, Dersch K, Bhakdi S, Husmann M. Pore-forming *Staphylococcus aureus* alpha-toxin triggers epidermal growth factor receptor-dependent proliferation. Cell Microbiol. 2006 Oct;8(10):1591-600. PMID: 16984414.

Staphylococcal alpha-toxin is an archetypal killer protein that homo-oligomerizes in target cells to create small transmembrane pores. The membrane-perforating beta-barrel motif is a conserved attack element of cytolysins of Gram-positive and Gram-negative bacteria. Following the recognition that nucleated cells can survive membrane permeabilization, a profile of abundant transcripts was obtained in transiently perforated keratinocytes. Several immediate early genes were found to be upregulated, reminiscent of the cellular response to growth factors. Cell cycle analyses revealed doubling of S + G2/M phase cells 26 h post toxin treatment. Determination of cell counts uncovered that after an initial drop, numbers increased to exceed the controls after 2 days. A non-lytic alpha-toxin mutant remained without effect. The alpha-toxin pore is too small to allow egress of cytosolic growth factors, and evidence was instead obtained for growth signalling via the epidermal growth factor receptor (EGFR). Inhibition of the EGFR or of EGFR-proligand-processing blocked the mitogenic effect of alpha-toxin. Western blots with phospho-specific antibodies revealed activation of the EGFR, and of the adapter protein Shc. Immediate early response and proliferation upon transient plasma membrane pore formation by bacterial toxins may represent a novel facet of the complex interaction between pathogen and host.

3. Manuscript in preparation.

4. Poster presentation. G. Veerachato, C. Neukirch, S. Bhakdi, M. Husmann. Translational *Stop and Go*: – an element of cellular survival strategies after attack by a pore forming toxin. Deutschen Gesellschaft für Hygiene und Mikrobiologie e.V. (DGHM) 2006. Würzburg.

Staphylococcus aureus α-toxin is a pore forming toxin that perforates plasma membranes of susceptible target cells by inserting small-diameter heptameric channels. As one consequence of perforation, intracellular ATP levels drop which may eventually lead to the demise of the toxin-attacked cells. However, in many cell types, loss of energy is transient, if moderate toxin-doses are applied. Thus, cells must be in command of strategies to cope with consequences of membrane perforation by α-toxin. We considered the possibility that shutdown of translation may form part of an early cellular response to membrane perforation. In fact, eIF2α proved to be rapidly phosphorylated in toxin-treated cells, leading to the inhibition of protein synthesis. Blockage of eIF-2α dephosphorylation improves ATP levels during the early phase of cellular response after toxin attack. The data lead us to propose that translational *stop and go* helps to control the metabolic derangement inflicted by α-toxin, and to reshape gene-expression patterns later on during recovery. Evidence is provided that this process is linked to stress-induced MAPK pathways.

5. Poster presentation. M. Husmann, K. Dersch1, W. Bobkiewicz1, E. Beckmann1, G. Veerachato, S. Bhakdi. Differential role of p38 MAPK for cellular defense against *S. aureus* alpha-toxin or Streptolysin O

Following the observation that cells are able to recover from membrane lesions incurred by *S. aureus* alpha-toxin and streptolysin O (SLO), we investigated the role of p38 in this process. p38 phosphorylation occurred in response to attack by both toxins, commencing within minutes after toxin treatment and waning after several hours. While SLO reportedly activates p38 via ASK1 and ROS, we find that this pathway is unlikely to play a major role for p38 induction in alpha-toxin treated cells. Strikingly divergent effects of p38 blockade were noted depending on the toxin employed. In the case of alpha-toxin, inhibition of p38 within the time frame of its activation led to disruption of the recovery process and to cell death. In contrast, blockade of p38 in SLO permeabilized cells did not affect the capacity of the cells to replenish their ATP stores.

6. Oral presentation. U. Haugwitz , W. Bobkiewicz, S.R. Han, E. Beckmann, G. Veerachato, S. Shaid, S. Biehl, K. Dersch, S. Bhakdi, M. Husmann. Pore-forming *Staphylococcus aureus* alpha-toxin triggers epidermal growth factor receptor-dependent proliferation.

7. REFERENCES

1. Ostfeld E, Segal J, Segal A, Bogokovski B. Bacterial colonization of the nose and external ear canal in newborn infants. Isr J Med Sci 1983;19(12):1046-9.
2. Namura S, Nishijima S, Higashida T, Asada Y. *Staphylococcus aureus* isolated from nostril anteriors and subungual spaces of the hand: comparative study of medical staff, patients, and normal controls. J Dermatol 1995;22(3):175-80.
3. Noble WC. Skin bacteriology and the role of *Staphylococcus aureus* in infection. Br J Dermatol 1998;139 Suppl 53:9-12.
4. Smith AJ, Jackson MS, Bagg J. The ecology of Staphylococcus species in the oral cavity. J Med Microbiol 2001;50(11):940-6.
5. Arvola T, Ruuska T, Keranen J, Hyoty H, Salminen S, Isolauri E. Rectal bleeding in infancy: clinical, allergological, and microbiological examination. Pediatrics 2006;117(4):e760-8.
6. Rice LB. Antimicrobial resistance in gram-positive bacteria. Am J Infect Control 2006;34(5 Suppl 1):S11-9; discussion S64-73.
7. Prevention CfDCa. *Staphylococcus aureus* resistant to vancomycin-United States. MMWR 2002;51:565-7.
8. Gray GS, Kehoe M. Primary sequence of the alpha-toxin gene from *Staphylococcus aureus* wood 46. Infect Immun 1984;46(2):615-8.
9. Fussle R, Bhakdi S, Sziegoleit A, Tranum-Jensen J, Kranz T, Wellensiek HJ. On the mechanism of membrane damage by *Staphylococcus aureus* alpha-toxin. J Cell Biol 1981;91(1):83-94.
10. Bhakdi S, Tranum-Jensen J. Alpha-toxin of *Staphylococcus aureus.* Microbiol Rev 1991;55(4):733-51.
11. Krishnasastry M, Walker B, Braha O, Bayley H. Surface labeling of key residues during assembly of the transmembrane pore formed by staphylococcal alpha-hemolysin. FEBS Lett 1994;356(1):66-71.
12. Song L, Hobaugh MR, Shustak C, Cheley S, Bayley H, Gouaux JE. Structure of staphylococcal alpha-hemolysin, a heptameric transmembrane pore. Science 1996;274(5294):1859-66.
13. Walev I, Martin E, Jonas D, Mohamadzadeh M, Muller-Klieser W, Kunz L, et al. Staphylococcal alpha-toxin kills human keratinocytes by permeabilizing the plasma membrane for monovalent ions. Infect Immun 1993;61(12):4972-9.
14. Jonas D, Walev I, Berger T, Liebetrau M, Palmer M, Bhakdi S. Novel path to apoptosis: small transmembrane pores created by staphylococcal alpha-toxin in T lymphocytes evoke internucleosomal DNA degradation. Infect Immun 1994;62(4):1304-12.

15. Valeva A, Walev I, Boukhallouk F, Wassenaar TM, Heinz N, Hedderich J, et al. Identification of the membrane penetrating domain of Vibrio cholerae cytolysin as a beta-barrel structure. Mol Microbiol 2005;57(1):124-31.

16. Olson R, Gouaux E. Crystal structure of the Vibrio cholerae cytolysin (VCC) pro-toxin and its assembly into a heptameric transmembrane pore. J Mol Biol 2005;350(5):997-1016.

17. Patel AH, Nowlan P, Weavers ED, Foster T. Virulence of protein A-deficient and alpha-toxin-deficient mutants of *Staphylococcus aureus* isolated by allele replacement. Infect Immun 1987;55(12):3103-10.

18. Haslinger B, Strangfeld K, Peters G, Schulze-Osthoff K, Sinha B. *Staphylococcus aureus* alpha-toxin induces apoptosis in peripheral blood mononuclear cells: role of endogenous tumour necrosis factor-alpha and the mitochondrial death pathway. Cell Microbiol 2003;5(10):729-41.

19. Menzies BE, Kourteva I. *Staphylococcus aureus* alpha-toxin induces apoptosis in endothelial cells. FEMS Immunol Med Microbiol 2000;29(1):39-45.

20. Alder GM, Austen BM, Bashford CL, Mehlert A, Pasternak CA. Heat shock proteins induce pores in membranes. Biosci Rep 1990;10(6):509-18.

21. Kultz D. Evolution of the cellular stress proteome: from monophyletic origin to ubiquitous function. J Exp Biol 2003;206(Pt 18):3119-24.

22. Leach JK, Van Tuyle G, Lin PS, Schmidt-Ullrich R, Mikkelsen RB. Ionizing radiation-induced, mitochondria-dependent generation of reactive oxygen/nitrogen. Cancer Res 2001;61(10):3894-901.

23. Mikkelsen RB, Wardman P. Biological chemistry of reactive oxygen and nitrogen and radiation-induced signal transduction mechanisms. Oncogene 2003;22(37):5734-54.

24. Kultz D. Phylogenetic and functional classification of mitogen- and stress-activated protein kinases. J Mol Evol 1998;46(5):571-88.

25. Fu H, Subramanian RR, Masters SC. 14-3-3 proteins: structure, function, and regulation. Annu Rev Pharmacol Toxicol 2000;40:617-47.

26. Wiens M, Diehl-Seifert B, Muller WE. Sponge Bcl-2 homologous protein (BHP2-GC) confers distinct stress resistance to human HEK-293 cells. Cell Death Differ 2001;8(9):887-98.

27. Craven RJ, Greenwell PW, Dominska M, Petes TD. Regulation of genome stability by TEL1 and MEC1, yeast homologs of the mammalian ATM and ATR genes. Genetics 2002;161(2):493-507.

28. Skorokhod A, Gamulin V, Gundacker D, Kavsan V, Muller IM, Muller WE. Origin of insulin receptor-like tyrosine kinases in marine sponges. Biol Bull 1999;197(2):198-206.

29. Leonarduzzi G, Arkan MC, Basaga H, Chiarpotto E, Sevanian A, Poli G. Lipid oxidation products in cell signaling. Free Radic Biol Med 2000;28(9):1370-8.

30. Spiteller G. Lipid peroxidation in aging and age-dependent diseases. Exp Gerontol 2001;36(9):1425-57.

31. Kultz D. Molecular and evolutionary basis of the cellular stress response. Annu Rev Physiol 2005;67:225-57.

32. Kaminska B. MAPK signalling pathways as molecular targets for anti-inflammatory therapy--from molecular mechanisms to therapeutic benefits. Biochim Biophys Acta 2005;1754(1-2):253-62.

33. English J, Pearson G, Wilsbacher J, Swantek J, Karandikar M, Xu S, et al. New insights into the control of MAP kinase pathways. Exp Cell Res 1999;253(1):255-70.

34. Chang L, Karin M. Mammalian MAP kinase signalling cascades. Nature 2001;410(6824):37-40.

35. Pearson G, Robinson F, Beers Gibson T, Xu BE, Karandikar M, Berman K, et al. Mitogen-activated protein (MAP) kinase pathways: regulation and physiological functions. Endocr Rev 2001;22(2):153-83.

36. Boulton TG, Yancopoulos GD, Gregory JS, Slaughter C, Moomaw C, Hsu J, et al. An insulin-stimulated protein kinase similar to yeast kinases involved in cell cycle control. Science 1990;249(4964):64-7.

37. Boulton TG, Nye SH, Robbins DJ, Ip NY, Radziejewska E, Morgenbesser SD, et al. ERKs: a family of protein-serine/threonine kinases that are activated and tyrosine phosphorylated in response to insulin and NGF. Cell 1991;65(4):663-75.

38. Zheng CF, Guan KL. Properties of MEKs, the kinases that phosphorylate and activate the extracellular signal-regulated kinases. J Biol Chem 1993;268(32):23933-9.

39. Derijard B, Raingeaud J, Barrett T, Wu IH, Han J, Ulevitch RJ, et al. Independent human MAP-kinase signal transduction pathways defined by MEK and MKK isoforms. Science 1995;267(5198):682-5.

40. Stein B, Brady H, Yang MX, Young DB, Barbosa MS. Cloning and characterization of MEK6, a novel member of the mitogen-activated protein kinase kinase cascade. J Biol Chem 1996;271(19):11427-33.

41. Yao Z, Diener K, Wang XS, Zukowski M, Matsumoto G, Zhou G, et al. Activation of stress-activated protein kinases/c-Jun N-terminal protein kinases (SAPKs/JNKs) by a novel mitogen-activated protein kinase kinase. J Biol Chem 1997;272(51):32378-83.

42. Zhou G, Bao ZQ, Dixon JE. Components of a new human protein kinase signal transduction pathway. J Biol Chem 1995;270(21):12665-9.

43. Lee JD, Ulevitch RJ, Han J. Primary structure of BMK1: a new mammalian map kinase. Biochem Biophys Res Commun 1995;213(2):715-24.

44. Cheng M, Zhen E, Robinson MJ, Ebert D, Goldsmith E, Cobb MH. Characterization of a protein kinase that phosphorylates serine 189 of the mitogen-activated protein kinase homolog ERK3. J Biol Chem 1996;271(20):12057-62.

45. Cuschieri J, Maier RV. Mitogen-activated protein kinase (MAPK). Crit Care Med 2005;33(12 Suppl):S417-9.

46. Wang X, Rao J, Studzinski GP. Inhibition of p38 MAP kinase activity up-regulates multiple MAP kinase pathways and potentiates 1,25-dihydroxyvitamin D(3)-induced differentiation of human leukemia HL60 cells. Exp Cell Res 2000;258(2):425-37.

47. Weitzman JB, Yaniv M. Signal transduction pathways and modulation of gene activity. Clin Chem Lab Med 1998;36(8):535-9.

48. Ratner AJ, Hippe KR, Aguilar JL, Bender MH, Nelson AL, Weiser JN. Epithelial cells are sensitive detectors of bacterial pore-forming toxins. J Biol Chem 2006;281(18):12994-8.

49. Stringaris AK, Geisenhainer J, Bergmann F, Balshusemann C, Lee U, Zysk G, et al. Neurotoxicity of pneumolysin, a major pneumococcal virulence factor, involves calcium influx and depends on activation of p38 mitogen-activated protein kinase. Neurobiol Dis 2002;11(3):355-68.

50. Stassen M, Muller C, Richter C, Neudorfl C, Hultner L, Bhakdi S, et al. The streptococcal exotoxin streptolysin O activates mast cells to produce tumor necrosis factor alpha by p38 mitogen-activated protein kinase- and protein kinase C-dependent pathways. Infect Immun 2003;71(11):6171-7.

51. Husmann M, Dersch K, Bobkiewicz W, Beckmann E, Veerachato G, Bhakdi S. Differential role of p38 mitogen activated protein kinase for cellular recovery from attack by pore-forming *S. aureus* alpha-toxin or streptolysin O. Biochem Biophys Res Commun 2006;344(4):1128-34.

52. Park JM, Ng VH, Maeda S, Rest RF, Karin M. Anthrolysin O and other gram-positive cytolysins are toll-like receptor 4 agonists. J Exp Med 2004;200(12):1647-55.

53. Han J, Lee JD, Bibbs L, Ulevitch RJ. A MAP kinase targeted by endotoxin and hyperosmolarity in mammalian cells. Science 1994;265(5173):808-11.

54. Lee JC, Laydon JT, McDonnell PC, Gallagher TF, Kumar S, Green D, et al. A protein kinase involved in the regulation of inflammatory cytokine biosynthesis. Nature 1994;372(6508):739-46.

55. Rouse J, Cohen P, Trigon S, Morange M, Alonso-Llamazares A, Zamanillo D, et al. A novel kinase cascade triggered by stress and heat shock that stimulates MAPKAP kinase-2 and phosphorylation of the small heat shock proteins. Cell 1994;78(6):1027-37.

56. Jiang Y, Chen C, Li Z, Guo W, Gegner JA, Lin S, et al. Characterization of the structure and function of a new mitogen-activated protein kinase (p38beta). J Biol Chem 1996;271(30):17920-6.

57. Stein B, Yang MX, Young DB, Janknecht R, Hunter T, Murray BW, et al. p38-2, a novel mitogen-activated protein kinase with distinct properties. J Biol Chem 1997;272(31):19509-17.

58. Li Z, Jiang Y, Ulevitch RJ, Han J. The primary structure of p38 gamma: a new member of p38 group of MAP kinases. Biochem Biophys Res Commun 1996;228(2):334-40.

59. Jiang Y, Gram H, Zhao M, New L, Gu J, Feng L, et al. Characterization of the structure and function of the fourth member of p38 group mitogen-activated protein kinases, p38delta. J Biol Chem 1997;272(48):30122-8.

60. Goedert M, Cuenda A, Craxton M, Jakes R, Cohen P. Activation of the novel stress-activated protein kinase SAPK4 by cytokines and cellular stresses is mediated by SKK3 (MKK6); comparison of its substrate specificity with that of other SAP kinases. Embo J 1997;16(12):3563-71.

61. Bode JG, Gatsios P, Ludwig S, Rapp UR, Haussinger D, Heinrich PC, et al. The mitogen-activated protein (MAP) kinase p38 and its upstream activator MAP kinase kinase 6 are involved in the activation of signal transducer and activator of transcription by hyperosmolarity. J Biol Chem 1999;274(42):30222-7.

62. Bode AM, Dong Z. Mitogen-activated protein kinase activation in UV-induced signal transduction. Sci STKE 2003;2003(167):RE2.

63. El Benna J, Han J, Park JW, Schmid E, Ulevitch RJ, Babior BM. Activation of p38 in stimulated human neutrophils: phosphorylation of the oxidase component p47phox by p38 and ERK but not by JNK. Arch Biochem Biophys 1996;334(2):395-400.

64. Krump E, Sanghera JS, Pelech SL, Furuya W, Grinstein S. Chemotactic peptide N-formyl-met-leu-phe activation of p38 mitogen-activated protein kinase (MAPK) and MAPK-activated protein kinase-2 in human neutrophils. J Biol Chem 1997;272(2):937-44.

65. Perregaux DG, Dean D, Cronan M, Connelly P, Gabel CA. Inhibition of interleukin-1 beta production by SKF86002: evidence of two sites of in vitro activity and of a time and system dependence. Mol Pharmacol 1995;48(3):433-42.

66. Guan Z, Buckman SY, Pentland AP, Templeton DJ, Morrison AR. Induction of cyclooxygenase-2 by the activated MEKK1 --> SEK1/MKK4 --> p38 mitogen-activated protein kinase pathway. J Biol Chem 1998;273(21):12901-8.

67. Da Silva J, Pierrat B, Mary JL, Lesslauer W. Blockade of p38 mitogen-activated protein kinase pathway inhibits inducible nitric-oxide synthase expression in mouse astrocytes. J Biol Chem 1997;272(45):28373-80.

68. Badger AM, Cook MN, Lark MW, Newman-Tarr TM, Swift BA, Nelson AH, et al. SB 203580 Inhibits p38 Mitogen-Activated Protein Kinase, Nitric Oxide Production, and Inducible Nitric Oxide Synthase in Bovine Cartilage-Derived Chondrocytes. The Journal of Immunology 1998;161:467-473.

69. Pietersma A, Tilly BC, Gaestel M, de Jong N, Lee JC, Koster JF, et al. p38 mitogen activated protein kinase regulates endothelial VCAM-1 expression at the post-transcriptional level. Biochem Biophys Res Commun 1997;230(1):44-8.

70. Craxton A, Shu G, Graves JD, Saklatvala J, Krebs EG, Clark EA. p38 MAPK is required for CD40-induced gene expression and proliferation in B lymphocytes. J Immunol 1998;161(7):3225-36.

71. Meja KK, Seldon PM, Nasuhara Y, Ito K, Barnes PJ, Lindsay MA, et al. p38 MAP kinase and MKK-1 co-operate in the generation of GM-CSF from LPS-stimulated human monocytes by an NF-kappa B-independent mechanism. Br J Pharmacol 2000;131(6):1143-53.

72. Zhang S, Liu H, Liu J, Tse CA, Dragunow M, Cooper GJ. Activation of activating transcription factor 2 by p38 MAP kinase during apoptosis induced by human amylin in cultured pancreatic beta-cells. Febs J 2006;273(16):3779-91.

73. Baan B, van Dam H, van der Zon GC, Maassen JA, Ouwens DM. The role of c-Jun N-terminal kinase, p38, and extracellular signal-regulated kinase in insulin-induced Thr69 and Thr71 phosphorylation of activating transcription factor 2. Mol Endocrinol 2006;20(8):1786-95.

74. Harper EG, Alvares SM, Carter WG. Wounding activates p38 map kinase and activation transcription factor 3 in leading keratinocytes. J Cell Sci 2005;118(Pt 15):3471-85.

75. Xia W, Longaker MT, Yang GP. P38 MAP kinase mediates transforming growth factor-beta2 transcription in human keloid fibroblasts. Am J Physiol Regul Integr Comp Physiol 2006;290(3):R501-8.

76. Stassen M, Klein M, Becker M, Bopp T, Neudorfl C, Richter C, et al. p38 MAP kinase drives the expression of mast cell-derived IL-9 via activation of the transcription factor GATA-1. Mol Immunol 2007;44(5):926-33.

77. Sii-Felice K, Pouponnot C, Gillet S, Lecoin L, Girault JA, Eychene A, et al. MafA transcription factor is phosphorylated by p38 MAP kinase. FEBS Lett 2005;579(17):3547-54.

78. Han J, Jiang Y, Li Z, Kravchenko VV, Ulevitch RJ. Activation of the transcription factor MEF2C by the MAP kinase p38 in inflammation. Nature 1997;386(6622):296-9.

79. Deak M, Clifton AD, Lucocq LM, Alessi DR. Mitogen- and stress-activated protein kinase-1 (MSK1) is directly activated by MAPK and SAPK2/p38, and may mediate activation of CREB. Embo J 1998;17(15):4426-41.

80. Cheng H, Kartenbeck J, Kabsch K, Mao X, Marques M, Alonso A. Stress kinase p38 mediates EGFR transactivation by hyperosmolar concentrations of sorbitol. J Cell Physiol 2002;192(2):234-43.

81. Zwang Y, Yarden Y. p38 MAP kinase mediates stress-induced internalization of EGFR: implications for cancer chemotherapy. Embo J 2006;25(18):4195-206.

82. van der Geer P, Hunter T, Lindberg RA. Receptor protein-tyrosine kinases and their signal transduction pathways. Annu Rev Cell Biol 1994;10:251-337.

83. Ullrich A, Coussens L, Hayflick JS, Dull TJ, Gray A, Tam AW, et al. Human epidermal growth factor receptor cDNA sequence and aberrant expression of the amplified gene in A431 epidermoid carcinoma cells. Nature 1984;309(5967):418-25.

84. Massague J, Pandiella A. Membrane-anchored growth factors. Annu Rev Biochem 1993;62:515-41.

85. Ullrich A, Schlessinger J. Signal transduction by receptors with tyrosine kinase activity. Cell 1990;61(2):203-12.

86. Heldin CH. Dimerization of cell surface receptors in signal transduction. Cell 1995;80(2):213-23.

87. Alroy I, Yarden Y. The ErbB signaling network in embryogenesis and oncogenesis: signal diversification through combinatorial ligand-receptor interactions. FEBS Lett 1997;410(1):83-6.

88. Prenzel N, Fischer OM, Streit S, Hart S, Ullrich A. The epidermal growth factor receptor family as a central element for cellular signal transduction and diversification. Endocr Relat Cancer 2001;8(1):11-31.

89. Merion M, Sly WS. The role of intermediate vesicles in the adsorptive endocytosis and transport of ligand to lysosomes by human fibroblasts. J Cell Biol 1983;96(3):644-50.

90. Vieira AV, Lamaze C, Schmid SL. Control of EGF receptor signaling by clathrin-mediated endocytosis. Science 1996;274(5295):2086-9.

91. Wang Y, Pennock S, Chen X, Wang Z. Endosomal signaling of epidermal growth factor receptor stimulates signal transduction pathways leading to cell survival. Mol Cell Biol 2002;22(20):7279-90.

92. Pennock S, Wang Z. Stimulation of cell proliferation by endosomal epidermal growth factor receptor as revealed through two distinct phases of signaling. Mol Cell Biol 2003;23(16):5803-15.

93. Carpenter G. Employment of the epidermal growth factor receptor in growth factor-independent signaling pathways. J Cell Biol 1999;146(4):697-702.

94. Takenobu H, Yamazaki A, Hirata M, Umata T, Mekada E. The stress- and inflammatory cytokine-induced ectodomain shedding of heparin-binding epidermal growth factor-like growth factor is mediated by p38 MAPK, distinct from the 12-O-tetradecanoylphorbol-13-acetate- and lysophosphatidic acid-induced signaling cascades. J Biol Chem 2003;278(19):17255-62.

95. Fischer OM, Hart S, Gschwind A, Prenzel N, Ullrich A. Oxidative and osmotic stress signaling in tumor cells is mediated by ADAM proteases and heparin-binding epidermal growth factor. Mol Cell Biol 2004;24(12):5172-83.

96. Fischer OM, Hart S, Gschwind A, Ullrich A. EGFR signal transactivation in cancer cells. Biochem Soc Trans 2003;31(Pt 6):1203-8.

97. Chen N, Ma WY, She QB, Wu E, Liu G, Bode AM, et al. Transactivation of the epidermal growth factor receptor is involved in 12-O-tetradecanoylphorbol-13-acetate-induced signal transduction. J Biol Chem 2001;276(50):46722-8.

98. Maki Y, Bos TJ, Davis C, Starbuck M, Vogt PK. Avian sarcoma virus 17 carries the jun oncogene. Proc Natl Acad Sci U S A 1987;84(9):2848-52.

99. Ball AR, Jr., Bos TJ, Loliger C, Nagata LP, Nishimura T, Su H, et al. Jun: oncogene and transcriptional regulator. Cold Spring Harb Symp Quant Biol 1988;53 Pt 2:687-93.

100. Ryder K, Lau LF, Nathans D. A gene activated by growth factors is related to the oncogene v-jun. Proc Natl Acad Sci U S A 1988;85(5):1487-91.

101. Hirai SI, Ryseck RP, Mechta F, Bravo R, Yaniv M. Characterization of junD: a new member of the jun proto-oncogene family. Embo J 1989;8(5):1433-9.

102. Ryder K, Lanahan A, Perez-Albuerne E, Nathans D. jun-D: a third member of the jun gene family. Proc Natl Acad Sci U S A 1989;86(5):1500-3.

103. Curran T, Peters G, Van Beveren C, Teich NM, Verma IM. FBJ murine osteosarcoma virus: identification and molecular cloning of biologically active proviral DNA. J Virol 1982;44(2):674-82.

104. Cohen DR, Curran T. fra-1: a serum-inducible, cellular immediate-early gene that encodes a fos-related antigen. Mol Cell Biol 1988;8(5):2063-9.

105. Zerial M, Toschi L, Ryseck RP, Schuermann M, Muller R, Bravo R. The product of a novel growth factor activated gene, fos B, interacts with JUN proteins enhancing their DNA binding activity. Embo J 1989;8(3):805-13.

106. Matsui M, Tokuhara M, Konuma Y, Nomura N, Ishizaki R. Isolation of human fos-related genes and their expression during monocyte-macrophage differentiation. Oncogene 1990;5(3):249-55.

107. Nishina H, Sato H, Suzuki T, Sato M, Iba H. Isolation and characterization of fra-2, an additional member of the fos gene family. Proc Natl Acad Sci U S A 1990;87(9):3619-23.

108. Karin M, Liu Z, Zandi E. AP-1 function and regulation. Curr Opin Cell Biol 1997;9(2):240-6.

109. Angel P, Karin M. The role of Jun, Fos and the AP-1 complex in cell-proliferation and transformation. Biochim Biophys Acta 1991;1072(2-3):129-57.

110. Nakabeppu Y, Ryder K, Nathans D. DNA binding activities of three murine Jun proteins: stimulation by Fos. Cell 1988;55(5):907-15.

111. Coso OA, Montaner S, Fromm C, Lacal JC, Prywes R, Teramoto H, et al. Signaling from G protein-coupled receptors to the c-jun promoter involves the MEF2 transcription factor. Evidence for a novel c-jun amino-terminal kinase-independent pathway. J Biol Chem 1997;272(33):20691-7.

112. Marinissen MJ, Chiariello M, Gutkind JS. Regulation of gene expression by the small GTPase Rho through the ERK6 (p38 gamma) MAP kinase pathway. Genes Dev 2001;15(5):535-53.

113. Haugwitz U, Bobkiewicz W, Han S-R, Beckmann E, Veerachato G, Shaid S, et al. Pore-forming *Staphylococcus aureus* α-toxin triggers epidermal growth factor receptor-dependent proliferation. Cellular Microbiology 2006;in press.

114. Harding HP, Calfon M, Urano F, Novoa I, Ron D. Transcriptional and translational control in the Mammalian unfolded protein response. Annu Rev Cell Dev Biol 2002;18:575-99.

115. Lu PD, Harding HP, Ron D. Translation reinitiation at alternative open reading frames regulates gene expression in an integrated stress response. J Cell Biol 2004;167(1):27-33.

116. Harding HP, Novoa I, Zhang Y, Zeng H, Wek R, Schapira M, et al. Regulated translation initiation controls stress-induced gene expression in mammalian cells. Mol Cell 2000;6(5):1099-108.

117. Scheuner D, Song B, McEwen E, Liu C, Laybutt R, Gillespie P, et al. Translational control is required for the unfolded protein response and in vivo glucose homeostasis. Mol Cell 2001;7(6):1165-76.

118. Lu PD, Jousse C, Marciniak SJ, Zhang Y, Novoa I, Scheuner D, et al. Cytoprotection by pre-emptive conditional phosphorylation of translation initiation factor 2. Embo J 2004;23(1):169-79.

119. Aridor M, Balch WE. Integration of endoplasmic reticulum signaling in health and disease. Nat Med 1999;5(7):745-51.

120. Zhang P, McGrath B, Li S, Frank A, Zambito F, Reinert J, et al. The PERK eukaryotic initiation factor 2 alpha kinase is required for the development of the skeletal system, postnatal growth, and the function and viability of the pancreas. Mol Cell Biol 2002;22(11):3864-74.

121. Chang RC, Wong AK, Ng HK, Hugon J. Phosphorylation of eukaryotic initiation factor-2alpha (eIF2alpha) is associated with neuronal degeneration in Alzheimer's disease. Neuroreport 2002;13(18):2429-32.

122. Novoa I, Zeng H, Harding HP, Ron D. Feedback inhibition of the unfolded protein response by GADD34-mediated dephosphorylation of eIF2alpha. J Cell Biol 2001;153(5):1011-22.

123. Harding HP, Zhang Y, Zeng H, Novoa I, Lu PD, Calfon M, et al. An integrated stress response regulates amino acid metabolism and resistance to oxidative stress. Mol Cell 2003;11(3):619-33.

124. Ma Y, Hendershot LM. Herp is dually regulated by both the endoplasmic reticulum stress-specific branch of the unfolded protein response and a branch that is shared with other cellular stress pathways. J Biol Chem 2004;279(14):13792-9.

125. Vattem KM, Wek RC. Reinitiation involving upstream ORFs regulates ATF4 mRNA translation in mammalian cells. Proc Natl Acad Sci U S A 2004;101(31):11269-74.

126. Prelich G, Kostura M, Marshak DR, Mathews MB, Stillman B. The cell-cycle regulated proliferating cell nuclear antigen is required for SV40 DNA replication in vitro. Nature 1987;326(6112):471-5.

127. Byrnes JJ, Downey KM, Black VL, So AG. A new mammalian DNA polymerase with 3' to 5' exonuclease activity: DNA polymerase delta. Biochemistry 1976;15(13):2817-23.

128. Imai H, Harland J, McCulloch J, Graham DI, Brown SM, Macrae IM. Specific expression of the cell cycle regulation proteins, GADD34 and PCNA, in the peri-infarct zone after focal cerebral ischaemia in the rat. Eur J Neurosci 2002;15(12):1929-36.

129. Mori K. Tripartite management of unfolded proteins in the endoplasmic reticulum. Cell 2000;101(5):451-4.

130. Bi M, Naczki C, Koritzinsky M, Fels D, Blais J, Hu N, et al. ER stress-regulated translation increases tolerance to extreme hypoxia and promotes tumor growth. Embo J 2005;24(19):3470-81.

131. Kimball SR. Eukaryotic initiation factor eIF2. Int J Biochem Cell Biol 1999;31(1):25-9.

132. Hershey JW, Asano K, Naranda T, Vornlocher HP, Hanachi P, Merrick WC. Conservation and diversity in the structure of translation initiation factor EIF3 from humans and yeast. Biochimie 1996;78(11-12):903-7.

133. Hentze MW. eIF4G: a multipurpose ribosome adapter? Science 1997;275(5299):500-1.

134. Merrick WC. Eukaryotic protein synthesis: an in vitro analysis. Biochimie 1994;76(9):822-30.

135. Pain VM. Initiation of protein synthesis in eukaryotic cells. Eur J Biochem 1996;236(3):747-71.

136. Clemens MJ, Bushell M, Jeffrey IW, Pain VM, Morley SJ. Translation initiation factor modifications and the regulation of protein synthesis in apoptotic cells. Cell Death Differ 2000;7(7):603-15.

137. Wek RC, Jiang HY, Anthony TG. Coping with stress: eIF2 kinases and translational control. Biochem Soc Trans 2006;34(Pt 1):7-11.

138. Hinnebusch AG. The eIF-2 alpha kinases: regulators of protein synthesis in starvation and stress. Semin Cell Biol 1994;5(6):417-26.

139. Anthony TG, McDaniel BJ, Byerley RL, McGrath BC, Cavener DR, McNurlan MA, et al. Preservation of liver protein synthesis during dietary leucine deprivation occurs at the expense of skeletal muscle mass in mice deleted for eIF2 kinase GCN2. J Biol Chem 2004;279(35):36553-61.

140. Hinnebusch AG, Natarajan K. Gcn4p, a master regulator of gene expression, is controlled at multiple levels by diverse signals of starvation and stress. Eukaryot Cell 2002;1(1):22-32.

141. Dong J, Qiu H, Garcia-Barrio M, Anderson J, Hinnebusch AG. Uncharged tRNA activates GCN2 by displacing the protein kinase moiety from a bipartite tRNA-binding domain. Mol Cell 2000;6(2):269-79.

142. Munn DH, Sharma MD, Baban B, Harding HP, Zhang Y, Ron D, et al. GCN2 kinase in T cells mediates proliferative arrest and anergy induction in response to indoleamine 2,3-dioxygenase. Immunity 2005;22(5):633-42.

143. Harding HP, Zhang Y, Bertolotti A, Zeng H, Ron D. Perk is essential for translational regulation and cell survival during the unfolded protein response. Mol Cell 2000;5(5):897-904.

144. Barber GN. The dsRNA-dependent protein kinase, PKR and cell death. Cell Death Differ 2005;12(6):563-70.

145. Lu L, Han AP, Chen JJ. Translation initiation control by heme-regulated eukaryotic initiation factor 2alpha kinase in erythroid cells under cytoplasmic stresses. Mol Cell Biol 2001;21(23):7971-80.

146. Boukamp P, Petrussevska RT, Breitkreutz D, Hornung J, Markham A, Fusenig NE. Normal keratinization in a spontaneously immortalized aneuploid human keratinocyte cell line. J Cell Biol 1988;106(3):761-71.

147. Hildebrand A, Pohl M, Bhakdi S. *Staphylococcus aureus* alpha-toxin. Dual mechanism of binding to target cells. J Biol Chem 1991;266(26):17195-200.

148. Smyth GK, Yang YH, Speed T. Statistical issues in cDNA microarray data analysis. Methods Mol Biol 2003;224:111-36.

149. Dudoit S, Yang YH, Callow MJ, Speed TP. Statistical methods for identifying genes with differential expression in replicated cDNA microarray experiments. Statistica Sinica 2002;12:111-139.

150. Livak KJ, Schmittgen TD. Analysis of relative gene expression data using real-time quantitative PCR and the 2(-Delta Delta C(T)) Method. Methods 2001;25(4):402-8.

151. Pfaffl MW. A new mathematical model for relative quantification in real-time RT-PCR. Nucleic Acids Res 2001;29(9):e45.

152. Dragneva Y, Anuradha CD, Valeva A, Hoffmann A, Bhakdi S, Husmann M. Subcytocidal attack by staphylococcal alpha-toxin activates NF-kappaB and induces interleukin-8 production. Infect Immun 2001;69(4):2630-5.

153. de Leeuw WJ, Slagboom PE, Vijg J. Quantitative comparison of mRNA levels in mammalian tissues: 28S ribosomal RNA level as an accurate internal control. Nucleic Acids Res 1989;17(23):10137-8.

154. Goidin D, Mamessier A, Staquet MJ, Schmitt D, Berthier-Vergnes O. Ribosomal 18S RNA prevails over glyceraldehyde-3-phosphate dehydrogenase and beta-actin genes as internal standard for quantitative comparison of mRNA levels in invasive and noninvasive human melanoma cell subpopulations. Anal Biochem 2001;295(1):17-21.

155. Lecomte F, Szpirer J, Szpirer C. The S3a ribosomal protein gene is identical to the Fte-1 (v-fos transformation effector) gene and the TNF-alpha-induced TU-11 gene, and its transcript level is altered in transformed and tumor cells. Gene 1997;186(2):271-7.

156. Brush MH, Weiser DC, Shenolikar S. Growth arrest and DNA damage-inducible protein GADD34 targets protein phosphatase 1 alpha to the endoplasmic reticulum and promotes dephosphorylation of the alpha subunit of eukaryotic translation initiation factor 2. Mol Cell Biol 2003;23(4):1292-303.

157. Kojima E, Takeuchi A, Haneda M, Yagi A, Hasegawa T, Yamaki K, et al. The function of GADD34 is a recovery from a shutoff of protein synthesis induced by ER stress: elucidation by GADD34-deficient mice. Faseb J 2003;17(11):1573-5.

158. Shaulian E, Karin M. AP-1 as a regulator of cell life and death. Nat Cell Biol 2002;4(5):E131-6.

159. Hodin RA, Meng S, Nguyen D. Immediate-early gene expression in EGF-stimulated intestinal epithelial cells. J Surg Res 1994;56(6):500-4.

160. Heinrich R, Kraiem Z. The protein kinase A pathway inhibits c-jun and c-fos protooncogene expression induced by the protein kinase C and tyrosine kinase pathways in cultured human thyroid follicles. J Clin Endocrinol Metab 1997;82(6):1839-44.

161. Crowe DL, Brown TN. Transcriptional inhibition of matrix metalloproteinase 9 (MMP-9) activity by a c-fos/estrogen receptor fusion protein is mediated by the proximal AP-1 site of

the MMP-9 promoter and correlates with reduced tumor cell invasion. Neoplasia 1999;1(4):368-72.

162. Simon C, Simon M, Vucelic G, Hicks MJ, Plinkert PK, Koitschev A, et al. The p38 SAPK pathway regulates the expression of the MMP-9 collagenase via AP-1-dependent promoter activation. Exp Cell Res 2001;271(2):344-55.

163. Sato H, Seiki M. Regulatory mechanism of 92 kDa type IV collagenase gene expression which is associated with invasiveness of tumor cells. Oncogene 1993;8(2):395-405.

164. Farina AR, Tacconelli A, Vacca A, Maroder M, Gulino A, Mackay AR. Transcriptional up-regulation of matrix metalloproteinase-9 expression during spontaneous epithelial to neuroblast phenotype conversion by SK-N-SH neuroblastoma cells, involved in enhanced invasivity, depends upon GT-box and nuclear factor kappaB elements. Cell Growth Differ 1999;10(5):353-67.

165. Benbow U, Brinckerhoff CE. The AP-1 site and MMP gene regulation: what is all the fuss about? Matrix Biol 1997;15(8-9):519-26.

166. Kaufman RJ. Stress signaling from the lumen of the endoplasmic reticulum: coordination of gene transcriptional and translational controls. Genes Dev 1999;13(10):1211-33.

167. Sheikh MS, Fornace AJ, Jr. Regulation of translation initiation following stress. Oncogene 1999;18(45):6121-8.

168. Connor JH, Weiser DC, Li S, Hallenbeck JM, Shenolikar S. Growth arrest and DNA damage-inducible protein GADD34 assembles a novel signaling complex containing protein phosphatase 1 and inhibitor 1. Mol Cell Biol 2001;21(20):6841-50.

169. Jiang HY, Wek SA, McGrath BC, Lu D, Hai T, Harding HP, et al. Activating transcription factor 3 is integral to the eukaryotic initiation factor 2 kinase stress response. Mol Cell Biol 2004;24(3):1365-77.

170. Mitsuhashi S, Matsuura N, Ubukata M, Oikawa H, Shima H, Kikuchi K. Tautomycetin is a novel and specific inhibitor of serine/threonine protein phosphatase type 1, PP1. Biochem Biophys Res Commun 2001;287(2):328-31.

171. Mitsuhashi S, Shima H, Tanuma N, Matsuura N, Takekawa M, Urano T, et al. Usage of tautomycetin, a novel inhibitor of protein phosphatase 1 (PP1), reveals that PP1 is a positive regulator of Raf-1 in vivo. J Biol Chem 2003;278(1):82-8.

172. Walev I, Palmer M, Martin E, Jonas D, Weller U, Hohn-Bentz H, et al. Recovery of human fibroblasts from attack by the pore-forming alpha-toxin of *Staphylococcus aureus*. Microb Pathog 1994;17(3):187-201.

173. Valeva A, Walev I, Gerber A, Klein J, Palmer M, Bhakdi S. Staphylococcal alpha-toxin: repair of a calcium-impermeable pore in the target cell membrane. Mol Microbiol 2000;36(2):467-76.

174. Basler M, Masin J, Osicka R, Sebo P. Pore-forming and enzymatic activities of Bordetella pertussis adenylate cyclase toxin synergize in promoting lysis of monocytes. Infect Immun 2006;74(4):2207-14.

175. Hewlett EL, Donato GM, Gray MC. Macrophage cytotoxicity produced by adenylate cyclase toxin from Bordetella pertussis: more than just making cyclic AMP! Mol Microbiol 2006;59(2):447-59.

176. Ehrmann IE, Gray MC, Gordon VM, Gray LS, Hewlett EL. Hemolytic activity of adenylate cyclase toxin from Bordetella pertussis. FEBS Lett 1991;278(1):79-83.

177. Zitzer A, Wassenaar TM, Walev I, Bhakdi S. Potent membrane-permeabilizing and cytocidal action of Vibrio cholerae cytolysin on human intestinal cells. Infect Immun 1997;65(4):1293-8.

178. Gray M, Szabo G, Otero AS, Gray L, Hewlett E. Distinct mechanisms for K+ efflux, intoxication, and hemolysis by Bordetella pertussis AC toxin. J Biol Chem 1998;273(29):18260-7.

179. Boumpas DT, Anastassiou ED, Tsokos GC, Thyphronitis G, Balow JE. Gene transcription during in vitro activation of human B lymphocytes with *Staphylococcus aureus* Cowan I strain. J Immunol 1990;145(8):2701-5.

180. Moreilhon C, Gras D, Hologne C, Bajolet O, Cottrez F, Magnone V, et al. Live *Staphylococcus aureus* and bacterial soluble factors induce different transcriptional responses in human airway cells. Physiol Genomics 2005;20(3):244-55.

181. Fragaki K, Kileztky C, Trentesaux C, Zahm JM, Bajolet O, Johnson M, et al. Downregulation by a long-acting beta2-adrenergic receptor agonist and corticosteroid of *Staphylococcus aureus*-induced airway epithelial inflammatory mediator production. Am J Physiol Lung Cell Mol Physiol 2006;291(1):L11-8.

182. Menzies BE, Kenoyer A. Signal transduction and nuclear responses in *Staphylococcus aureus*-induced expression of human {beta}-defensin-3 in skin keratinocytes. Infect Immun 2006.

183. Xu Y, Voorhees JJ, Fisher GJ. Epidermal Growth Factor Receptor Is a Critical Mediator of Ultraviolet B Irradiation-Induced Signal Transduction in Immortalized Human Keratinocyte HaCaT Cells. Am J Pathol 2006;169(3):823-30.

184. Kaufmann K, Thiel G. Epidermal growth factor and thrombin induced proliferation of immortalized human keratinocytes is coupled to the synthesis of Egr-1, a zinc finger transcriptional regulator. J Cell Biochem 2002;85(2):381-91.

185. Pain VM, Clemens MJ. Assembly and breakdown of mammalian protein synthesis initiation complexes: regulation by guanine nucleotides and by phosphorylation of initiation factor eIF-2. Biochemistry 1983;22(4):726-33.

186. Siekierka J, Manne V, Ochoa S. Mechanism of translational control by partial phosphorylation of the alpha subunit of eukaryotic initiation factor 2. Proc Natl Acad Sci U S A 1984;81(2):352-6.

187. Rolfe DF, Brown GC. Cellular energy utilization and molecular origin of standard metabolic rate in mammals. Physiol Rev 1997;77(3):731-58.

188. Buttgereit F, Brand MD. A hierarchy of ATP-consuming processes in mammalian cells. Biochem J 1995;312 (Pt 1):163-7.

189. Novoa I, Zhang Y, Zeng H, Jungreis R, Harding HP, Ron D. Stress-induced gene expression requires programmed recovery from translational repression. Embo J 2003;22(5):1180-7.

190. Doutheil J, Gissel C, Oschlies U, Hossmann KA, Paschen W. Relation of neuronal endoplasmic reticulum calcium homeostasis to ribosomal aggregation and protein synthesis: implications for stress-induced suppression of protein synthesis. Brain Res 1997;775(1-2):43-51.

191. Kumar R, Azam S, Sullivan JM, Owen C, Cavener DR, Zhang P, et al. Brain ischemia and reperfusion activates the eukaryotic initiation factor 2alpha kinase, PERK. J Neurochem 2001;77(5):1418-21.

192. DeGracia DJ, Kumar R, Owen CR, Krause GS, White BC. Molecular pathways of protein synthesis inhibition during brain reperfusion: implications for neuronal survival or death. J Cereb Blood Flow Metab 2002;22(2):127-41.

193. Harding HP, Zeng H, Zhang Y, Jungries R, Chung P, Plesken H, et al. Diabetes mellitus and exocrine pancreatic dysfunction in perk-/- mice reveals a role for translational control in secretory cell survival. Mol Cell 2001;7(6):1153-63.

194. Kimball SR, Jefferson LS. Regulation of protein synthesis by modulation of intracellular calcium in rat liver. Am J Physiol 1992;263(5 Pt 1):E958-64.

195. Kazemi S, Papadopoulou S, Li S, Su Q, Wang S, Yoshimura A, et al. Control of alpha subunit of eukaryotic translation initiation factor 2 (eIF2 alpha) phosphorylation by the human papillomavirus type 18 E6 oncoprotein: implications for eIF2 alpha-dependent gene expression and cell death. Mol Cell Biol 2004;24(8):3415-29.

196. O'Loghlen A, Perez-Morgado MI, Salinas M, Martin ME. Reversible inhibition of the protein phosphatase 1 by hydrogen peroxide. Potential regulation of eIF2 alpha phosphorylation in differentiated PC12 cells. Arch Biochem Biophys 2003;417(2):194-202.

197. Munoz F, Martin ME, Manso-Tomico J, Berlanga J, Salinas M, Fando JL. Ischemia-induced phosphorylation of initiation factor 2 in differentiated PC12 cells: role for initiation factor 2 phosphatase. J Neurochem 2000;75(6):2335-45.

198. Carlson M. Glucose repression in yeast. Curr Opin Microbiol 1999;2(2):202-7.

199. Kemp BE, Mitchelhill KI, Stapleton D, Michell BJ, Chen ZP, Witters LA. Dealing with energy demand: the AMP-activated protein kinase. Trends Biochem Sci 1999;24(1):22-5.

200. Sanz P, Alms GR, Haystead TA, Carlson M. Regulatory interactions between the Reg1-Glc7 protein phosphatase and the Snf1 protein kinase. Mol Cell Biol 2000;20(4):1321-8.

201. Frerichs KU, Smith CB, Brenner M, DeGracia DJ, Krause GS, Marrone L, et al. Suppression of protein synthesis in brain during hibernation involves inhibition of protein initiation and elongation. Proc Natl Acad Sci U S A 1998;95(24):14511-6.

202. Wang J, Laschinger C, Zhao XH, Mak B, Seth A, McCulloch CA. Mechanical force activates eIF-2alpha phospho-kinases in fibroblast. Biochem Biophys Res Commun 2005;330(1):123-30.

203. Li J, Holbrook NJ. Elevated gadd153/chop expression and enhanced c-Jun N-terminal protein kinase activation sensitizes aged cells to ER stress. Exp Gerontol 2004;39(5):735-44.

204. Misra UK, Deedwania R, Pizzo SV. Activation and cross-talk between Akt, NF-kappaB, and unfolded protein response signaling in 1-LN prostate cancer cells consequent to ligation of cell surface-associated GRP78. J Biol Chem 2006;281(19):13694-707.

205. Crozier SJ, Zhang X, Wang J, Cheung J, Kimball SR, Jefferson LS. Activation of signaling pathways and regulatory mechanisms of mRNA translation following myocardial ischemia-reperfusion. J Appl Physiol 2006;101(2):576-82.

206. Williams BR. PKR; a sentinel kinase for cellular stress. Oncogene 1999;18(45):6112-20.

207. Goh KC, deVeer MJ, Williams BR. The protein kinase PKR is required for p38 MAPK activation and the innate immune response to bacterial endotoxin. Embo J 2000;19(16):4292-7.

208. He Y, Tan SL, Tareen SU, Vijaysri S, Langland JO, Jacobs BL, et al. Regulation of mRNA translation and cellular signaling by hepatitis C virus nonstructural protein NS5A. J Virol 2001;75(11):5090-8.

209. Rodriguez-Hernandez CJ, Sanchez-Perez I, Gil-Mascarell R, Rodriguez-Afonso A, Torres A, Perona R, et al. The immunosuppressant FK506 uncovers a positive regulatory cross-talk between the Hog1p and Gcn2p pathways. J Biol Chem 2003;278(36):33887-95.

210. Huffman DL, Abrami L, Sasik R, Corbeil J, van der Goot FG, Aroian RV. Mitogen-activated protein kinase pathways defend against bacterial pore-forming toxins. Proc Natl Acad Sci U S A 2004;101(30):10995-1000.

211. Vitale G, Bernardi L, Napolitani G, Mock M, Montecucco C. Susceptibility of mitogen-activated protein kinase kinase family members to proteolysis by anthrax lethal factor. Biochem J 2000;352 Pt 3:739-45.

212. Park JM, Greten FR, Li ZW, Karin M. Macrophage apoptosis by anthrax lethal factor through p38 MAP kinase inhibition. Science 2002;297(5589):2048-51.

213. Garsin DA, Sifri CD, Mylonakis E, Qin X, Singh KV, Murray BE, et al. A simple model host for identifying Gram-positive virulence factors. Proc Natl Acad Sci U S A 2001;98(19):10892-7.

214. Sifri CD, Begun J, Ausubel FM, Calderwood SB. Caenorhabditis elegans as a model host for *Staphylococcus aureus* pathogenesis. Infect Immun 2003;71(4):2208-17.

215. Sifri CD, Begun J, Ausubel FM. The worm has turned--microbial virulence modeled in Caenorhabditis elegans. Trends Microbiol 2005;13(3):119-27.

216. Berman K, McKay J, Avery L, Cobb M. Isolation and characterization of pmk-(1-3): three p38 homologs in Caenorhabditis elegans. Mol Cell Biol Res Commun 2001;4(6):337-44.

217. Aballay A, Drenkard E, Hilbun LR, Ausubel FM. Caenorhabditis elegans innate immune response triggered by Salmonella enterica requires intact LPS and is mediated by a MAPK signaling pathway. Curr Biol 2003;13(1):47-52.

218. Lettre G, Kritikou EA, Jaeggi M, Calixto A, Fraser AG, Kamath RS, et al. Genome-wide RNAi identifies p53-dependent and -independent regulators of germ cell apoptosis in C. elegans. Cell Death Differ 2004;11(11):1198-203.

219. Bennett TA, Lynam EB, Sklar LA, Rogelj S. Hydroxamate-based metalloprotease inhibitor blocks shedding of L-selectin adhesion molecule from leukocytes: functional consequences or neutrophil aggregation. J Immunol 1996;156(9):3093-7.

8. CURRICULUM VITAE

Name: Gunnaporn Veerachato
Date of Birth: 21 January 1972
Place of Birth: Bangkok, Thailand
Citizenship: Thai
Residence: Pathum Thani, Thailand
E-mail: pookmainz@gmail.com

Education:

2003-present Ph.D Student,

Johannes Gutenberg-University of Mainz / Faculty of Biology & Institute of Medical Microbiology and Hygiene (Germany)

1999-2003 Master of Science (Veterinary Microbiology),

University of Saskatchewan/Western College of Veterinary Medicine (Canada)

1996-1998 Master of Science (Molecular Genetics-Genetic Engineering),

Mahidol University/Institute of Molecular Biology and Genetics (Thailand)

1989-1995 Doctor of Veterinary Medicine (DVM.),

Chulalongkorn University/Faculty of Veterinary Science (Thailand)

Research Experience:

2003 Oral Presentation: The Second Thai Student Academic Conference, Aachen University of Technology

Study of host response to *Streptococcus dysgalactiae*

2003 M.Sc thesis project, University of Saskatchewan

Streptococcus dysgalactiae: Interactions with host cells and characterization of *gap*C (Advisors-Profs. Lorne A. Babiuk and Andrew A. Potter)

2002 Poster Presentation: The Ninth Annual Life Sciences Student Research Day, University of Saskatchewan

1998 M.Sc thesis project, Mahidol University

Studies on *Escherichia coli* expression of classical swine fever virus *gp*55 and its antigenic characterization (Advisor - Prof.Sakol Panyim)

1995 Case Study, Chulalongkorn University

Canine parvovirus (CPV) serum antibody titres in canine pups before the first innoculation of CPV vaccine (Advisors - Assoc.Prof. Kanisak Oraveerakul and Assist.Prof. Supote Methiyapun)